Vapor-Liquid Equilibrium of Monoethanolamine/Piperazine/Water at 35 – 70 ^{0}C

by

John Arthur McLees, Jr., B.S.

Thesis

Presented to the Faculty of the Graduate School of

The University of Texas at Austin

in Partial Fulfillment

of the Requirements

for the Degree of

Master of Science in Engineering

The University of Texas at Austin

May, 2006

Vapor-Liquid Equilibrium of Monoethanolamine/Piperazine/Water at 35 – 70 ^{0}C

Approved by
Supervising Committee:

_____

Gary T. Rochelle, Supervisor

_____

Frank Seibert

Dedication

To my parents, John and Susan McLees. You believed in my every step of the way to this point, and I hope I make you proud.

Acknowledgements

I would like to thank first and foremost Dr. Gary Rochelle for his support throughout this project. His guidance and suggestions were always welcomed as they provided me with valuable insight on many occasions. He allowed me to pursue ideas freely and openly listened to my input, and I really feel like he taught me far more than he will ever realize. I want to thank him for taking me into his group and being my mentor for the past 2 years as it was an experience I will always cherish.

George Goff may very well have been the most important member of Dr. Rochelle's group that I interacted with during my stay here. I wish I would have had more time to spend with George as I only got to know him for a little over a year, but during that short time I was able to learn so much from him that I would have struggled to pick up on my own. George taught me everything I know about my experimental methods from running the FTIR system to data analysis, and even the kinds of questions to expect during presentations. George was also gracious enough to help me with problems even after he left the group, and I am extremely appreciative of that.

Mark Nelson from Air Quality Analytical, Inc. has been my most valuable contact outside of the University during my time in Austin. I am forever grateful for his patience with me in taking the time to teach me concepts in vibrational spectroscopy that were critical to the completion of this project. Mark always had time to answer my questions and even make trips to the site where I was working if I had problems, and there is no question I could not have completed this project without his help.

Frank Seibert has been a great person to interact with during my stay at the University of Texas. He has provided me with invaluable experience working in pilot plant level projects, and his knowledge in this area is extensive. Aside from that, he took

a genuine interest not only in my experimental work but also my life outside of school, of which I am really grateful. I would also like to thank Chris Lewis, Robert Montgomery, and Steve Briggs from Pickle Research Campus for all the assistance they provided me during the two projects I was involved in there.

Over the past few months, I have been fortunate to work closely with Marcus Hilliard as a lab partner, and this experience has taught me many things not only about engineering, but life in general. His input and ideas have been very insightful, and his help in running experiments in addition to modeling work was essential to the completion of this work. I want to thank him for giving me much-needed direction to go in my work when I found myself lost at times, and that he played a vital role in its achievement.

Andrew Sexton has been many things for me during my time in Austin. Not only has he been a roommate and fellow Rochelle group member, I am proud to call him my one of my best friends. We have been through so many things together from joint experiments, University of Texas football games, and road trips that I am very excited to be staying here in Austin to watch him progress through his graduate school career. I would also like to thank fellow roommate and friend Jason Cantor for his almost daily (and more often than not, unintentional) humorous actions that make me confident that I would not have had nearly as much fun had these two not been in my life.

Eric Chen has probably been one of the most valuable people I have met for a variety of reasons. He is the most seasoned member of Dr. Rochelle's group, and consequently has a lot of knowledge and experience that no other members have. He has been very willing to go out of his way to help me with my work or at least point me in the right direction, and not once complained. I am honored to also call Eric one of my good friends that I have had the pleasure of interacting with during my graduate studies.

I would like to thank the other members of Dr. Rochelle's group that have already left or are still here: Tim Cullinane, Chuck Okoye, Ross Dugas, Babatunde Oyenekan, Jason Davis, Bob Tsai, and Lane Salgado. You guys have all had some form of influence in my work, and I always appreciated your suggestions and thoughts during the weekly group meetings. Hopefully, I'll still be able to make appearances in the labs from time to time or drop in on one of our weekly Thursday pilgrimages to Chipotle.

Lastly, I want to thank my family and friends back home in South Carolina. You guys have been there for me even though we don't get to see each other quite as much as we would like to, and I know you are all right there supporting me throughout this project. I hope I made you all proud.

This thesis was prepared with the support of the U.S. Department of Energy, under Award No. DE-FC26-02NT41440. However, any opinions, findings, conclusions, or recommendations expressed herein are those of the authors and do not necessarily reflect the views of the DOE or other sponsors.

May 5, 2006

Abstract

Vapor-Liquid Equilibrium of Monoethanolamine/Piperazine/Water at 35 – 70 ^{0}C

John Arthur McLees, Jr., M.S.E.

The University of Texas at Austin, 2006

Supervisor: Gary T. Rochelle

The equilibrium partial pressures of monoethanolamine (MEA), piperazine (PZ), and water were measured in a stirred reactor with a recirculating vapor phase by FTIR analysis at 35 – 70 ^{0}C. MEA and PZ volatility were measured in two separate pilot plant campaigns to capture CO_2 from flue gas under a range of absorber conditions. The laboratory data were regressed to determine NRTL binary interaction parameters that predicted the experimental points within 10 – 20%. It was proven that MEA volatility ($0.45<\gamma_{MEA}<0.55$) is a viable concern in CO_2 capture processes from an economic, environmental, and overall health perspective. PZ, on the other hand, was not observed to be as volatile ($0.06<\gamma_{PZ}<0.08$) as predicted by previous models and therefore volatility loss would not be a significant drawback for using it as a CO_2 capture solvent. Pilot plant results show an average MEA gas phase concentration at the absorber outlet to be

approximately 45 ppm while the PZ concentrations averaged 6 ppm and 8 ppm at the absorber inlet and outlet, respectively.

Table of Contents

List of Tables

List of Figures

Chapter 1: Introduction

The purpose of this chapter is to introduce the current process for CO_2 capture by absorption/stripping and to identify the types of amine losses associated with it. A second objective will be to discuss the reasons for using a particular solvent, and the benefits and drawbacks associated with the different types. Lastly, the specific scope and objectives of this particular project will be discussed.

1.1. CO_2 CAPTURE BY AQUEOUS ABSORPTION/STRIPPING

Absorption/stripping with aqueous amines will be an important technology for CO_2 capture from coal-fired power plants. Monoethanolamine (MEA) is the most widely used solvent for this purpose, and will be discussed further in this chapter. However, other solvent possibilities exist such as K_2CO_3/Piperazine (Cullinane 2005), MEA/PZ (Okoye 2005), and MDEA/PZ (Bishnoi 2000). Figure 1.1 below shows the typical flowsheet of the absorption/stripping process and where the different types of losses would typically occur.

Flue gas containing approximately 12 mol% CO_2 is counter-currently contacted with the liquid amine solvent in the absorber column. The rich amine solution is then sent through a cross-exchanger for pre-heating before being pumped into the top of the stripper column.

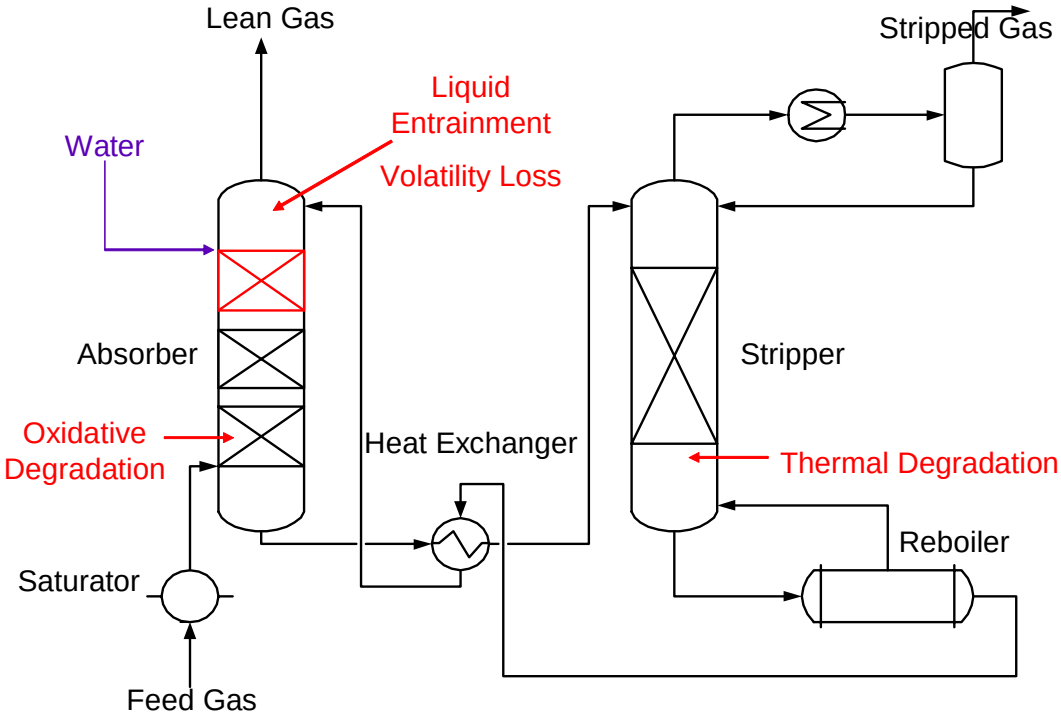

Figure 1.1: Process Flowsheet for CO_2 Capture from Flue Gas by Aqueous Amine Absorption/Stripping (Regions Associated With Amine Losses Are Shown in Red)

The stripper is heated by steam in the reboiler, which is the main driving force to release the CO_2 from the amine solution. The gas coming off the top of the stripper is sent to a cooler to knock out the water to recover the CO_2. The heated lean amine solution is pumped through the cross-exchanger to be cooled before it is regenerated and recycled to the top of the absorber column.

1.2. AMINE LOSS MECHANISMS

There are several ways in which amines can be lost in the aqueous absorption/stripping process. This work will focus on amine loss through volatility, which is a way of describing how likely this compound is to evaporate from the liquid phase into the gas phase. Most alcohols and amine solvents, for example, are very

volatile. Volatility is quantified by the parameter γ, which is introduced by a relationship known as modified Raoult's Law, as seen in Equation 1.1.

$$y_i P = x_i \gamma_i P_i^{sat} \tag{1.1}$$

Where y_i is the mole fraction of component i in the vapor phase, P is the total pressure of the system, x_i is the liquid mole fraction of component i, γ_i is the activity coefficient of component i, and P_i^{sat} is the pure liquid vapor pressure of component i at a given temperature. The closer the activity coefficient is to 1, the more ideal the system is.

Amine volatility is significant because of its environmental implications, economic costs, and safety concerns. The most important reason to be concerned with amine volatility is the potential environmental impact these compounds may have when they get into the atmosphere and react. Amines react with sulfuric and nitric acid in the presence of sunlight to produce aerosols and secondary particulate (Seinfeld 1997). Amines can also react with NO_x gases in the presence of sunlight in the atmosphere to produce ozone (Seinfeld). Amines can also be a source of volatile organic compounds (VOCs) which can have different environmental impacts from contributing to global warming (MVOCs) or non-methane VOCs (NMVOCs) that can include carcinogenic products such as benzene (U.S. EPA). Furthermore, any waste that develops as a result of being used in the CO_2 capture process is potentially hazardous, and must be disposed of accordingly.

The second reason to study amine volatility is the potential economic losses associated with it. Current amine prices are \$0.70/lb MEA (ICIS Pricing 2006) and \$2.50/lb PZ (CMR 2005). CO_2, on the other hand, gets merely \$0.50/ton (CMR 2005). Compared on a lb-mol basis, any amine volatility greater than 40 – 50 ppm would result in a net financial loss as compared to the market value for the CO_2 being recovered.

Thus, it can be seen that there exists some breakeven point where losing amines through volatility is actually costing more than the CO_2 being recovered is worth. Along the same lines, amine solvents and their degradation products are highly corrosive materials that would result in lost profits due to replacing or repairing process equipment.

Amine volatility also raises some health and safety concerns. MEA, for example, has a threshold limit value (TLV) of 3 ppm or a 6 mg/m^3 time weighted average (OSHA). Above this limit, exposure to MEA for an extended period can cause irritation or damage to the skin, eyes, nose, or respiratory system. Similarly, PZ has no established workplace exposure limits, but has been shown to irritate the eyes, skin, and nose and cause blurred vision, weakness, coughing/weezing, and skin rash if exposed to for extended periods of time.

Oxidative degradation of amines is significant in the presence of oxygen or air. Flue gas scrubbing contains a significant amount of O_2, and thus oxidative degradation is commonly seen, most likely in the absorber column (see Fig. 1.1). The major degradation product of MEA in the presence of O_2 is NH_3 as predicted by both the electron abstraction mechanism and hydrogen abstraction mechanism (Goff 2005). Goff (2005) also proposed the following degradation products for MEA when exposed to oxygen as seen below in Table 1.1. These products can cause corrosion in plant equipment such as pumps, reactors, and pipes, not to mention adversely effect the kinetics involved in the reaction.

1.3. CURRENT AQUEOUS AMINE SOLVENTS

1.3.1. Monoethanolamine (MEA)

Monoethanolamine is the most common solvent currently used for CO_2 absorption/stripping. One reason for choosing MEA is that it has a high capacity for

CO_2, meaning it can absorb a significant quantity of CO_2 on a molar basis. Typically, primary and secondary amines have a limiting loading factor of 0.5 mol CO_2/mol amine, but this number can be increased at higher CO_2 partial pressures due to free amine liberation from the hydrolysis of the carbamate ions. Secondly, MEA has fast reaction kinetics, meaning the MEA reacts quickly with the CO_2 to form a carbamate molecule which binds the CO_2 into the liquid phase. This carbamate is thought to be the source of the high CO_2 absorption rates of primary and secondary amines. Kohl and Nielsen (1997) also show MEA to have a high CO_2 removal efficiency. Some of the drawbacks to using MEA include a large heat duty needed for solvent regeneration and corrosion issues. Because the absorption of CO_2 into an aqueous MEA solution is highly exothermic, there is a large heat duty required by the reboiler to regenerate the solvent. This heat duty represents the single biggest contribution to the overall cost of the CO_2 capture, which currently operates at a cost of about \$150/ton CO_2 (U.S. DOE 2006). MEA in the absence of CO_2 has been shown to be corrosion inhibitor (Riggs 1973), but the MEA carbamate molecules formed are known to complex with species such as Fe and result in increased corrosion rates (Nakayanagi 1996).

1.3.2. Piperazine (PZ)

Current work is being done to improve the CO_2 capture process by defining new innovative solvents. One such way of doing this is to add an activator to a conventional amine solvent (such as MEA), and one of the more prominent activators for this purpose is PZ. Piperazine is a diamine molecule, meaning it has two moles of amine available to react with CO_2 whereas a primary amine (such as MEA) only has one. PZ is also attractive because it has a lower heat of reaction than MEA, and blending the two solvents offers the benefits of fast reaction kinetics associated with the primary amine coupled with the higher CO_2 capacity and lower heat of reaction of PZ. BASF (Appl et

all, 1982) showed an MDEA/PZ blend to be a more effective CO_2 remover than conventional blends such as DEA/MDEA. Bishnoi (2000) proposed that MEA/PZ and K_2CO_3/PZ systems could possibly reduce the amount of packing in the absorber column by up to a factor of 2.

1.4. RESEARCH OBJECTIVES AND SCOPE OF THIS WORK

The main objective of this work is to measure amine volatility for several different solvents at various concentrations and use these measurements to be able to verify or refute current model predictions. Specifically, the focus will be on MEA-H_2O, PZ-H_2O, and MEA-PZ-H_2O systems over a temperature range that brackets typical absorber conditions (35 – 70 ^{0}C). The concentrations used will represent typical concentrations seen in industrial CO_2 capture conditions, as well as some other concentrations to generate sufficient data to model these systems using standard binary NRTL parameters. Current partial pressure measurements for these systems (especially PZ-H_2O and blended amine systems) are limited (see Chapter 2) and thus reliable data will need to be generated. The effects of CO_2 loading on these measurements will not be included in this work.

A second objective will be to gather and analyze gas partial pressure data from two separate pilot plant campaigns carried out at the JJ Pickle Research Campus. The first campaign used 7 m MEA as the solvent, while the second campaign featured two different compositions of a K_2CO_3/PZ blend solvent (5 m K^+/2.5 m PZ and 6.4 m K^+/1.6 m PZ). These types of experiments differ from those carried out in the laboratory in that they have a longer timeframe as well as offer an opportunity to quantify other unknown compounds that may be present in the process as a result of degradation or corrosion. Additionally, the air is continuously recirculated which allows for accumulation of degradation products. Furthermore, these experiments deal with the effects of CO_2

loading, so it will not be possible to compare these results to models derived from laboratory data.

Chapter 2: Literature Review

This chapter will discuss previous work done in the areas of vapor-liquid equilibrium and thermodynamics for MEA and PZ solvents. By reviewing work from previous studies, it provides a motivation and direction for this work. Additionally, some of the results will be comparable to the results seen later in this work. Figure 2.1 shows some published data for several amines used in CO_2 capture processes. All values shown in Figure 2.1 are available from the DIPPR database. This graph shows that for the majority of amine solvents used in CO_2 capture, very little VLE data exists in the 40 – 60 ^{0}C temperature range typically seen in absorber columns.

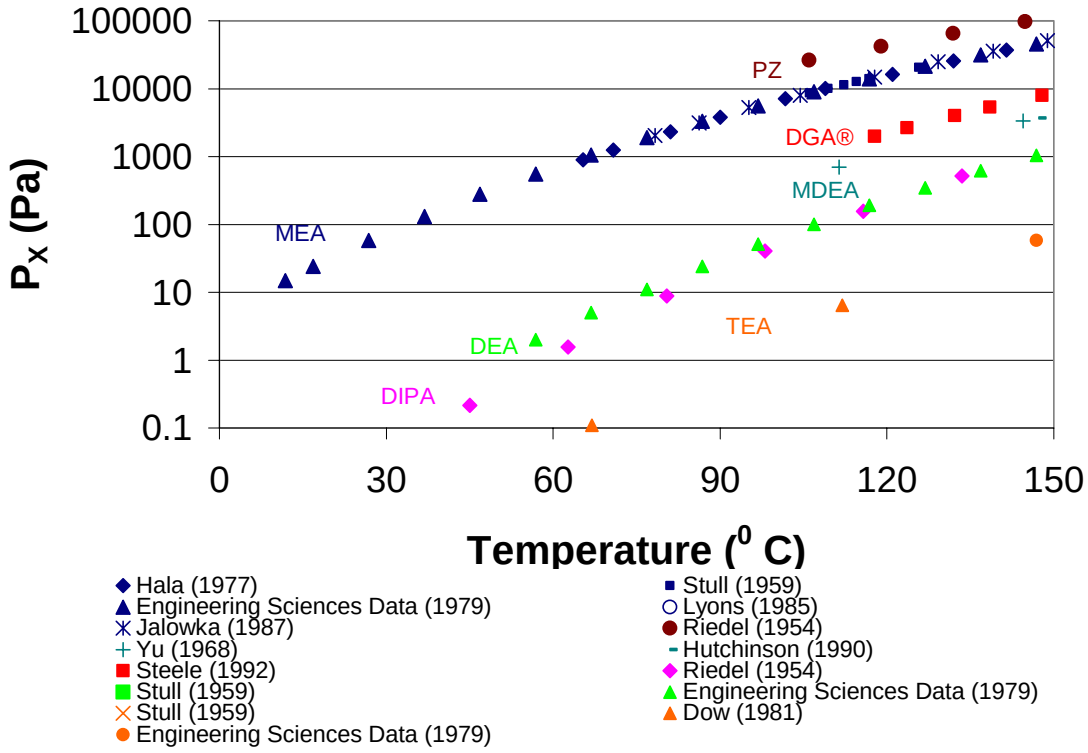

Figure 2.1. Previous amine volatility works in DIPPR database

2.1. PREVIOUS MEA STUDIES

As seen in Figure 2.1, there is some MEA partial pressure data available in the temperature range of interest for this work (40 – 60 ^{0}C). Table 2.1 below summarizes the previous MEA data that was reviewed for this work.

Table 2.1. Previous MEA literature

Author	Data type	Concentration/mole frac	Temperature/^{o}C	Pressure/kPa	
Touhara et al. (1982)	TX	0.0 - 0.9	25 - 35	0.212 - 5.466	1982
Nath and Bender (1983)	TX	0.1 - 0.9	60 - 92	1.307 - 69.101	1983
Lénard et al. (1990)	TXY	0.3 - 1.0	70 - 90	5.770 - 70.290	1990
Texaco (1994)	PX	0.0 - 1.0	100 - 163	101.325	1994
Texaco (1994)	TX	0.1 - 0.8	40 - 147	6.762 - 99.027	1994
Texaco (1994)	TXY	0.0 - 1.0	44 - 95	5.770 - 68.965	1994
Cai et al. (1996)	TXY	0.0 - 1.0	100 - 170	101.325	1996
Park and Lee (1997)	TXY	0.0 - 1.0	100 - 170	101.325	1997
Tochigi et al. (1999)	TXY	0.0 - 1.0	90	4.020 - 70.070	1999

Author	Concentration/mole frac	FPD/^{o}C	
Chang et al. (1993)	0.0 - 1.0	0.5 - 20.5	1993

Author	Concentration/mole frac	Temperature/^{o}C	Heat of Mixing/-J*mol^{-1}	
Touhara et al. (1982)	0.0 - 1.0	25	2395 - 72	1982
Posey (1996)	0.2 - 07	25 - 70	2269 - 1391	1996

Author	Concentration/mole frac	Temperature/^{o}C	Heat Capacity/J*(mol*K)$^{-1}$	
Page	0.0 - 1.0	10 - 40	75 - 180	1993
Weiland et al. (1997)	0.03 - 0.16	25	79 - 91	1997
Chiu and Li (1999)	0.2 - 0.8	30 - 80	94 - 164	1999

Touhara et al (1982) measured vapor pressures of binary mixtures of H_2O-MEA, H2O-N-methyl-2-aminoethanol, and H2O-N,N-dimethyl-2-aminoethanol at 298.15 and 308.15 K. Furthermore, this study also quantified the excess enthalpies and densities of these mixtures at 298.15 K using and isothermal displacement calorimeter and pyknometer. Lastly, the excess thermodynamic quantities G^E, H^E, TS^E, and V^E were calculated. The results showed all mixtures (except where $x > 0.5$ for H_2O-N,N-dimethyl-2-aminoethanol) had small negative deviations from Raoult's law in regards to vapor pressure.

Nath and Bender (1983) measured total pressure VLE for pure substances as well as binary and ternary mixtures of alcohols, alkanolamines, and water from 60 – 95 ^{0}C in a vapor-recycle equilibrium cell. Specifically, the MEA-H_2O system was studied at 60, 78, and 91.7 ^{0}C. Activity coefficients for each system were calculated using the Wilson and UNIQUAC equations and were seen to have negative deviations from an ideal solution.

Lénard et al (1990) measured VLE data for MEA-H_2O systems at 343.2 K and 363.2 K using a Stage-Muller dynamic equilibrium still that recirculated both liquid and vapor phases. Vapor and liquid phases were determined by gas chromatography (as opposed to FTIR analysis in this work) using a Hewlett-Packard 5790 A gas chromatograph. These experimental data had a mean absolute average deviation of less than 0.01 for the vapor fraction of MEA, and these data were represented using a three parameter Redlich-Kister expansion. The resulting excess Gibbs energy model was used to predict P-x-y curves for the MEA-H_2O systems at the two temperatures studied the experimental results compared very favorably to the model predictions. Furthermore, Lénard et al used their model to predict P-x-y curves at 298.15 K and 308.15 K and these values compared reasonably well to data measured by Touhara (1982).

Cai et al (1996) measured isobaric VLE for a MEA-H_2O system at 101.33 kPa and 66.66 kPa as well as DEA-H_2O and MEA-DEA systems at 6.66 kPa. Again, these measurements were carried out at a higher temperature range (373.15 – 443.38 K) and the liquid and vapor compositions were determined using the standard curve of refraction index vs mole fraction of the binary mixture at 20 ^{0}C with a precision of 0.001. The liquid phase activity coefficients were calculated with the UNIFAC group contribution model as published by Larsen et al (1987). The average absolute deviation for the vapor composition was less than 0.012 for the MEA-H_2O system. Therefore, Cai et al

concluded that UNIFAC relationships could be used to accurately define the ethanolamine systems.

Park and Lee (1997) measured isobaric VLE for MEA-H_2O and MEA-ethanol in an equilibrium cell that allowed circulation of both liquid and vapor phases at atmospheric pressure. Activity coefficients for both systems were calculated using the Wilson, NRTL, and UNIQUAC models and fugacity coefficients were calculated using the virial equation of state with the second virial coefficients. This work is to Park and Lee in that all partial pressure experiments will be carried out at atmospheric conditions, although the stirred reactor in the laboratory only circulates the vapor phase through the liquid phase. This work also used NRTL binary interaction parameters to calculate activity coefficients for the MEA-H_2O system as well as the PZ-H_2O and MEA-PZ-H_2O blend systems. Park and Lee's data were acquired at a higher temperature range (100 – 170 ^{0}C) than this work.

Tochigi et al (1999) measured VLE for a ternary system consisting of H_2O-MEA-dimethyl sulfoxide as well as the three binary systems at 363.15 K in an equilibrium still. The vapor pressure for pure MEA was also measured at a range of temperatures from 357.63 – 439.69 K (124.48 – 166.54 ^{0}C) which was outside of the temperature range of pure MEA for this work. Experimental activity coefficients for each system were calculated via modified Raoult's law and compared to values predicted by the NRTL model. The results of Tochigi et al compared favorably to those published earlier by Lenard et al (1987) at the same temperature, although the Lenard data did not pass the area consistency test of Redlich-Kister (1948). It was found that the average deviation between experimental and predicted vapor phase composition and total pressure were 1.1 mol% and 2.94%, respectively.

Pagé et al (1992) measured the density, isobaric heat capacity, and isentropic compressibility of MEA-H_2O systems at 10, 25, and 40 ^{0}C over the entire composition range and these results were used to calculate various thermodynamic excess and partial molar functions. These results were compared to previous work done on water-ethylene glycol and water-2-methoxyethanol systems, and the differences were explained based on different component features as well as cooperative fluctuations and hydrogen-bonding connectivity in aqueous solutions.

Chang et al (1993) measured water freezing point data in several amine-water systems. These measurements were used to regress binary interaction parameters using the NRTL model, and the results showed strong interactions between MDEA and H_2O near 0 ^{0}C. Furthermore, the measurements helped to rank the nonidealities of the amine-water systems such that MDEA ≈ DGA® > dimethylmonoethanolamine (DMMEA) > triethanolamine (TEA) > DEA > MEA. Lastly, the freezing point depression data was combined with total pressure data to predict a significant temperature dependence of solution properties.

Posey and Rochelle (1996) measured heat of mixing for pure MDEA, DEA, and MEA into 0.1 M NaOH at 25 ^{0}C and 70 ^{0}C. This data combined with total pressure, freezing point depression, and VLE data was used to regress NRTL parameters for MEA-H_2O, DEA-H_2O, and MDEA-H_2O systems. The regressions show that this new heat of mixing data improves modeling capabilities for the amine systems. The best case model for MEA-H_2O in this work has good agreement with total pressure data from Touhara et al (1982) and Nath and Bender (1983) but tends to slightly overpredict in many cases. The activity coefficients for MEA in a 20 wt% aqueous solution are predicted to be about the same at 50 ^{0}C by all three models, but there is a significant discrepancy between model predictions at 120 ^{0}C. Thus, the heat of mixing data was shown to make a 50%

difference in predicted amine vapor pressure depending on whether or not it was included in the regression.

Weiland et al (1997) measured heat capacities of CO_2-loaded solutions of aqueous MEA, DEA, MDEA, and MEA/MDEA and DEA/MDEA blends at 25 ^{0}C. Their measurements showed that the heat capacities of the amine-water solutions decrease as a function of loading, and the solutions become increasingly sensitive to CO_2 loading at higher amine concentrations. The heat capacity of the amine blend solutions showed no significant dependence on the relative proportions of the amines at a constant total amine concentration.

Chiu and Li (1999) measured heat capacity data for several aqueous amine solutions from 30 – 80 ^{0}C using a differential scanning calorimeter at alkanolamine liquid mole fractions of 0.2, 0.4, 0.6, and 0.8. The results of the measurements were used to calculate an excess molar heat capacity expression in the form of the Redlich-Kister model, and the overall average absolute deviations for excess molar heat capacity and heat capacity were 11.9% and 0.29%, respectively, compared to their experimental measurements.

Goff (2005) quantified the oxidative degradation rate of MEA by measuring the NH3 concentrations in the vapor phase through FTIR analysis at 55 ^{0}C. Other parameters such as Fe, Cu, MEA, and O_2 concentrations, CO_2 loading and pH of the solution were studied to quantify their effect on MEA degradation under typical absorber conditions.

2.2. PREVIOUS PZ STUDIES

Because PZ is not used to the extent of MEA in CO_2 capture processes currently, there is not much literature available on PZ-H_2O binary systems like MEA that was previously discussed. Aroua and Salleh (2004) measured CO_2 solubility in aqueous PZ in a stirred cell reactor at 20, 30, 40, and 50 ^{0}C with CO_2 partial pressures between 0.4 –

4.95 kPa. It was found that the aqueous PZ solvent behaves in much the same way as commonly-used alkanolamines in that increasing the CO_2 partial pressure results in an increased CO_2 loading but a temperature or concentration increase will have the reverse effect on CO_2 loading. These measurements further lead to the conclusion that the PZ forms stable carbamate ions in solution. These measurements were used to regress a model using the Kent-Eisenberg (1979) approach, and these model predictions were in agreement with the experimental data, particularly at higher temperatures.

Derks et al (2005) measured CO_2 solubility in 0.2 and 0.6 M aqueous PZ solutions at 25, 40, and 70 ^{0}C. These measurements were used to correlate an electrolyte equation of state model as proposed by Furst and Renon (1997). The final model consisted of seven ionic parameters that was able to predict the experimental CO_2 partial pressure data with an average deviation of 16%.

Wilson and Wilding (1994) measured P-T-x data for PZ-H_2O systems at 112.9 ^{0}C and 198.8 ^{0}C, but these two temperatures are well outside the temperature range of this project.

2.3. PREVIOUS BLENDED AMINE/AMINE-PROMOTED K_2CO_3 STUDIES

As mentioned previously, it is often desired to blend primary and secondary amines with an activator such as PZ to obtain a solvent with the positive characteristics of both components. Dang (2001) measured CO_2 absorption into MEA/PZ blended systems to derive a model based on equilibrium constants and also showed PZ to be an effective promoter of MEA. Bishnoi (2000) used CO_2 absorption measurements into MDEA/PZ blended solutions to derive a rigorous thermodynamic model for this system. Cullinane (2005) measured CO_2 flux on a wetted-wall column to define the thermodynamics and kinetics of an innovative 2.5 m K_2CO_3/5 m PZ solution that was shown to be effective in

CO_2 absorption. Hilliard (2005) regressed a rigorous electrolyte NRTL model of the K_2CO_3/PZ based on the experimental data acquired by previous studies.

Chapter 3: Experimental Methods and Apparatus

This chapter covers the experimental methods used to quantify amine volatility in the different solvents used throughout this project.

3.1 CHEMICALS AND SOLUTION PREPARATION

Monoethanolamine (99% purity) was purchased from Acros Organics. Anhydrous piperazine (≥ 98% purity) was purchased from Fluka. CO_2 and nitrogen (N_2) gases were obtained from Matheson Tri-Gas and the Cryogenics Laboratory at The University of Texas at Austin at a purity of 99.5 mol% and 99.0 mol%, respectfully. Ultra-pure deionized water was available from the Department of Chemical Engineering at The University of Texas at Austin. All solutions were prepared gravimetrically.

3.2 EXPERIMENTAL EQUIPMENT

3.2.1 Laboratory Stirred Reactor Apparatus

Nitrogen was saturated to water and amine in the laboratory by recirculating it through an amine solution in a stirred reactor placed in a temperature controlled bath. A schematic of this setup can be seen in Figure 3.1. The amine solution was placed in the stirred reactor and temperature set to a predetermined value. The gas was pumped through a heated sample line (T = 180 ^{0}C) to the FTIR for gas analysis. Once the gas passed through the FTIR analyzer, it was recirculated back to the bottom of the reactor through another heated sample line (T = 95 ^{0}C).

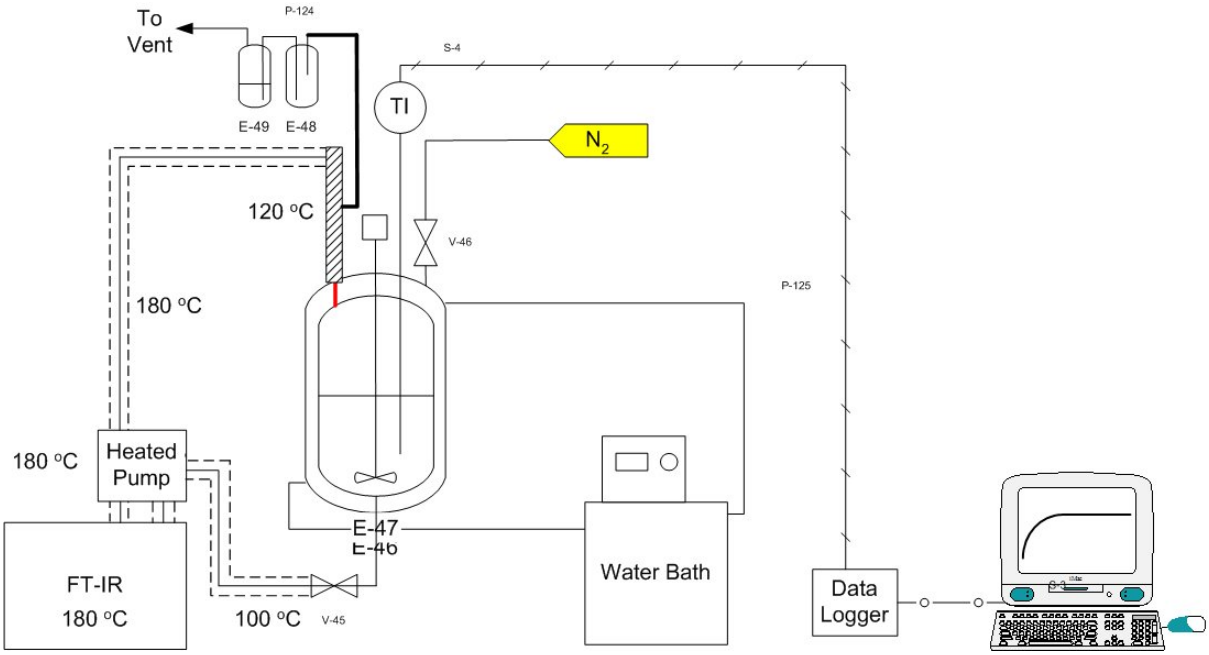

Figure 3.1: Partial Pressure Experiments Process Flowsheet

Data was taken at 40, 50, 60, and 70^{0}C settings on the temperature bath, and each data point required approximately 1.5 – 2 hours to reach equilibrium, which was determined by observing when the temperature measurement had stabilized to within 0.5%. The specific amines evaluated and their respective concentrations can be seen below in Table 3.1.

Table 3.1: Summary of Experimental Conditions for Partial Pressure Experiments

Amine-H_2O System	Temperature Range	Concentration
MEA	30 - 70 ^{0}C	100 mol %
		30 mol%
		7.0 m
		3.5 m
PZ	30 - 70 ^{0}C	0.9 m
		1.8 m
		2.5 m
		3.6 m
MEA/PZ	30 - 70 ^{0}C	3.5 m/1.8 m
		3.5 m/3.6 m
		7 m/1.8 m
		7 m/3.6 m

3.2.1.1 Temperature Controllers

The temperature of the liquid amine solution was controlled by an IsoTemp 3016H temperature bath produced by Fisher Scientific International. This particular bath used di-methyl silicone oil (50 cSt viscosity) purchased from Krayden, Inc. as a heat transfer fluid. The temperature inside the reactor was controlled to within ± 0.1 ^{0}C by the bath, and the actual solution temperature was recorded by a K-type thermocouple connected to Pico Limited Technology PT-104 converter. The thermocouple has a readability of ± 0.01 ^{0}C. The PT-104 converter reads a millivolt signal from the thermocouple and converts this signal to a temperature through a calibration formula programmed into the PicoLog Recorder software on the laboratory computer. The formula was developed by setting the temperature of the heat bath and recording the millivolt signal from the K-type thermocouple. A Pt-resistance thermocouple was used as a standard temperature, and thus the correlation between millivolt signal and Pt-resistance thermocouple temperature was plotted over a temperature range of 0 ^{0}C – 100

^{0}C. The experiment was carried out in a sealed bomb in a 500 cc Zipperclave manufactured by Autoclave Engineers, Inc. Figure 3.2 shows the corresponding calibration curve.

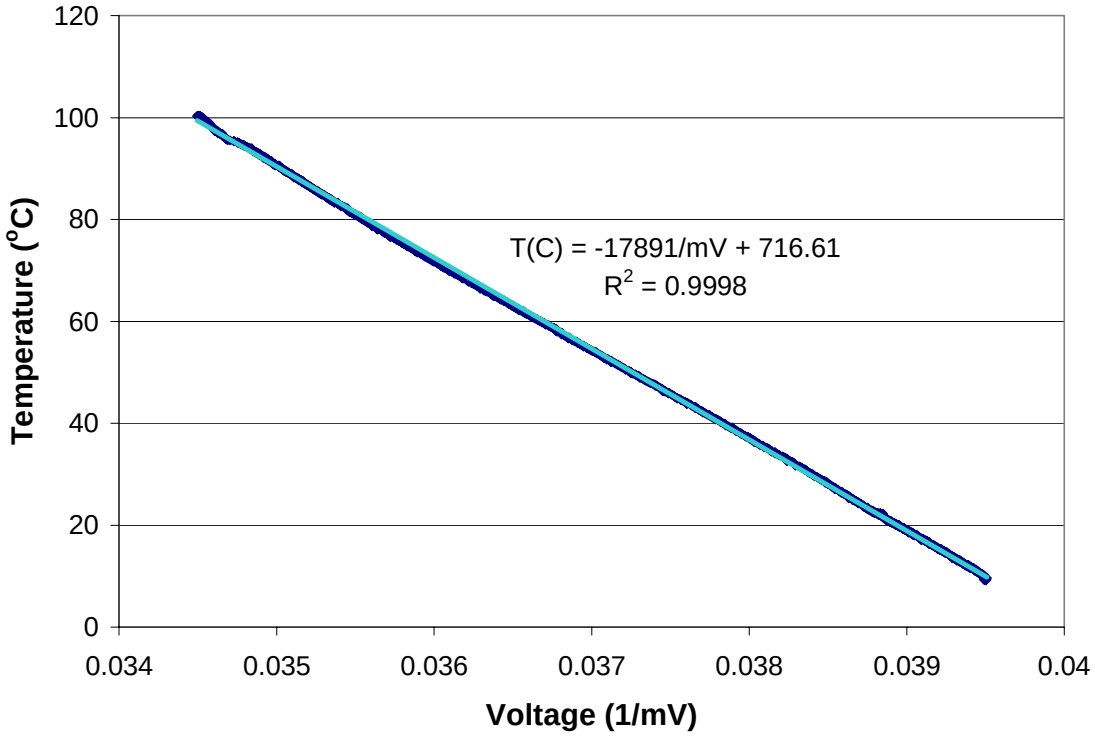

Figure 3.2: Calibration Curve for K-Type Thermocouple Used in Partial Pressure Experiments

3.2.1.2 Stirred Reactor System

The stirred reactor, which was purchased from Ace Glass, Inc. was a 1L jacketed reactor with 5 necks at the top and an 8 mm drain tube at the bottom, which served as the reactor gas inlet. This is the same reactor that was used by Goff (2005). The reactor had an inner diameter of 10 cm and a liquid depth of 15 cm. The entire reactor was insulated using Frost King ® reflective water heater insulation (1 in. thickness) cut to fit the reactor dimensions. The large neck at the top of the reactor served as a port for the StedFast™

SL 1200 stirrer produced by Fisher Scientific International. The stirrer is constructed out of stainless steel with a single blade paddle, and the agitator was capable of speeds up to 1450 RPM, although typical agitation rates for the partial pressure experiments were around 360 RPM. The stirrer was inserted through a Teflon® connector that made an airtight seal when screwed into the reactor.

One of the three medium-sized necks was used as a gas outlet where the FTIR heated sample line could be connected through a 3/8 – inch PFA Teflon® Tee. A mist eliminator for the gas outlet line was constructed from NaturalAire Cut-to-fit material and stuffed into the Teflon® connector on the reactor neck as well as inside the PFA Tee. This was also done to negate liquid entrainment in the heated gas sample line. The branch of the tee was connected to insulated tubing that ran to a system of two gas washing bottles that was used as a pressure relief system. This entire system of Swagelok® connections was insulated using BriskHeat electronic heating wrap plugged into a Variac ($T = 120\ ^{0}C$) which served to eliminate the risk of condensation in the Teflon fittings.

Another of the medium necks was used as a port for the K-type thermocouple and was connected using Swagelok® stainless steel connections. One of these was a ¼ -- inch stainless steel tee that branched into PTX-610 Pressure Transmitter manufactured by Druck Incorporated. The pressure inside the reactor was then recorded via the PicoLog Recorder software. The remaining two necks were not used in the experiments.

Goff's reactor setup utilized the same glass reactor and temperature bath setup as described above, but the rest of that system was different compared to the current setup. The biggest difference between Goff's reactor and the one in this work is that Goff's reactor did not have the heated gas recirculation line (i.e, the second 15 ft heated line). Rather, Goff's reactor was setup in a single pass mode where the gas left the top of the reactor through a single 15 ft heated sample line at 180 0C and after being sent through

the FTIR analyzer, was simply vented into the fume hood. This setup required longer times for solutions to come to equilibrium, and was one of the main motivations for implementing the heated recirculation line in this current setup. Secondly, Goff's reactor was not insulated as well as the current setup. The current setup is wrapped with water heater insulation while Goff's was exposed to ambient air. Another improvement to the current reactor setup is the use of the BriskHeat wrap around the PFA Swagelok® connections between the reactor and the heated sample line. Goff insulated these connections with cooking hot pads, but entrainment was still possible, and thus it seems the electronic heating from the BriskHeat wrap is the preferred method. Lastly, the pressure relief system described previously is an upgrade to Goff's reactor in the sense that it offers not only a easy way to verify system pressure (using the water level in the gas washing bottles) but is also a good safety feature built into the system.

3.2.1.3 FTIR Gas Analysis System

A portable FTIR gas phase analysis system (analyzer and sample pump) was purchased from Air Quality Analytical, Inc. The analyzer was a Temet Gasmet™ DX-4000 that could analyze up to 50 separate components through a temperature controlled gas cell set at 180 ^{0}C. Therefore, the gas could be analyzed without having to dry or dilute it to knock out water which would interfere with the IR absorption.

The SB4000 sample pump had separate temperature controllers for both the 15 ft. heated sample line as well as the sample pump. Furthermore, the sample pump also had separate pressure gauges for sample inlet and vent ports. The heated sample lines used in the laboratory experiments were both 15 ft long insulated Teflon® with 3/8 – in inner diameter PFA tubing inside. The sample pump and heated line temperatures for the gas outlet line from the reactor were controlled at 180 ^{0}C, while the temperature of the sample line for the gas recirculation line to the reactor inlet was set at 95 ^{0}C.

3.2.2 FTIR Gas Sampling System for PRC MEA Campaign (Campaign 3)

Since the FTIR is capable of measuring up to 50 components simultaneously in the gas phase, it was incorporated into the pilot plant CO_2 absorber/stripper system located at the JJ Pickle Research Campus in Austin, TX. For this particular study (which was carried out from 04/06 – 04/13/05), the only sample point was located in the gas outlet line, an 8-in. stainless steel pipe where the sample probe was located about 12 feet from the top of the absorber and about 6 feet before the cooler. Figures 3.3 and 3.4 give a

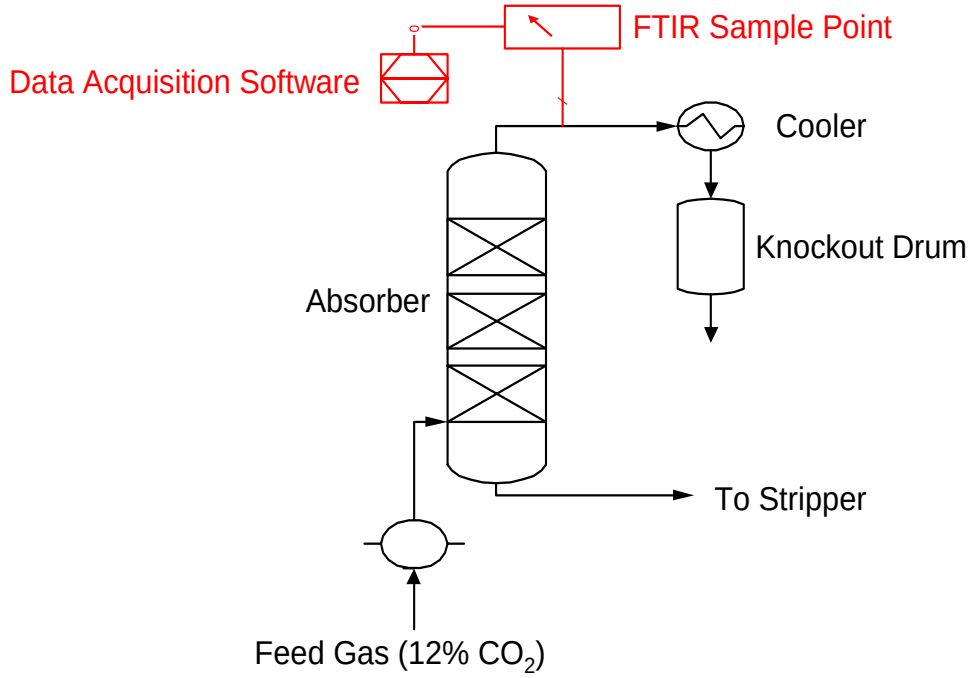

schematic of the experimental setup.

Figure 3.3: FTIR Sample Point Shown in PRC Process Flowsheet for PRC MEA Baseline Campaign

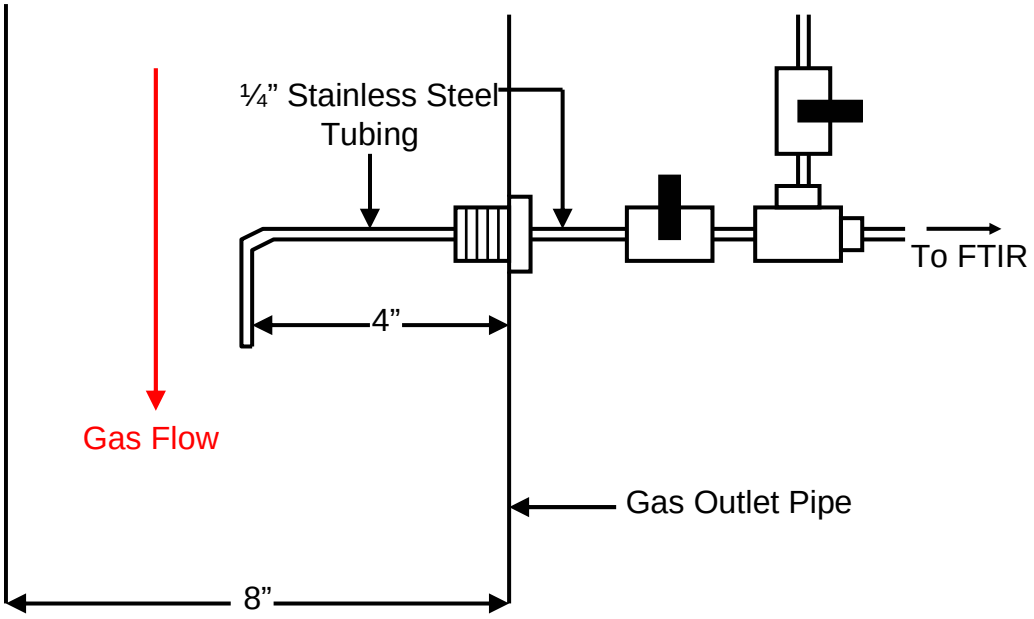

Figure 3.4: FTIR Sample Probe Used in PRC MEA Baseline Campaign

All of the FTIR analyzer equipment as well as the computer were located outside on the second level of the structure's platform for this project. The sample probe was constructed of ¼" stainless steel tubing and positioned parallel to the gas flow in the 8" I.D. gas outlet pipe. The probe was made long enough so that it was sampling gas flowing in the middle of the line. Two Swagelok® on/off valves allowed for switching between absorber gas and nitrogen purge streams, which was necessary when it became time for the instrument to be recalibrated. Since the instrument was located outside, it was necessary to recalibrate it several times daily due to significant changes in ambient temperature which cause drift in the optics sensors. Once the instrument was calibrated correctly using dry nitrogen gas, the software was set up to record samples at 3 minute intervals.

3.2.3 FTIR Gas Sampling System for PRC Campaign 4 (PZ/K_2CO_3 Campaign)

The gas sampling method for Campaign 4 proved to be a major upgrade from the method used in Campaign 3. First, it was desired to measure gas compositions at both the absorber inlet as well as outlet locations. In fact, the absorber outlet point was to be located inside the absorber head this time as opposed to some distance down the line in the absorber gas outlet stream as in the previous Campaign. The main reason for this was to measure the gas composition as close to the top of the absorber as possible and not allow for the gas sample to cool (and therefore condense water and amines) before it got to the sample point. Furthermore, locating the sample point inside the absorber head allowed for more faith in the temperature measurement from the nearest thermocouple (TT4078), and thus more accurate model predictions could be made (see Fig. 3.4). Secondly, it was imperative to locate all the FTIR equipment and associated hardware indoors in a laboratory for safety reasons. Thirdly, the operators at PRC requested all FTIR data be linked to their Delta V control system so they could monitor gas phase compositions from the control room.

There were also significant changes to the materials of construction of the sample probe itself. For Campaign 4, it was desired to construct the probe with as little stainless steel as possible so as to minimize heat loss. Thus, the material of construction was to be 3/8" PFA Teflon® tubing rather than stainless steel. Because PFA is not as rigid as stainless, it is impossible to shape into something practical by itself, so the PFA tubing was placed inside a ½" stainless steel tube so that rigid shapes could be made while the gas was only exposed to the PFA (see Fig. 3.4 below).

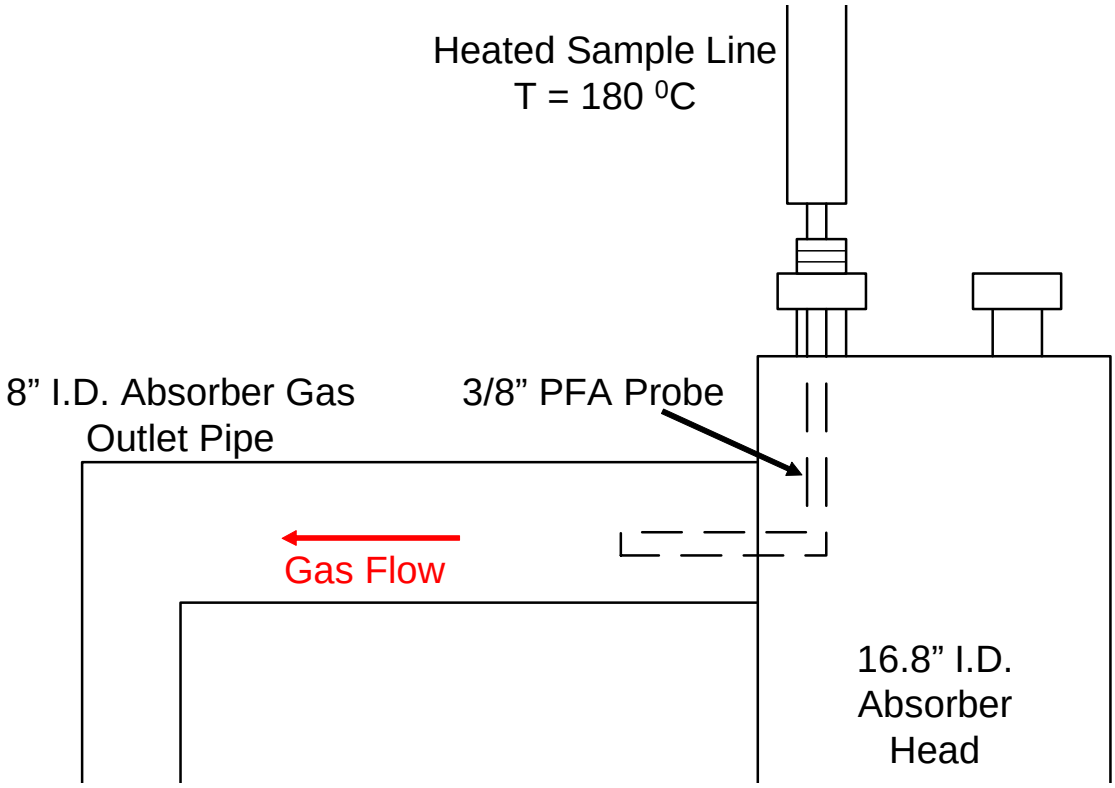

Figure 3.4: FTIR Absorber Head Sample Probe Used in PRC Campaign 4

The secondary sample point in this Campaign was located downstream of the steam injection point right before the absorber inlet gas line. Because the FTIR can analyze wet gases (as opposed to the Vaisala analyzers only being capable of analyzing gases on a dry basis), this particular location was deemed more important than one that could have been located closer to the Vaisala, which was before the steam injection. This particular sample probe was constructed out of 3/8 – in PFA Teflon® tubing wrapped inside ½ - in stainless steel tubing to maintain rigidity. The only difference between the absorber inlet and absorber outlet sample probes was that the inlet probe was significantly smaller in size due to the fact that it did not have to traverse the length of a column head. This probe had a length of about 4 in. and was placed in an existing

penetration in the absorber gas inlet pipe, with the probe pointed in the direction of gas flow so as to minimize entrainment and wall effects.

Since there were two sample points to be analyzed in this Campaign with only one FTIR analyzer, it was necessary to construct a valve switching system to allow operators to easily switch between sample points. Two Swagelok® "60" Series 3-way ball valves were mounted inside a custom made temperature controlled oven box from Environmental Supply Company, Inc. and were plumbed so that one sample point flowed to the FTIR analyzer while the other was sent to vent in a fume hood inside the laboratory. Figure 3.5 shows the basic flowsheet of how this was set up.

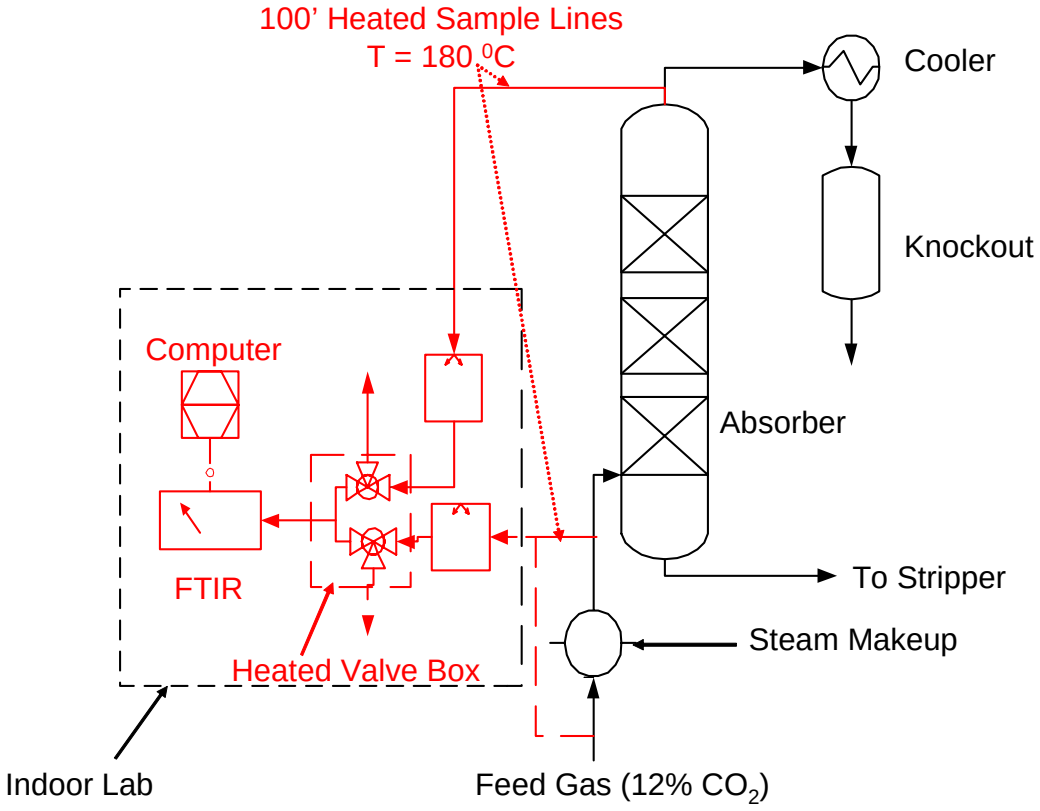

Figure 3.5: FTIR Sample Points in PRC Process Flowsheet for Campaign 4

One major advantage to having all the equipment indoors was the lack of a need to recalibrate the analyzer several times a day. This leads to less downtime and more data that can be collected. Both sample probes as well as all exposed Teflon® tubing inside the laboratory were well insulated to alleviate sample condensation. Once the analyzer was initially calibrated, it was allowed to collect data sets at three minute intervals from 01/10/06 until 01/20/06. After the solvent composition changed from 5 m K^+/2.5 m PZ to 6.4 m K^+/1.6 m PZ, the analyzer was recalibrated on 01/23/06 and allowed to collect data samples in three minute intervals from 01/23/06 until 01/26/06.

3.3 ANALYTICAL METHODS

The only analytical method used in this work was Fourier Transform Infrared (FTIR) analysis. FTIR analysis was carried out using the gas analyzer system previously described. The major benefit of FTIR analysis is that this system has the capability to measure wet gases of up to 50 separate components simultaneously, and can record the data automatically, thus allowing for experiments requiring long sampling times. Goff (2005) detailed the theory and mathematics behind FTIR analysis, and this work will serve to describe the process by which the system is calibrated, a sample is analyzed, and the creation of reference files for new components. A brief overview of this process will be given here, but for a detailed description refer to Appendix A.

3.3.1 FTIR Gas Phase Analysis

The FTIR is a valuable instrument for this type of work because it can analyze the gas phase composition of a hot wet gas sample. To do this analysis, however, the FTIR software needs something to compare the sample spectra to and this is known as a reference spectrum. Each component that will be included in the analysis must have reference spectra for given concentrations saved in the correct directory on the computer; otherwise the Calcmet™ software will not "look" for it and will give false readings for that particular component. Many reference spectra are included in the Calcmet™ libraries, so the only spectra that need to be generated are components not in that library or components with reference spectra that are deemed suspect (see Appendix A for this procedure).

It was necessary to create reference files specifically for MEA and PZ for these series of laboratory experiments since they were not included with the Calcmet™ software library. MEA reference files were created using the GASMET™ Calibrator at concentrations of 5, 10, 25, 50, 100, 500, 5000, 10000, and 15000 ppm by varying the N_2

flowrate (via the Brooks flow controller) and pumping rate of the liquid MEA through the syringe pump control to achieve the desired concentration. This process is given in detail in Appendix A. PZ reference files at concentrations of 2, 40, 59, 105, 140, 151, 188, 232, 407, and 471 ppm were created by placing a pre-weighed sample of dried PZ into a sealed bomb in the Isotemp temperature bath at a set temperature and N_2 flowrate. Nitrogen was passed over the PZ for a specified amount of time, and after this time had elapsed, the PZ was weighed again to determine the amount of PZ that had evaporated. The evaporation rate was assumed to be constant, and since the molar flow of N_2 was known through the flow controller calibration curves, it was possible to calculate a PZ concentration in the gas phase, which could be converted into a ppm value. The PZ concentration could be varied by adjusting the bath temperature and/or the N_2 flowrate.

Once all the reference spectra are organized, the FTIR has to be given a zero baseline to start from, and this is done by flowing pure N_2 through the system and running a Zero Calibration through the software. Once all the component values are verified to read "0.00", then it is possible to start taking measurements. A detailed description of this process and multi-component gas phase analysis is given in Appendix A. Once this calibration procedure is completed, the temperature bath was set to the desired temperature and allowed to equilibrate. Once this had occurred, the software was initialized to acquire sample spectra at 3 minute intervals until the solution had reached equilibrium, which was established when the bath temperature was stable to within 0.5% according to the PicoLog software. At this point it was possible to average the gas phase concentrations for each component for the 5 previous samples to get representative values for the gas phase compositions at this particular temperature.

Chapter 4: MEA Baseline Campaign Results

This chapter focuses on the partial pressure and subsequent volatility results for the MEA Baseline Campaign carried out at the JJ Pickle Research Campus in Austin, Texas from April 6 – April 13, 2005. The experimental procedure for this campaign was outlined in Chapter 3. This campaign was conducted under industrial CO_2 capture conditions, and the effects of temperature and CO_2 loading on MEA volatility are presented.

4.1 METHOD DEVELOPMENT AND DATA ANALYSIS

The initial results of the FTIR analysis came back with very high residuals, meaning that the absorbance peaks of the compounds being measured compared poorly with those peaks in the reference files, and thus many of the values initially reported were deemed suspect. Some causes of this were poor or misplaced reference files, higher than expected concentrations of some compounds, and analyzing for absorbances of compounds in the wrong wave regions. With FTIR analysis, it is possible to re-evaluate results even after the experiment is complete (granted the background scan is good) by changing the wave regions where absorbance is being analyzed for in certain compounds.

The first step of the new method development was to generate new NH_3 reference files, as it was believed the ones that were initially used were dated and possibly inaccurate. To do this, a 1000 ppm NH_3/N_2 blend was mixed with pure N_2 at different flowrates and passed through the heated sample line back in the laboratory. The N_2 flow was varied to give different NH_3 concentrations. New reference files were generated at 100 ppm, 250 ppm, 500 ppm, 750 ppm, and 1000 ppm., and then added to the analysis settings.

Secondly, the analysis regions for different compounds were changed. For NH_3, absorbances were only analyzed for in the 995-1073 and 1096-1250 cm^{-1} region. Analysis for NO was turned off, but the results yielded higher residuals than previously found for H_2O, so NO was added back to the list of compounds to be analyzed. For CO_2, it was found to be impossible to analyze in the region between 980-1130 cm^{-1}, but proved to be insignificant in terms of affecting the concentrations as this region is normally just used for baseline correction purposes. Also, due to the high H_2O residuals, it was not practical to use the region between 3400 and 3800 cm^{-1} for CO_2, and it was removed. An additional analysis region for MEA was added (2416-2601 cm^{-1}), and another region was experimented with (980-1119 cm^{-1}), but the residuals increased, and this latter region was removed. Another reference file for methanol was added (10 ppm), and the analysis regions were changed to 995-1073 cm^{-1}, 1095-1150 cm^{-1}, and 2450-3180 cm^{-1}. This caused a drop from in MEA concentration from 29.2 ppm to 2.9 ppm for the same sample. Furthermore, an additional region was added for acetaldehyde from 3200-3350 cm^{-1}. Finally, the methylamine analysis regions were changed to 2022-2223 cm^{-1}, 2450-2650 cm^{-1}, and 2800-3203 cm^{-1}, with the first two regions to account for baseline correction. This new method greatly improved the residuals on every compound, with noticeable improvements in CO_2, H_2O, NH_3, and MEA.

4.2 EXPERIMENTAL RESULTS

This section will present the key findings from the MEA Baseline Campaign FTIR analysis. The components that made up the final analysis were H_2O, CO_2, CO, N_2O, NO, NO_2, NH_3, formaldehyde, MEA, and CH_4. The main focus was on the H_2O, CO_2, NH_3, and MEA concentrations. Comprehensive tables listing raw data for all components can be found in the appendix.

4.2.1 MEA and H2O Activity Coefficient Results

Since there is no other alternative way of measuring concentrations of any compounds other than CO_2 in the gas phase at PRC, the measured partial pressure of H_2O and MEA was compared to the pure liquid vapor pressure which is predicted by Posey (1994), given by Equations 4.1 and 4.2 below, and the results are shown in Figure 4.1. (Note that both Equations. 4.1 and 4.2 apply to binary amine-water solutions and thus do not account for CO_2 loading.)

$$\text{H}_2\text{O: } P^*_{H_2O}(Pa) = \exp\left(72.55 - \frac{7206.7}{T(K)} - 7.1385\ln T(K) + 4.046E-6T(K)^2\right) \qquad 4.1$$

$$\text{MEA: } P^*_{MEA}(Pa) = \exp\left(172.78 - \frac{13492}{T(K)} - 21.914\ln T(K) + 1.3779E-5T(K)^2\right) \qquad 4.2$$

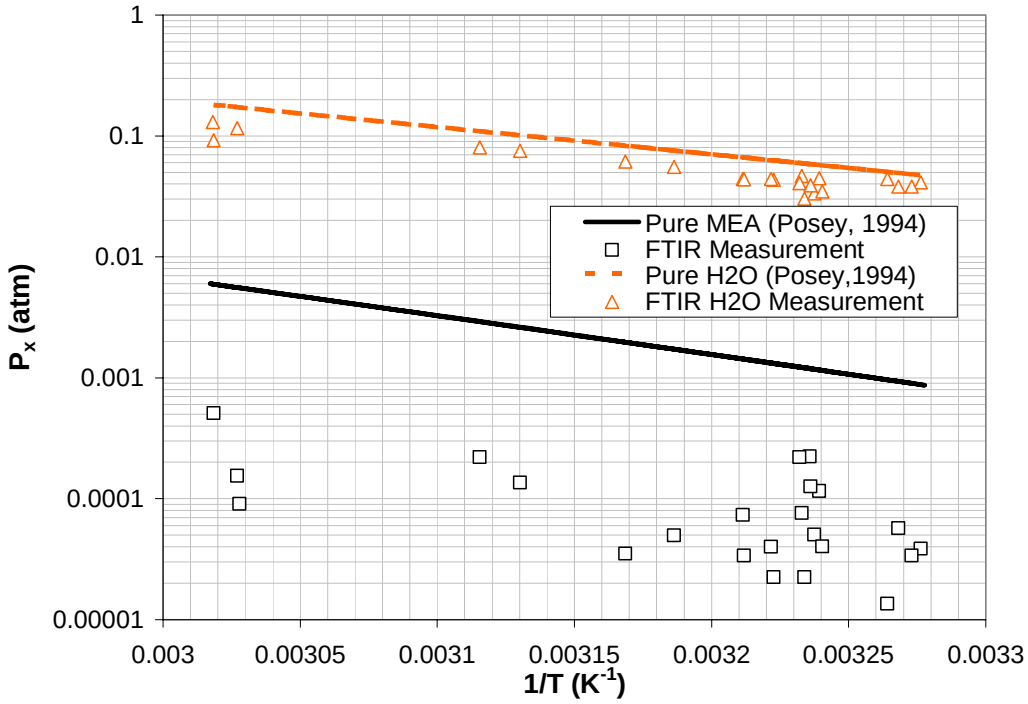

Figure 4.1: Experimental and predicted values for MEA and H_2O partial pressure (in atm) versus inverse temperature (K^{-1}).

It is observed that in both cases, the actual measured vapor pressures in a loaded solution for both compounds are somewhat lower than predicted for the unloaded scenario. Apparent activity coefficients for each compound were calculated by Equations. 4.3 and 4.4, and then plotted as a function of absorber lean loading in Figures 4.3 and 4.4.

$$\text{MEA:}\quad \gamma_{MEA} = \frac{P_{MEA,meas}}{P^*_{MEA,calc}(T) * x_{MEA} * (1-2\alpha)} \tag{4.3}$$

$$\text{H2O:}\quad \gamma_{H_2O} = \frac{P_{H_2O,meas}}{P^*_{H_2O,calc}(T) * x_{H_2O}} \tag{4.4}$$

where α is the absorber lean loading (mol CO_2/mol MEA), a_{H2O} is the activity of water ($P_{H2Omeas}/P^*_{H2Ocalc}$), x_{H20} and x_{MEA} are the mole fractions of free water and MEA,

respectively in unloaded solutions. These values correspond to 55/62 for water, and 7/62 for MEA.

Chang (1993) and Posey (1994) predict an activity coefficient of approximately 0.96 for water in a binary water-MEA solution, and our data seem to be a scatter with values ranging from approximately 0.5-1, while most are consistently lower than 0.96. The same study also predicts MEA activity coefficients between 0.4 and 0.45 for a binary water-MEA system between the temperatures of 30 ^{0}C and 60 ^{0}C. Our studies show that, in this temperature range, we again see a scatter of points at both loading conditions, but the majority of the points are somewhat higher than this prediction. Both of these deviations are accounted for by the fact that the loaded CO_2 decreases the amount of free MEA in the system, and thus the differences in the activity coefficients.

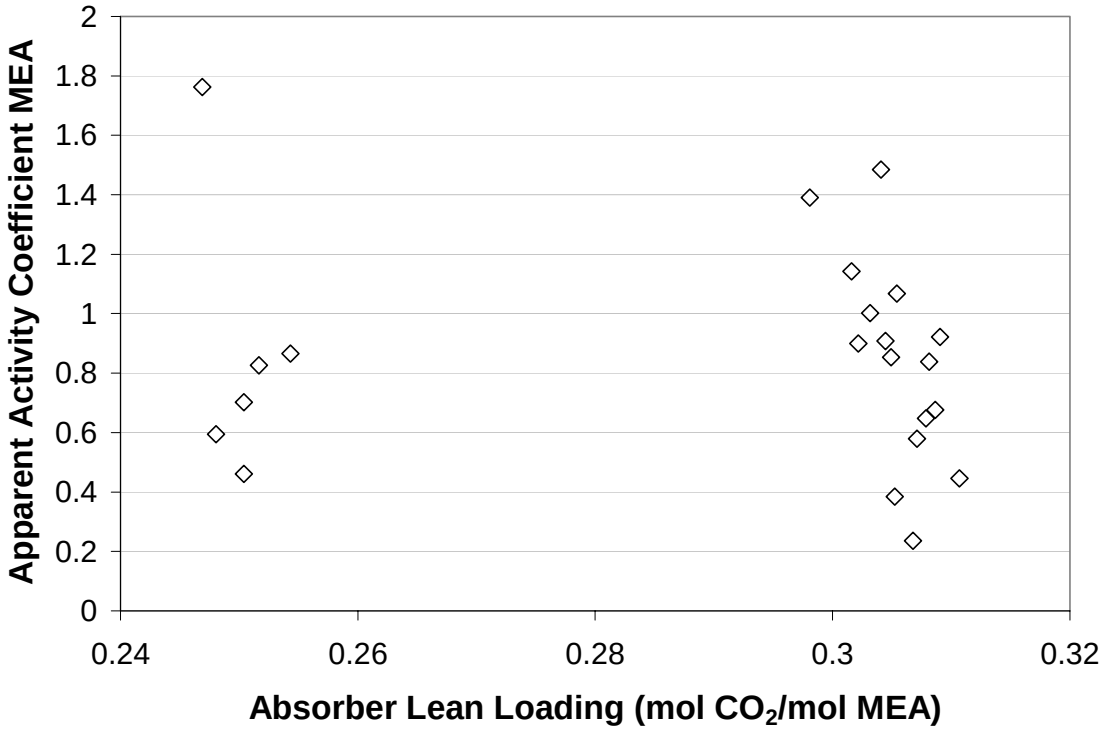

Figure 4.3: Measured activity coefficients for MEA as a function of absorber lean loading for MEA Baseline Campaign

For most of the experiment, NH_3 concentrations at the top of the absorber were very high, some exceeding 1000 ppm. Currently, it is not possible measure NH_3 past this limit since 1000 ppm is the upper limit in reference spectra, and since the FTIR cannot extrapolate values beyond its known references (due to the severe non-linearity of absorbance peaks), the NH_3 concentrations given by the FTIR above 1000 ppm are more than likely significantly under-predicted. This creates a slight problem in that NH_3 absorbs in many of the same places as compounds such as H_2O, CO_2, and MEA; so if the NH_3 concentrations are incorrect, there is a good chance that some of the other values are not entirely correct.

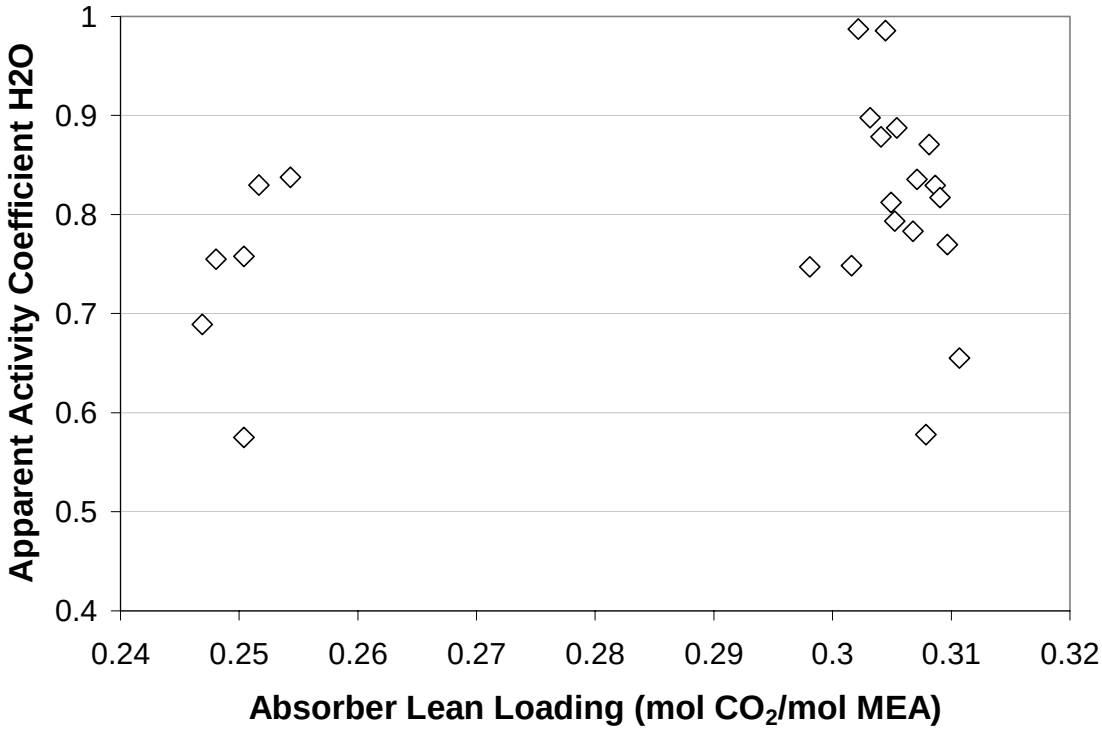

Figure 4.4: Measured activity coefficients for H_2O as a function of absorber lean loading for MEA Baseline Campaign

4.2.2 CO_2 Results

The secondary goal of this FTIR study was to evaluate whether or not FTIR analysis could be a viable alternative to the current Horiba and Vaisala instruments as an in-line analyzer. One way to check this was to compare the concentrations of CO_2 measured at the top of the absorber. Figure 4.5 below presents the measured concentrations of CO_2 by the FTIR (averaged over a period of 15 minutes) and the instantaneous readings of the Vaisala Al404 analyzer. The FTIR value was obtained by finding the time of the FTIR sample that was closest to the time the liquid samples were taken by the operators, and then averaging that value with the FTIR samples that occurred 3 and 6 minutes before and after the chosen FTIR sample. The values for the

Vaisala analyzer had to be corrected to account for the fact that the gas being analyzed is wet, and since the Vaisala is calibrated with dry gas, the actual FTIR values were divided by (1+%H_2O) to give the concentrations shown in Figure 4.5.

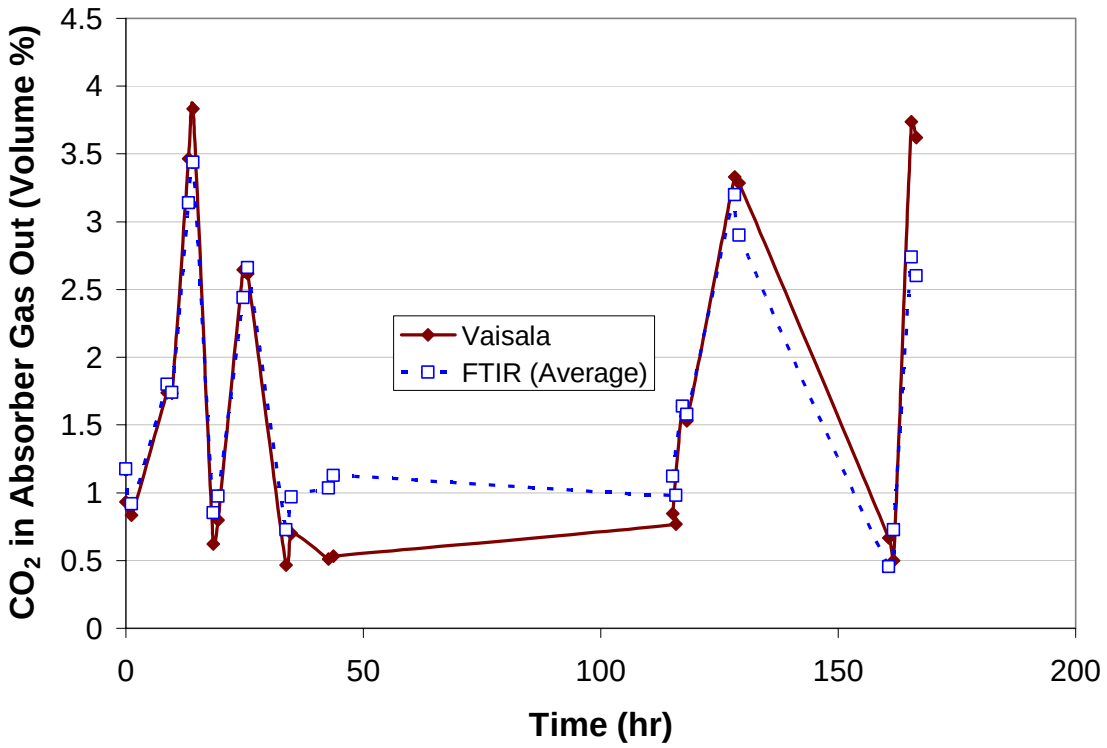

Figure 4.5: Carbon dioxide concentrations (in volume %) measured over the seven day time period of the FTIR analysis

It is clear that the FTIR is a very adequate instrument in analyzing compositions of wet gases for CO_2 for the majority of the experiment. The values differed on average by approximately 20% for the vast majority of the points not counting the last two, and one possible explanation for this may be a calibration issue with the Vaisala instruments. As will be seen in Chapter 5, it is important to calibrate both analyzers on the same basis. The FTIR is calibrated on a vol % basis, and the Vaisala analyzers are typically calibrated with gas standards that are assumed to be in wt %. If these gas standard cylinders are in

fact filled on a vol% basis (which is the standard procedure, unless specified otherwise), then the Vaisala readings would be erroneous and be off by a factor of about 30%.

Figure 4.6 below shows the direct correlation between gas outlet temperature and H_2O concentration, and because the last two sample points occur at a higher than normal temperature, the H_2O concentration is significantly higher, and thus the measured CO_2 concentrations are not in agreement. Secondly, the sample probe into the column had approximately 4-5 inches of exposed stainless steel tubing, and thus the gas may have cooled 2-3 degrees over this short distance, causing some water to condense (along with some CO_2), and this may contribute to the different values, especially at the higher temperature runs.

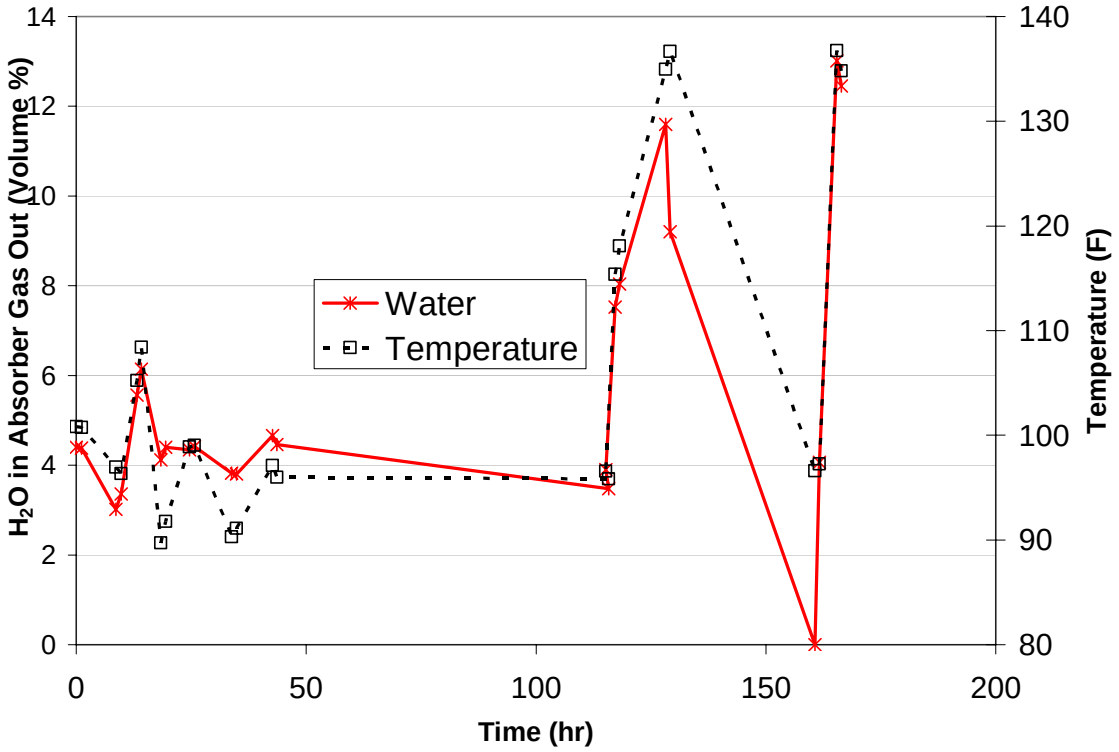

Figure 4.6: Water concentration (volume %) and temperature (^{0}F) over the course of the seven day time period

4.3 CONCLUSIONS AND RECOMMENDATIONS

This initial gas sampling and FTIR analysis proved to be a useful way to gain amine volatility data under real world industrial conditions. MEA was found to be not as volatile as predicted by Posey's model over the range of temperatures that were studied, but there were some instances where MEA concentrations reached higher than 500 ppm, which is still a concern from both an environmental and economic perspective. It is noted, however, that the absorber/stripper configuration was operated without a water wash stage, so that may account for the high levels of MEA seen in these instances. Because the majority of sample points for all the compounds that were analyzed for correspond to residuals less than 0.01, it can be said that the resulting measured concentrations are precise. MEA does have a few sample points where its residual is greater than 0.02, meaning the spectra do not agree very well with the supplied references. One explanation for this could be that there is some other compound present in the gas phase that is not being accounted for, and thus the software is falsely giving the residual peaks to MEA when in fact they correspond to this unknown compound. It is helpful to have a good understanding of the chemistry associated with the compound that are being analyzed for beforehand, but this chemistry is not as well understood as simple amine-water systems, so it is very possible that an intermediate could be present in the gas phase. Also, the pilot plant facility is not an exclusive CO_2 recovery unit, and thus many different types of distillation and extraction experiments are carried out on the same process units that were used in this campaign. It is plausible, in fact, that there is some left over hydrocarbon or amine from a previous experiment that has found its way into this campaign, and the software is falsely attributing its peaks to the compounds that are currently being analyzed for.

Another conclusion is that the MEA used in the campaign was already degraded to a significant degree. Goff (2005) suggests that NH_3 is the primary oxidative degradation product of MEA, and the FTIR data from this campaign clearly show steadily increasing NH_3 concentrations, some to levels exceeding 1000 ppm (and thus the range of our calibrations). Therefore, this solvent definitely undergoes degradation under these conditions, and the losses due to exposure to air should not be ignored.

For future experiments of this type, it is recommended that all analytical equipment be placed indoors in a controlled environment. This would greatly reduce all errors in the detector associated with drifting due to large swings in ambient temperature and decrease the amount of downtime devoted to re-calibration of the instrument. In addition, locating the hardware indoors allows for closer operator supervision since the equipment is located near the control room. Secondly, the absorber outlet point should be located closer to the top of the absorber head so that sample condensation due to cooling is minimized, and the fact the temperature of the sample being analyzed is closer to that recorded by the TT4078. Thirdly, the sample probe itself should be constructed in such a way as to minimize heat loss. A way to do this would be to fabricate the probe out of a material that does not conduct heat as well as stainless steel. Furthermore, it has been suggested that these hot flue gases may react with the stainless steel and cause the aldehydes to off-gas, and this could explain why the aldehyde concentrations were so low.

Chapter 5: K_2CO_3/PZ Pilot Plant Campaign Results

This chapter details the partial pressure results for the K_2CO_3/PZ Campaign carried out at the Pickle Research Campus from January 10 – January 26, 2006. The experimental procedure for this campaign was outlined in Chapter 3. The experimental conditions for this particular campaign were set to mirror those that might occur in an industrial application of this technology.

5.1 Method Development and Data Analysis

All gas samples for this campaign were initially analyzed using the same reference files and corresponding analysis regions for the final MEA Campaign analysis. New reference spectra were generated for PZ at concentrations of 2, 40, 59, 105, 140, 151, 188, 232, 407, and 471 ppm using the GASMET™ Calibrator instrument in the laboratory. Figure 4.1 shows the reference spectrum for the 290 ppm PZ reference file. For the final analysis, however, only the 59, 105, 188, and 407 ppm reference files were used to measure for PZ.

The initial FTIR results showed high residuals for most compounds, and thus a different analysis method had to be developed post-experimentally (similar to the MEA Baseline Campaign). The initial results showed concentrations of NO_x gases in excess of 700 ppm, and this unexpected result generated great concern for operator safety if this was indeed true. It was later discovered, however, that hexane was used in an extraction experiment at the pilot plant facility just prior to the campaign, and the analysis settings were modified to include hexane in the analysis. Because the original analysis settings did not include hexane, the Calcmet™ software had to assign the hexane peaks to a component that was included in the analysis, and so it falsely assigned the hexane peaks to the NOx gases, which explained the high concentrations originally observed. As a

result of adding hexane to the gas phase analysis, the concentrations of NO_x gases dropped to the 2 – 5 ppm range for most of the experiment.

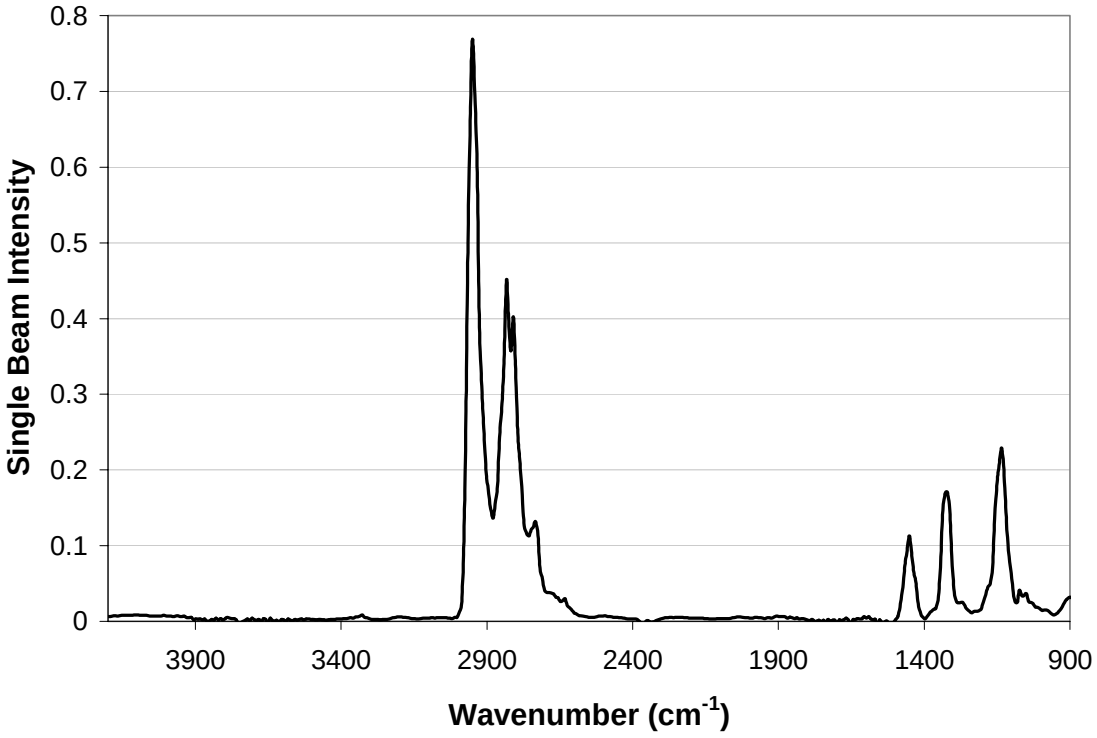

Figure 5.1: 290 ppm reference spectrum for PZ (T = 180 ^{0}C, path length = 500 cm)

The unexpected presence of hexane in the gas phase caused another data analysis problem. Figure 5.2 below shows the measured hexane concentrations in the gas phase (in ppm) over the course of the campaign. For the first solvent composition (5 m K+/2.5 m PZ), the concentrations of hexane at both sample points vary in range from approximately 10 – 100 ppm, but this concentration jumps significantly to almost 1000 ppm during the second solvent composition (6.4 m K+/1.6 m PZ). The sudden increase in hexane concentration for the second solvent composition made analyzing for PZ impossible at the absorber outlet because hexane and PZ absorb in the same regions and

the PZ peak was being engulfed by the enormous hexane peak in the sample spectra. As a result, the Calcmet™ software gives false negative concentrations for PZ during the vast majority of sample spectra measured during the 6.4/1.6 solvent composition testing.

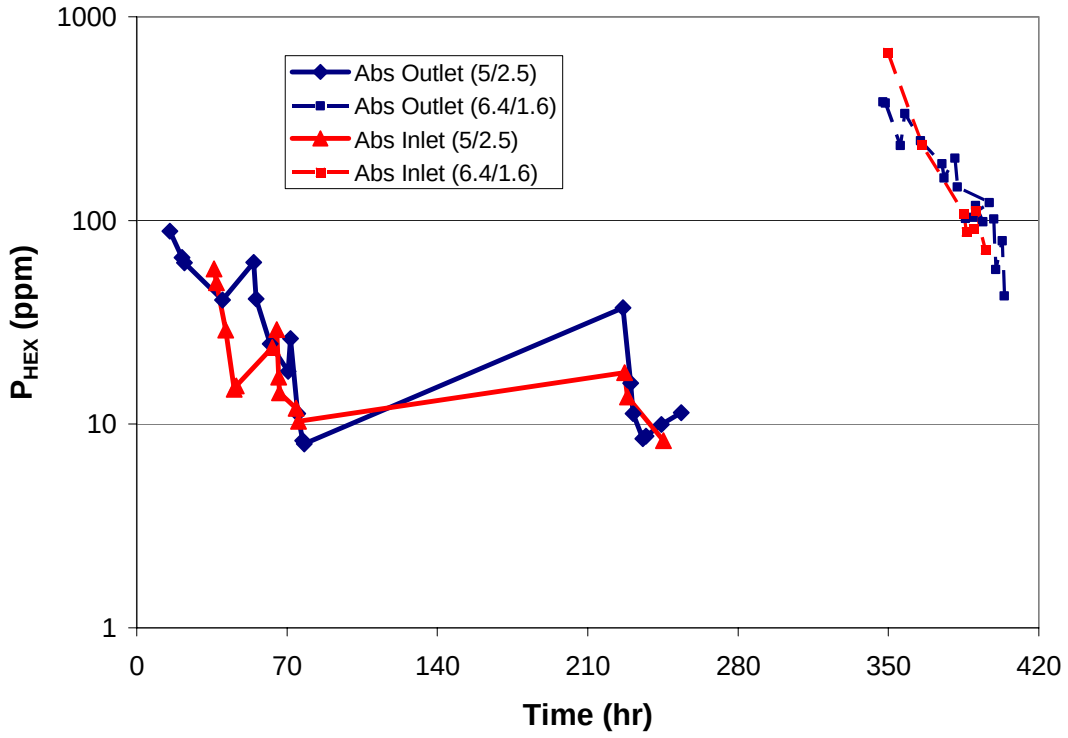

Figure 5.2: Gas Phase Hexane Concentrations as Measured by the FTIR Analyzer

Once hexane was added to the list of components in the analysis software, the residuals became significantly lower (less than 0.01 in most cases) and it appeared that the analysis was finished. Upon closer inspection, however, it turns out that there was still an appreciable amount of an unknown compound (more than likely an amine) left when all other spectra were "subtracted out" of a given sample spectra. Figure 5.3 below shows the reference spectra for the unknown compound that was generated by the residual method. Only two regions (895 – 1296 and 2550 – 3450 cm^{-1}) were used in the analysis settings.

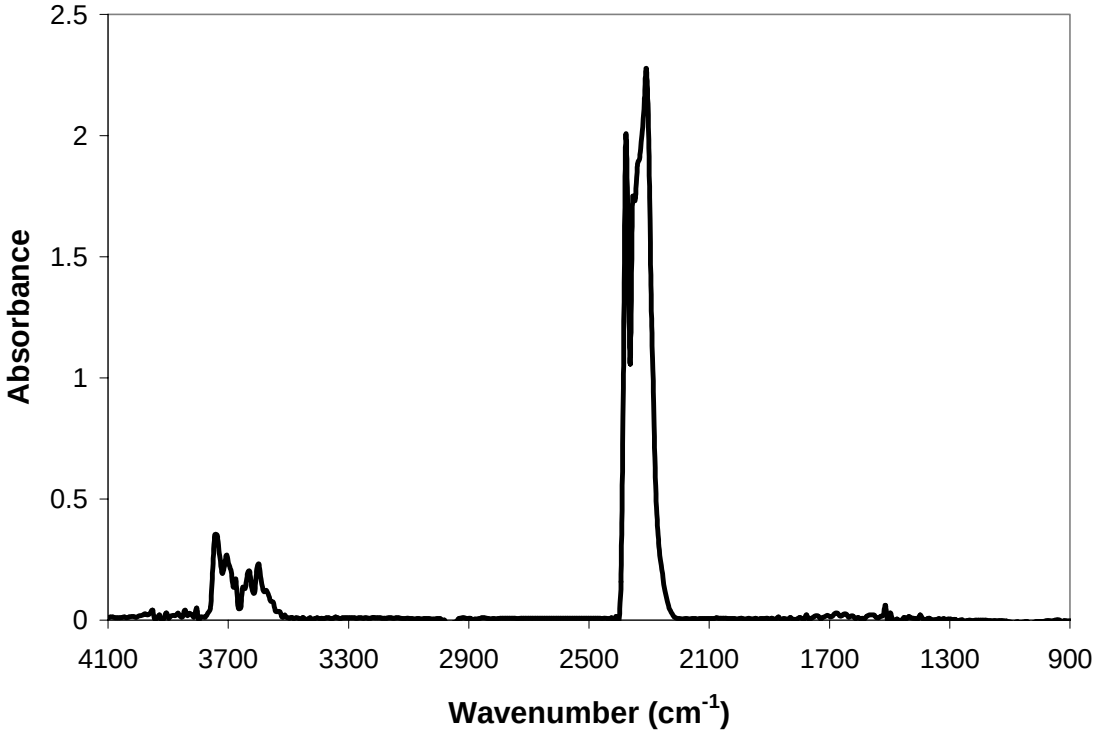

Figure 5.3: Reference spectrum for the unknown compound from the K_2CO_3/PZ pilot plant campaign

The first hypothesis for the identity of this unknown compound was ethylenediamine. Piperazine is produced commercially by reacting dichloroethane in excess NH_3 to produce 1-amino, 2-chloroethane and ammonium chloride (Reaction 5.1). The 1-amino, 2-chloroethane reacts with NH_3 to produce ethylenediamine (EDA) and ammonium chloride (Reaction 2). The EDA reacts with itself to form 1-amino, 4-chloro aminobutane (Reaction 3) which reacts with NH_3 to form PZ (Reaction 4). Another possible explanation is that EDA may be a product of oxidative degradation of PZ as shown by Sexton (2006).

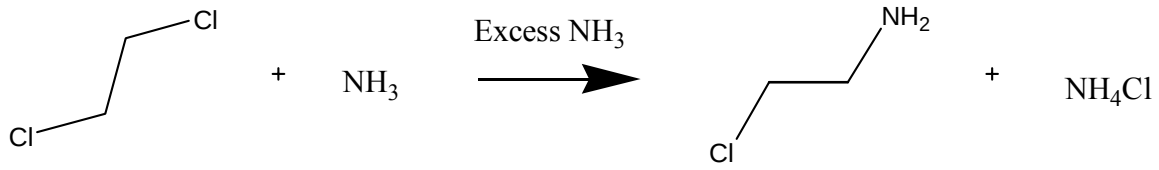

(1)

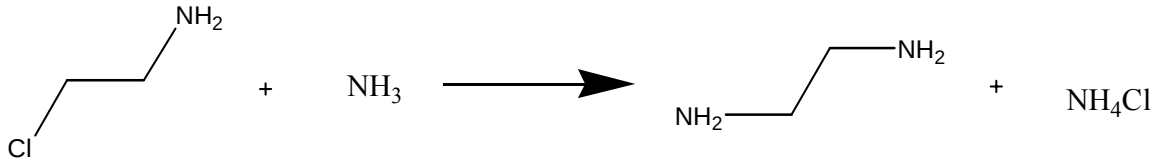

(2)

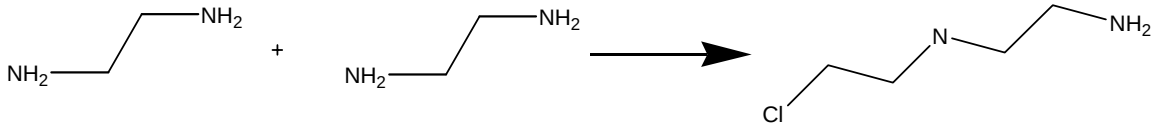

(3)

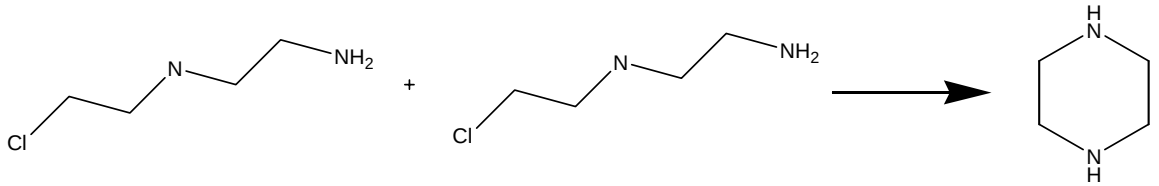

(4)

Based on the reaction mechanisms above, it is not improbable to think that there could be some EDA formed through reaction with NH_3 in the system, or present beforehand due to oxidative degradation taking place. Fortunately, there were two separate reference spectra for ethylenediamine (10 and 100 ppm) available in the Calcmet™ software library, and the 100 ppm spectrum is shown below in Figure 5.4.

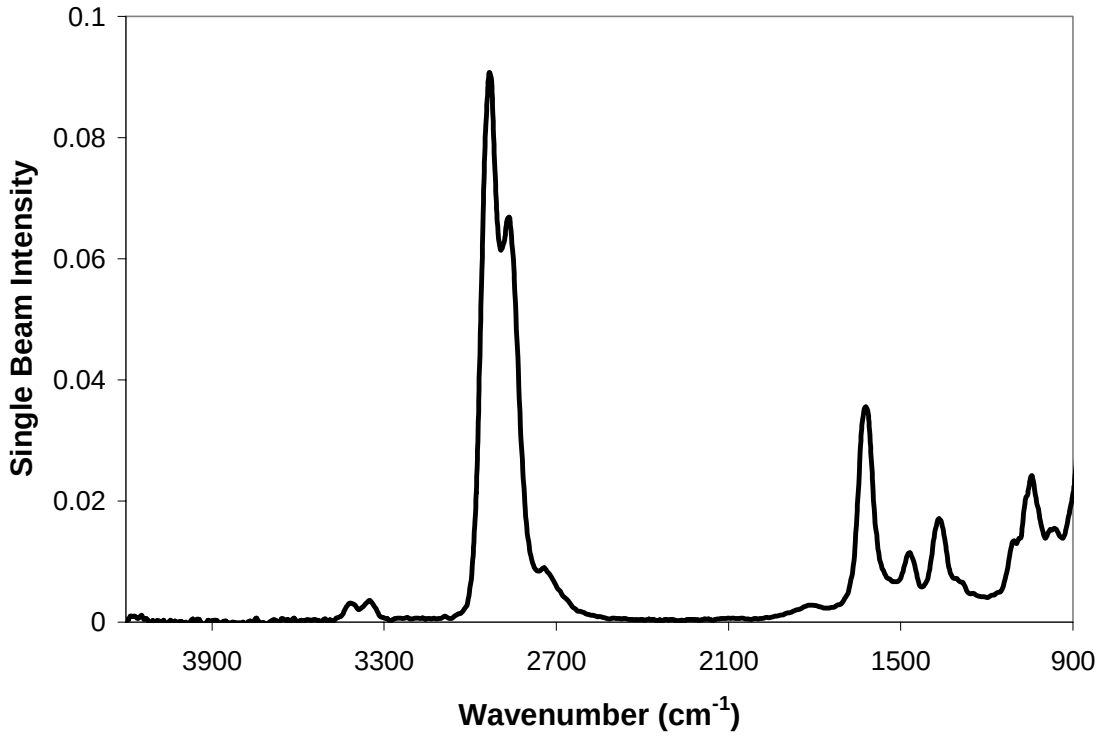

Figure 5.4: 100 ppm ethylenediamine reference spectrum (T = 180 ^{0}C, path length = 500 cm)

While the ethylenediamine reference spectra looks somewhat similar in shape to that of the unknown compound at first glance, it is important to point out that the large double peak in the unknown occurs at around 2300 cm^{-1} while this same peak occurs at around 2800 cm^{-1} for ethylenediamine. Similarly, the smaller peaks for the unknown compound occur around 3500 – 3800 cm^{-1} while this same peak shows up at around 3300 – 3400 cm^{-1} for ethylenediamine. Nevertheless, ethylenediamine was added to the analysis, but only showed up in concentrations less than 1 ppm, so it was subsequently removed.

The next compound that was believed to be the unknown amine present was ethylamine. Sexton (2006) has shown the presence of an unknown degradation product

through IC analysis of K_2CO_3/PZ solutions, and one of the components suggested was ethylamine. By including ethylamine in the analysis (and if indeed this was the Unknown Amine), it would serve to qualify that hypothesis. Unfortunately, there were no reference spectra available for ethylamine available in the Calcmet™ software library, so one had to be generated. Pure ethylamine was not available for this procedure, so a 100 ppm ethylamine reference spectrum was generated from a 70 wt% ethylamine/30 wt% H_2O mixture. Figure 5.5 below shows the resulting spectrum.

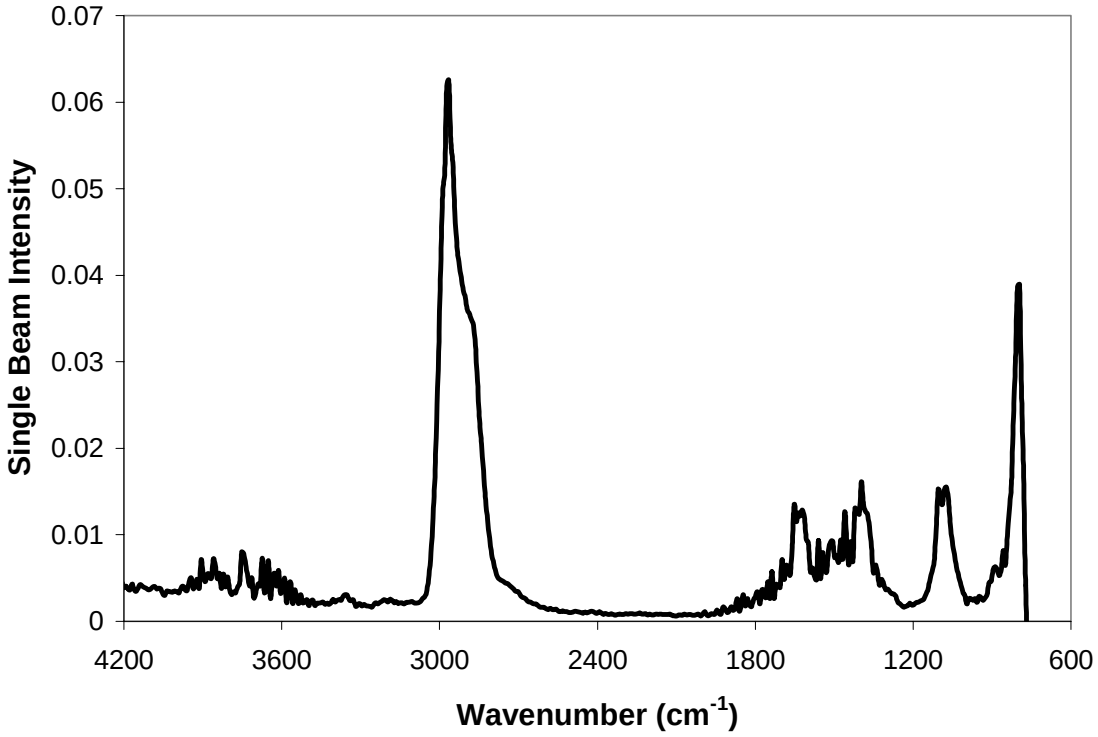

Figure 5.5: 100 ppm reference spectrum for ethylamine (T = 180 ^{0}C, path length = 500 cm)

Similarly to ethylenediamine, the large peak for ethylamine (2700 – 3050 cm^{-1}) does not show up at the same wavenumber as the unknown compound (2200 – 2400 cm^{-1}). Also, the smaller peaks at the higher wavenumbers do not match up either. Thus,

when ethylamine was added to the analysis, it showed up in very little amounts (1 – 2 ppm), and was subsequently removed from the analysis. The other two components used in the hexane extraction experiment were toluene and sulfolane, of which toluene was not present in any significant amounts and there is currently no reference spectra available for sulfolane.

The identity of the unknown compound is still undetermined at the time of writing this thesis, and from here on in this chapter will be referred to as Unknown Amine. The remainder of the chapter will serve to examine the results of the campaign; namely the PZ partial pressure results, CO_2 measurements and how they differed from the inline analyzers, and some preliminary Unknown Amine results.

5.2. EXPERIMENTAL RESULTS

This section details the important FTIR analysis results from the K_2CO_3/PZ Campaign. The components that made up the final analysis were H_2O, CO_2, N_2O, NO, NO_2, NH_3, hexane, formaldehyde, acetaldehyde, methylamine, PZ, and Unknown Amine. The main focus was on the H_2O, CO_2, NO_x, NH_3, hexane, PZ, and Unknown Amine concentrations as these were the main constituents of the gas samples. A sample spectra and analysis listing the concentrations of all components can be found in the appendix.

5.2.1. PZ Partial Pressure Results

Because of the severe lack of published PZ partial pressure data (as opposed to MEA), it was pretty unclear what level of volatility to expect under the experimental conditions. Riedel (1954) used an equation that he developed to predict the vapor pressure of PZ as a function of temperature, but the minimum temperature used in his regression was 106 ^{0}C – far from the 40 – 60 ^{0}C range observed in absorber conditions. It was noted that in some preliminary laboratory tests that the partial pressure of PZ was

measured at around 10 – 20 ppm using the stirred reactor setup for some degradation experiments at 55 ^{0}C.

Figure 5.6 below shows the trends of the PZ gas phase concentration over the course of the experiment. As mentioned previously, it was impossible to analyze for PZ at the absorber outlet due to the excess hexane present in the gas phase during the phase of the campaign corresponding to the 6.4 m K^{+}/1.6 m PZ solvent, so those data points have been thrown out. Most of the data points lie in the 0 – 15 ppm range for both inlet and outlet sample points, with the exception of the first two absorber outlet points. It is noted that when there are data points for both the absorber inlet and outlet occurring at near the same time, the PZ concentration seems to be about the same for both. An explanation for this would be the route that the gas takes after exiting the column. After the gas leaves the absorber column, it is sent to a cooler and then a knockout drum, where water (and possibly PZ) condense out. This cool, dry air is then passed through a fan. Condensate from the stripper overhead stream (which may contain PZ) is vaporized and then fed into the air stream before reaching the inlet sample point.

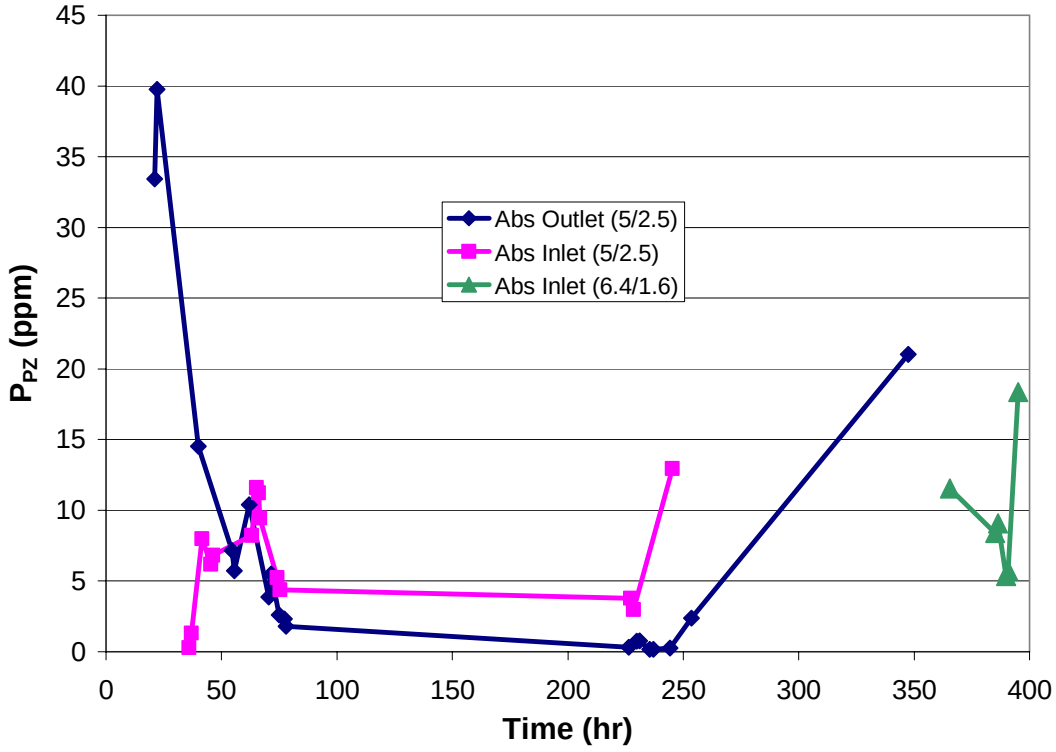

Figure 5.6: Measured PZ partial pressure (in ppm) during the course of the K_2CO_3/PZ pilot plant campaign

Hilliard (2003) regressed an electrolyte NRTL model in Aspen™ to predict vapor-liquid equilibrium data for K_2CO_3/PZ/CO_2 systems based on factors such as temperature, CO_2 loading, and solvent composition. Figures 5.7 and 5.8 below show how the partial pressure of PZ (as measured by the FTIR analyzer) compare to the PZ partial pressure as predicted by the model at the absorber outlet and inlet, respectively. Model predictions were made based upon experimental temperature and measured absorber lean loadings (taken from the data logsheet) that were entered into a flash calculation in Aspen™.

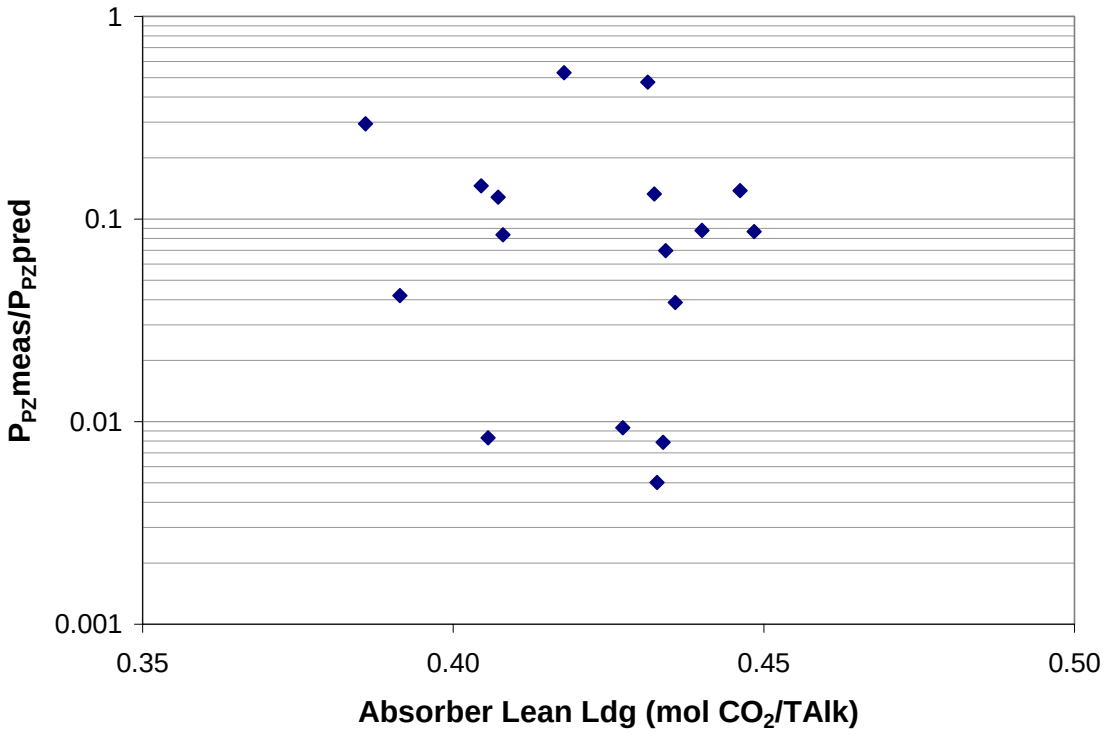

Figure 5.7: PZ partial pressure ratios at the absorber outlet sample point (5 m K^+/2.5 m PZ solvent only)

As shown in Figure 5.7 above, the measured PZ partial pressures are 2.5 to 100 times lower than the model predictions. Furthermore, there is no apparent correlation between the partial pressure ratio and absorber lean loading, which was calculated based on TOC and IC measurements of the sample solutions. This result tends to suggest that either the data are bad or that the model is not giving accurate predictions. Based on the intense method development used in the FTIR analysis, it would seem the FTIR measurements are pretty accurate, and thus maybe the model should be refined.

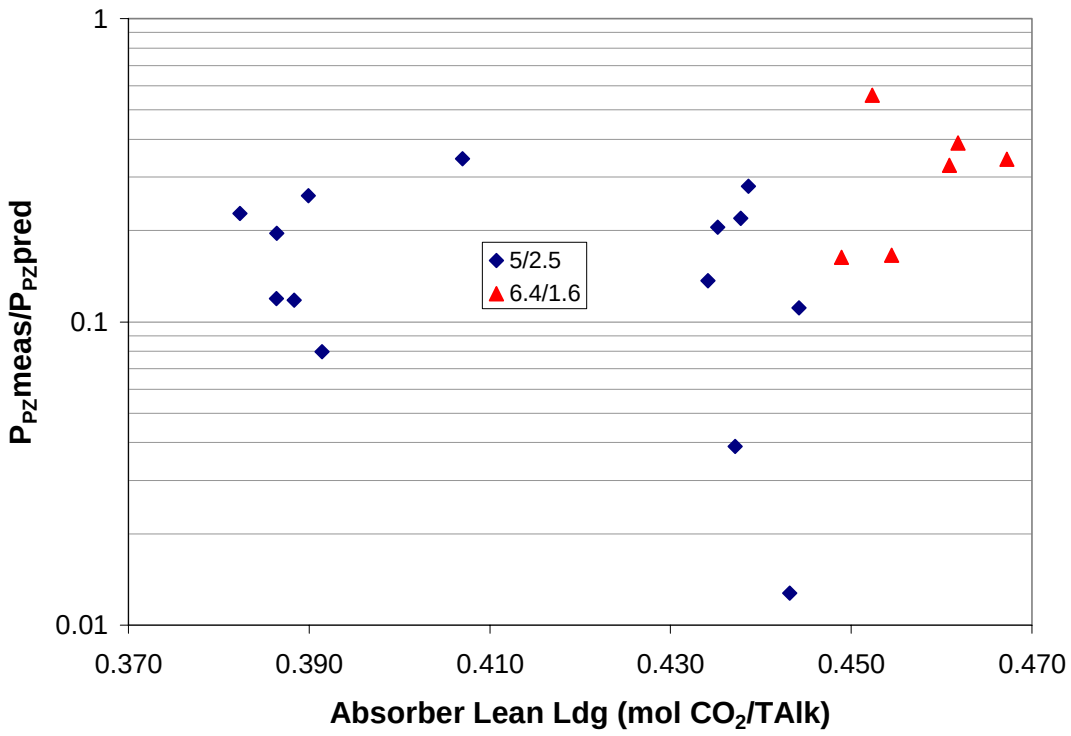

Figure 5.8: PZ partial pressure ratios at absorber inlet sample point for both solvent compositions

The partial pressure ratios at the absorber inlet sample point (Figure 5.8) exhibit some similarities as well as some differences when compared to those ratios at the absorber outlet (Figure 5.7). At the absorber inlet, it was possible to quantify PZ concentrations for some of the sample times during the second solvent composition, and thus have been included in the analysis. While the data in Figure 5.8 do have somewhat of a scatter similar to the absorber outlet data, the points appear to have a slight linear correlation with absorber lean loading (if the two outlier points at the bottom are disregarded); a result that was not seen at the absorber outlet. The measured PZ partial pressures are still significantly lower than their predicted values; with the majority a factor of 2 – 10 lower than the predicted value. Again, based on these results, PZ

appears to be significantly less volatile than model predictions, and thus if these results are indeed correct, PZ loss as a result of volatility would not be a major concern for this particular solvent.

5.2.2. CO_2 Results

As was the case in the MEA Baseline Campaign, a secondary objective for the FTIR analyzer during the K_2CO_3/PZ Campaign was to verify the measurements of the inline Vaisala and Horiba CO_2 analyzers. Additionally, the FTIR was to be the primary CO_2 measurement capability under certain experimental conditions due to the fact that these conditions were outside the ranges of the Horiba and Vaisala devices. It was quickly observed that a discrepancy existed between the measured CO_2 values between the FTIR and the Vaisala analyzers. The FTIR was consistently reading approximately 30 – 40% higher than the Vaisala analyzers when comparing samples taken at the same time, as shown in Figure 5.9. This graph shows a ratio of CO_2 partial pressures between the FTIR and Vaisala as a function of gas temperature (in ^{0}F) at the absorber inlet or outlet sample point. If these two values were identical, the ratio should be 1, but since the FTIR is consistently reading higher than the Vaisala, the ratio is greater than 1. It can also be seen that there is a greater scatter in the data at the absorber outlet points (the blue and red data points) than is seen at the absorber inlet (purple and green points). This could be due to the use of the cross-exchanger to tightly control the approach temperature at the gas inlet, which would hence dictate water composition, which may or may not have an effect on the Vaisala instruments as they are somewhat sensitive to wet gas. After much investigation, it was deduced that the Vaisalas had been mistakenly calibrated under the assumption that the calibration gas cylinders were filled on a wt% basis when in fact they were filled on a vol% basis.

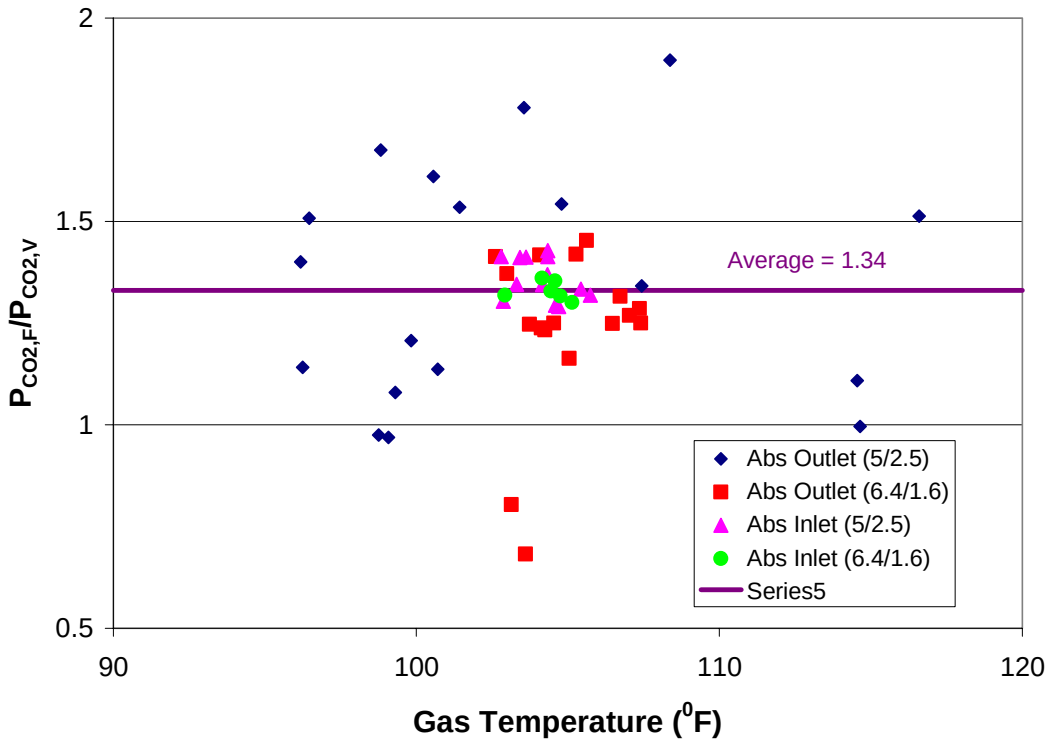

Figure 5.9: CO_2 partial pressure discrepancies between the FTIR and Vaisala as a function of gas inlet/outlet temperature (in ^{0}F)

5.2.3. H_2O Results

Since there was such a great deal of uncertainty in the actual value of the gas sample being analyzed from the MEA Baseline Campaign (due mainly to sample point location), it was imperative for this campaign to be able to say with certainty what the actual temperature was. Because H_2O is a compound that tracks well with temperature (refer to Figure 4.6) and the FTIR has the capability to measure H_2O concentrations with a great deal of precision, it is possible to use measured H_2O concentrations as an indication of temperature. The method that was used in this analysis was to plot the measured partial pressures of H_2O (as gathered by the FTIR) as a function of temperature over the time that the experiment was carried out and compare these values to partial

pressure values calculated by the DIPPR model using temperature readings from the various inline probes. Figures 5.10 and 5.11 below show the results for the absorber inlet and outlet sample points, respectively.

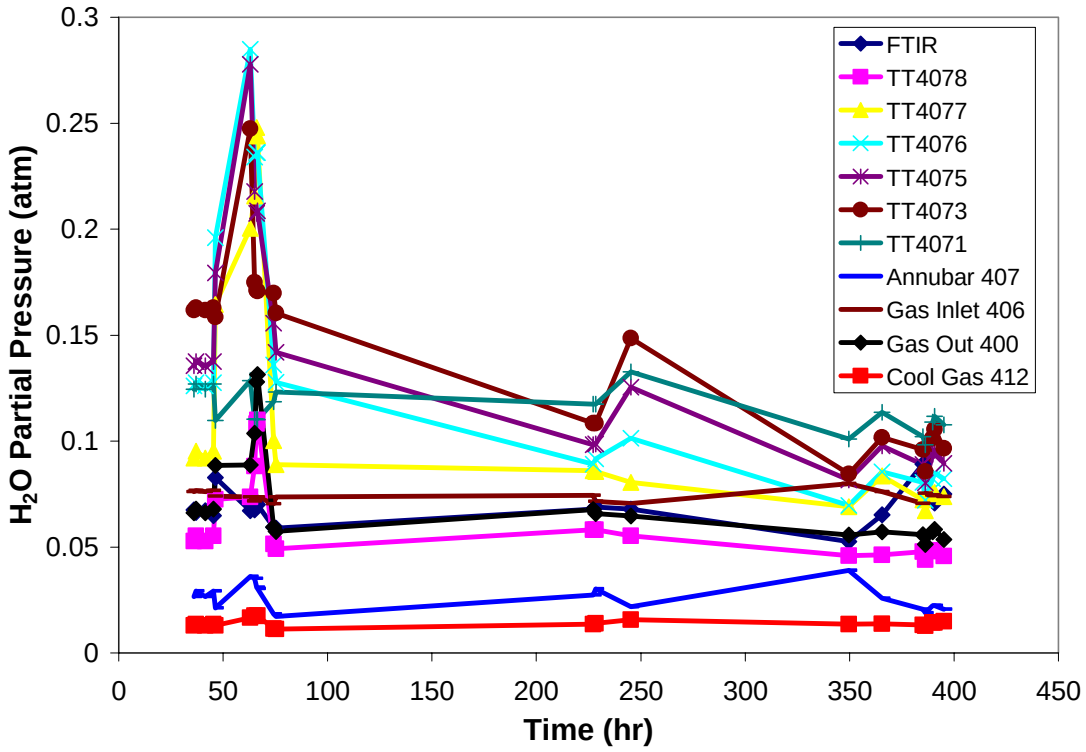

Figure 5.10. H_2O partial pressures as a function of temperature at the absorber inlet sample point

The dark blue diamond points indicate experimental measurements from the FTIR. As one can see from the graph, there are several temperature analyzers that give similar partial pressures, indicating that these points are indicative of similar temperature readings. The most interesting result is that two of the analyzers that track the inlet FTIR measurements well (TT 4078 and TT400) are located at the top of the absorber column and in the gas outlet line, respectively. That leaves the third option, TT 406, which is located in the gas inlet line after the steam injection point, and this was ultimately chosen

as the reference temperature for the absorber inlet sample point. The last point to be made about this plot is that there is a degree of uncertainty associated with these temperature measurements in that even though TT 406 does match up well with the FTIR at some points, at others there is a bit of a discrepancy and that perhaps the more representative sample temperature would be given by another probe. Figure 5.11 below shows partial pressure ratios (experimental/predicted) as a result of using TT406 as the representative temperature.

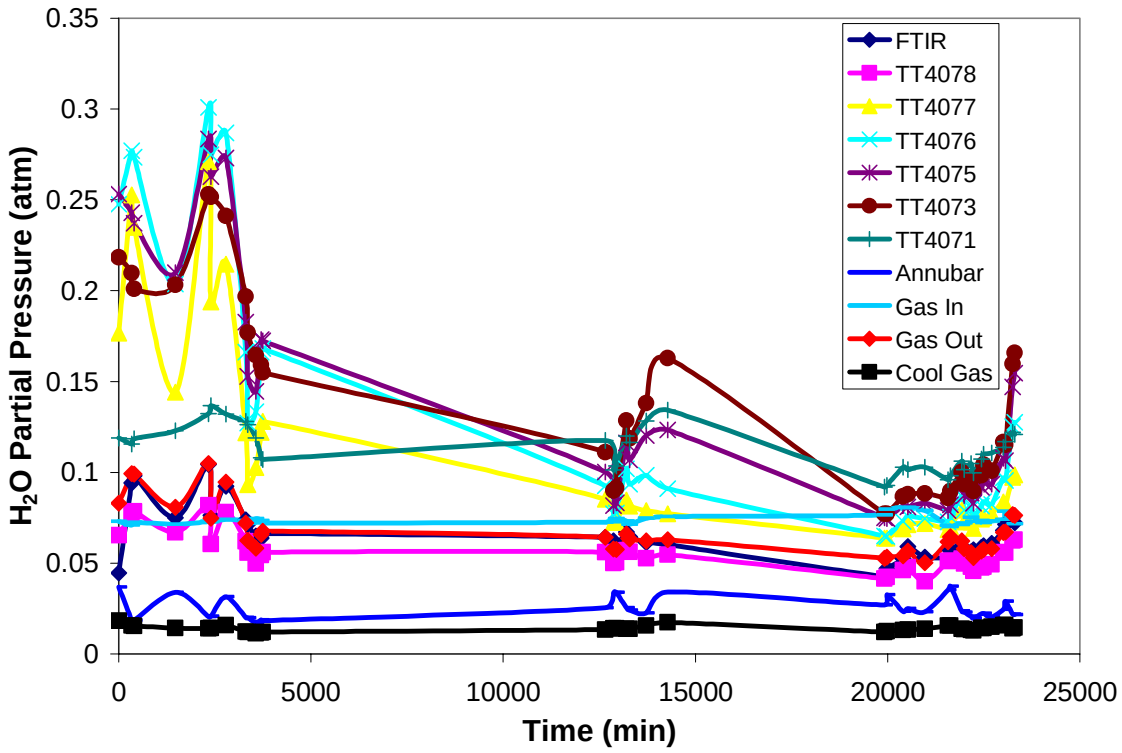

Figure 5.11. H_2O partial pressures as a function of temperature at the absorber outlet sample point

Figure 5.11 depicts H_2O partial pressures as measured by the FTIR at the absorber outlet point versus values calculated from the DIPPR model using temperatures from the various inline analyzers. The blue diamond points represent the FTIR measurements, and

from the figure above, it can be seen that there are two analyzers that appear to be very similar in temperature to the FTIR because they are giving near the same H_2O partial pressure. These two sensors, TT4078 and TT400, are located at the top of the absorber column, right above the top of the packing and in the gas outlet line, respectively. Because these two instruments read so close to each other and the FTIR, it is concluded that the sample temperature must be nearly the same between the top of the packing and the absorber outlet sample point. As a result, the temperature readings from the TT 400 instrument were chosen as representative gas sample temperatures, although it would not have been incorrect to use values from the TT4078 (as was done in the previous MEA Baseline Campaign). Figure 5.12 below gives H_2O partial pressure ratios (experimental/predicted) that were calculated for both the absorber inlet and outlet sample points using the two selected inline temperature analyzers. It can be seen that that temperature measurements at the absorber outlet are slightly more consistent with that of the FTIR as the ratios are nearer to 1. Even though the temperature measurements at the absorber inlet sample point are not as close to 1 as at the outlet, there is still approximately only 6% error, which is a reasonable number. The absorber inlet data have more scatter because this particular temperature sensor was right near the steam injection, so some mixing effects may be the explanation. Secondly, there's not as big of a range of temperature for the absorber inlet data as that is one of the control variables that the operators use to manipulate the system, and it was set to a nominal value with a stricter confidence interval than compared to the absorber outlet temperature.

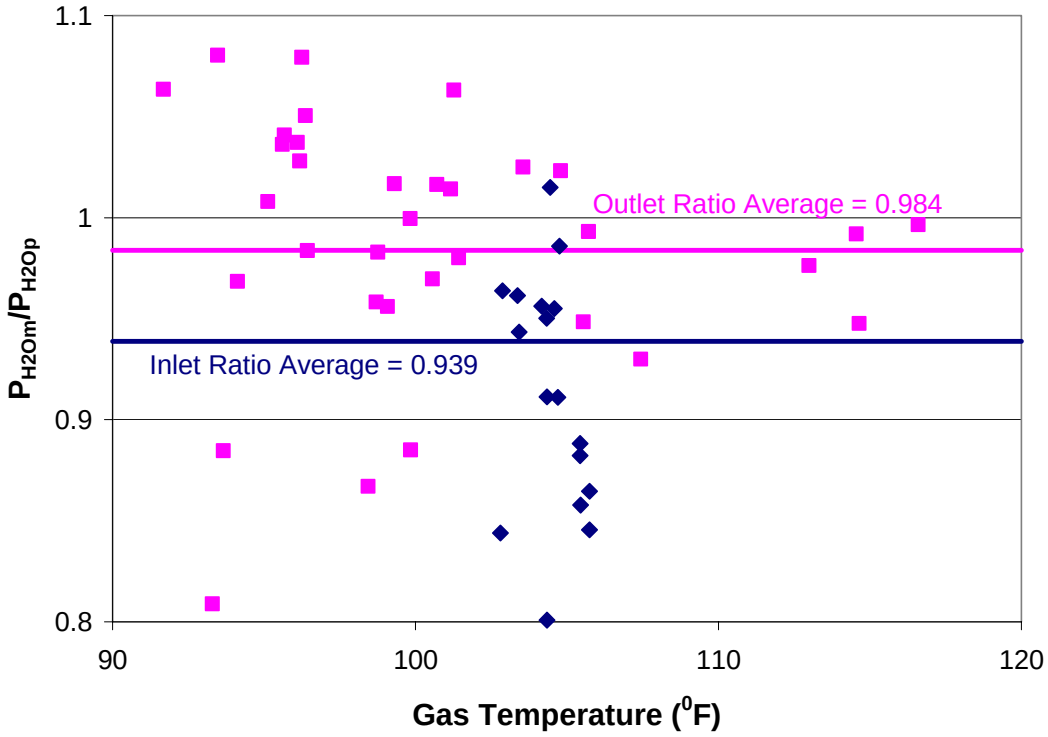

Figure 5.12. H_2O partial pressure ratios (experimental/predicted) for absorber inlet and outlet sample points as a function of gas temperature

5.3. CONCLUSIONS AND RECOMMENDATIONS

On the whole, the experimental method for this particular campaign was so much more successful than the one associated with the MEA Baseline Campaign. The superior design of sample probes for this campaign coupled with the better choice of sample point locations seem to give much more reliable results since it was easier to match the gas sample temperature with one of the inline thermocouples and not have to worry about samples cooling and condensing before getting into the heated lines. Secondly, locating all the analyzer equipment indoors in a controlled environment led to less downtime associated with re-calibration of the FTIR (associated with changes in ambient temperature) and thus allowed more time to be devoted to recording data. This setup

seemed to be convenient to operate and is the recommended setup for any more experiments of this nature.

It would be helpful to know beforehand when running these types of experiments if and when any other types of experiments were ran using the pilot plant facility so that these components can be added to the analysis. This would cause less anxiety in worrying that a potentially harmful component (NO_x in this particular case) is showing up in dangerous levels when in fact it is not. Furthermore, adding all of the correct components to the analysis from the start would decrease time refining the analysis method after the experiment is completed, which was the determining factor in the amount of time it took to gather results.

The precision of the results presented in this chapter are limited by two factors: the large presence of hexane (especially during the second solvent composition) and the presence of the Unknown Amine. Because the PZ levels were consistently in the 10 – 20 ppm range, it would be hard to gain any more precision since the peaks used in the analysis are buried in the enormous hexane peaks in the sample spectra. In a perfect experiment, the hexane would not have been present, but since this facility is meant to simulate industrial conditions, experimental conditions are far from perfect and thus it is impossible to analyze for PZ at some sample times. The Unknown Amine looks similar to ethylenediamine and ethylamine in terms of reference spectra, but does not match up completely, and thus the Unknown is neither of these components. As of this work's publication, its identity was still undetermined, but there are other ways to determine possible identities of the Unknown, such as IC chromatography. Once the Unknown Amine's identity is positively determined, it would just be a matter of generating a reference file (if one if not already available) and adding this reference to the analysis method to determine actual concentrations.

The PZ concentrations that were able to be measured showed very low residuals (less than 0.01) for both the absorber inlet and outlet sample points, and since the analysis method has been vigorously refined, it is speculated that these results are accurate. If this assumption is indeed true, it appears that PZ was not nearly as volatile as predicted by models, and thus PZ loss due to volatility would not be a major concern. It would be necessary to generate more data in a controlled laboratory setting with both of these solvents over a representative range of CO_2 loadings to completely validate these initial results and to improve model performance.

As was the case in the MEA Baseline Campaign, the FTIR gas analyzer proved to be a very capable alternative in determining CO_2 levels at a given point in the facility. In fact, it may be even more useful than the Horibas and Vaisalas in that it can measure wet gas and would eliminate the need for a cooler and water knockout. This would provide operators with real-time measurements of not only CO_2 but also water concentration in the gas phase which they currently do not have. The most logical explanation for why the FTIR consistently read higher than the Vaisalas was that the Vaisalas were calibrated incorrectly on a wt% basis when in fact the calibration gas cylinders were filled on a vol% basis. This hypothesis was verified by using the Vaisalas to measure a third CO_2 cylinder and comparing the results to measurements from a gas chromatograph.

Finally, temperature measurements were verified by using H_2O partial pressure calculations as a function of the temperature given by the various inline analyzers. As a result, the absorber inlet gas sample temperature was given by TT 406 and the absorber outlet gas sample temperature by TT 400 (although TT4078 could also have been used). To verify the validity of this method, the actual H_2O partial pressure value measured by the FTIR was compared to a H_2O partial pressure calculated by the DIPPR model as a function of the analyzers' temperature readings at each sample time. As a result, the

average absorber inlet partial pressure ratio was approximately 0.94 while the ratio at the absorber outlet was better than 0.98.

Chapter 6: Laboratory Partial Pressure Results and Binary NRTL Modeling

The focus of this chapter is to present the gas partial pressure and subsequent amine volatility results obtained from experiments carried out in the stirred reactor setup detailed in Chapter 3. This chapter will be broken up into 3 major sections; each detailing the results of the three different systems that were studied (MEA-H_2O, PZ-H_2O, and MEA-PZ-H_2O). Once the results are presented, the second part of each section will detail how the results were used in generating NRTL binary interaction parameters in Aspen™ to predict activity coefficients.

6.1. NRTL MODEL

The choice of model for this work was the Nonrandom Two Liquid (NRTL) model. Specifically, the NRTL model is an excess Gibbs energy function and is used to predict activity coefficients for a binary system. The excess Gibbs energy function can be represented as:

$$\frac{G^{ex}}{RT} = x_1 x_2 \left(\frac{\tau_{21} G_{21}}{x_1 + x_2 G_{21}} + \frac{\tau_{12} G_{12}}{x_2 + x_1 G_{12}} \right) \tag{6.1}$$

Where i and j are the species indexes (1: H_2O and 2: amine), x_i is the liquid mole fraction of component i, τ_{ij} is the binary interaction parameter between component i and j, α_{ij} is the molecule-molecule nonrandomness factor (set at 0.2), $G_{12} = \exp(-\alpha_{12}\tau_{12})$, and $G_{21} = \exp(-\alpha_{21}\tau_{21})$.

The binary interaction parameters were assumed to be temperature dependent, and fitted in the following way:

$$\tau_{12} = A_{12} + \frac{B_{12}}{T} \tag{6.2}$$

$$\tau_{21} = A_{21} + \frac{B_{21}}{T} \tag{6.3}$$

Equation 6.4 below shows that by taking the appropriate derivative (with respect to component *i* or *j*) of Equation 6.1, it is possible to determine the activity coefficient of component *i* or *j* (Equation 6.5).

$$\ln \gamma_i = \left[\frac{\partial \left(nG^{ex} / RT \right)}{\partial n_i} \right] \tag{6.4}$$

$$\ln \gamma_2 = x_1^2 \left[\tau_{12} \left(\frac{G_{12}}{x_2 + x_1 G_{12}} \right)^2 + \frac{\tau_{21} G_{21}}{(x_1 + x_2 G_{21})^2} \right] \tag{6.5}$$

After all experimental data was tabulated, it was first regressed in Aspen™ using the method outlined above to fit the binary interaction parameters using all 4 contributions: A_{ij}, B_{ij}, A_{ji}, and B_{ji}. This model was called the full model because it used all 4 parameters to obtain τ_{12} and τ_{21}.

The next step after obtaining values for the binary interaction parameters using the full model was to use different sub models to determine their values and compare the results to the full model. The purpose of using sub models was to determine if simpler forms of the binary interaction parameters could capture the same behavior as the full model. The first case was to delete the B_{12} parameter and regress the binary interaction parameters with just A_{12}, A_{21}, and B_{21}. The second sub model regressed the binary interaction parameters while excluding the B_{21} parameter, and the third sub model regressed the binary interaction parameters by using only A_{12} and A_{21} parameters.

The parameters and corresponding standard deviations for each sub model were compared to that of the full model, and the sub model with the lowest weighted sum of squares was chosen to as a starting point for further regression. This process was repeated until the entire system could be modeled by only one parameter, and afterwards all sub model cases were ranked based on logic test and correlation criteria. The logic test criterion was that the standard deviation of the parameter had to be less than the estimate itself, and the correlation criterion was that any two parameters that had a

correlation coefficient between them of greater than ± 0.9 were said to have no correlation. The third factor that was used to rank the sub models was the weighted sum of squares for each sub model and the percentage deviation as compared to the weighted sum of squares average associated with the full model.

6.2. MEA-H_2O EXPERIMENTAL RESULTS

The gas partial pressures for MEA and H_2O were measured for the binary system at 4 different concentrations: pure MEA, 23.8 m MEA (x_{MEA} = 0.3), 7 m MEA (x_{MEA} = 0.112), and 3.5 m MEA (x_{MEA} = 0.0593). Each of these solutions were measured at 35, 45, 55, and 65 ^{0}C, and the results (see Table 6.1) were compared to the pure liquid vapor pressure as predicted by the DIPPR model, which is in the form given in Equation 6.6 below.

$$P_X^{sat} = A + \frac{B}{T} + C\ln(T) + DT^E \tag{6.6}$$

Where P_X^{sat} is in Pa and T is in K. Table 6.2 below gives the values for the DIPPR coefficients.

Table 6.1. Measured vapor pressures for MEA-H_2O system

Date	Composition	T (^oC)	MEA (ppm)	H_2O (vol%)	Total P (kPa
3/2/2006	Pure MEA	50.61	2972	0	107
3/3/2006		58.03	4376	0	108.6
3/24/2006		38.79	1371	0	116.6
3/24/2006		45.78	2165	0	116.4
3/24/2006		53.92	3676	0	116.2
3/23/2006	23.8 m MEA	42.77	239	4.78	114.6
3/23/2006		49.95	441	6.6	115.3
3/23/2006		53.87	602	8.15	115.3
3/23/2006		61.69	1387	11.96	115.5
3/10/2006	7 m MEA	72.7	800	29.43	125.3
3/14/2006		64.7	445	20.45	117.8
3/22/2006		42.1	57	6.55	114.8
3/22/2006		49.3	115	9.23	114.8
3/22/2006		52.8	163	10.99	114.6
3/22/2006		56.8	209	13.02	114.8
3/22/2006		61.4	282	15.28	115.1
3/15/2006	3.5 m MEA	45.95	58	8.65	113.7
3/15/2006		51.21	100	11.79	113.5
3/15/2006		58.87	169	16.61	113.5
3/15/2006		65.29	240	20.95	113.6
3/21/2006		42.70	37	6.82	115.4
3/21/2006		49.40	73	9.74	115.6
3/21/2006		56.31	140	13.62	116.2
3/21/2006		65.47	227	19.83	117.8

Table 6.2. Values for coefficients used in DIPPR model for amine-water systems

$$P_X^{sat}(Pa) = A + \frac{B}{T(K)} + C\ln(T) + DT^E$$

Component	A	B	C	D	E	Min T (K)	Max T (K)
Water	73.649	-7258.2	-7.3037	4.17E-06	2	273.16	647.13
MEA	92.624	-10367	-9.4699	1.90E-18	6	283.65	678.2
PZ	70.503	-7914.5	-6.6461	5.21E-18	6	379.15	638

The results from all four MEA-H_2O solvent compositions can be seen below in Figure 6.1 over the entire temperature range where the single points represent

experimental data and the solid lines are predictions from the NRTL sub model 33 (explained in detail later in this chapter) based on temperature and solvent composition. It can be seen that the points compare very favorably to the NRTL predictions, especially the numerous points at 3.5 m and 7 m MEA solutions that were acquired on different days. The NRTL model has an error of approximately 10%, as opposed to the 2% error associated with the FTIR analyzer. This means that the vast majority of the points are within the model's range of accuracy.

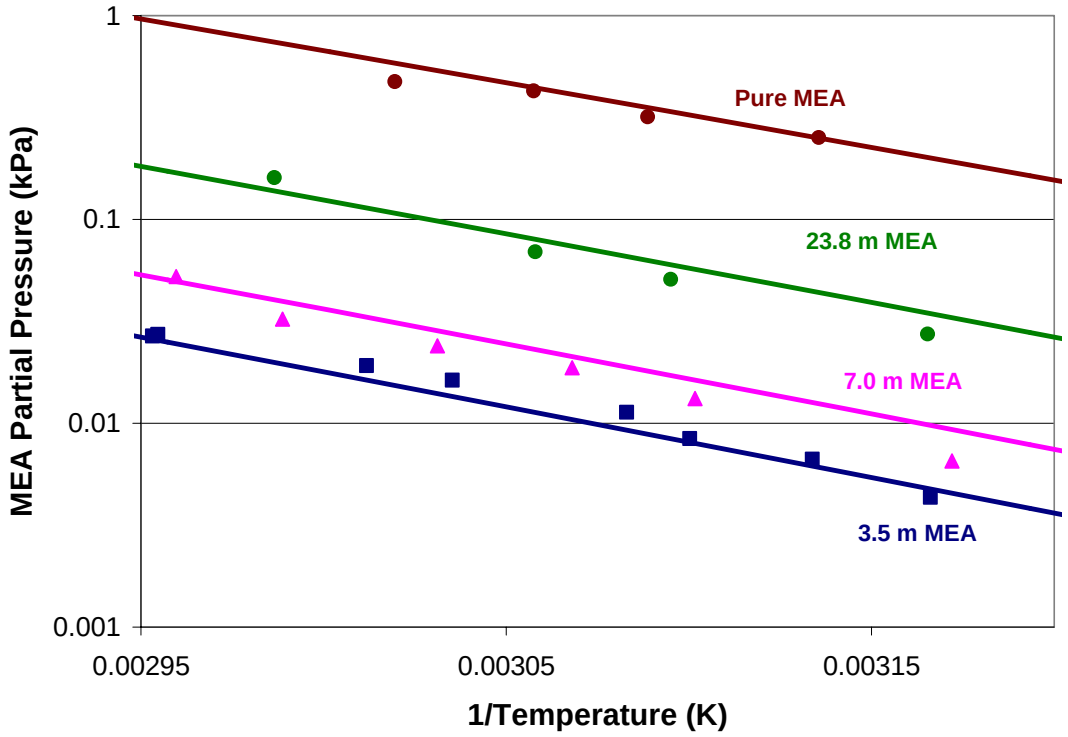

Figure 6.1. Experimental MEA equilibrium partial pressure points and curves predicted by NRTL sub model 33

Once the MEA partial pressure data was tabulated, it was possible to determine activity coefficients for each system based on the measured partial pressure, calculated DIPPR saturation pressure (as a function of experimental temperature), and MEA liquid

mole fraction. Figure 6.2 below is a plot of the experimental MEA activity coefficients (points) and activity coefficients predicted by the NRTL sub model 33 binary interaction parameters (solid lines). The scatter in the data reflects the uncertainty associated with the FTIR measurements as there are a few measurements that reflect the model predictions while others at the same solvent composition are not quite as accurate.

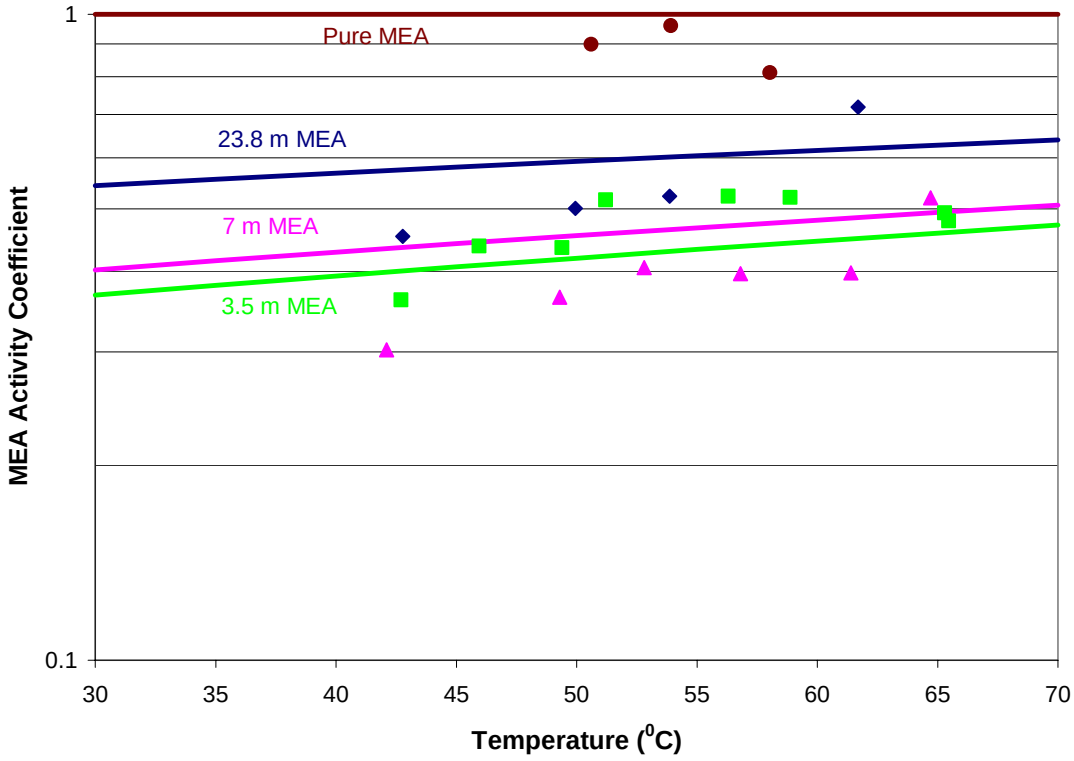

Figure 6.2. MEA activity coefficients for MEA-H_2O, curves predicted by NRTL sub model 33

Figure 6.3 below shows the water activity data from these experiments. The error bars on the experimental data points represent the 2% error associated with the FTIR analyzer equipment. The solid lines are NRTL predictions, which have about a 10% error associated with them. Recall from Chapter 1 that activity coefficients are derived from modified Raoult's Law, and by dividing both sides of Equation 1.1 by P_i^{sat}, the ratio

of P_i/P_i^{sat} is known as the activity, which in theory should be independent of temperature. The data for pure H_2O, 3.5 m MEA (x_{H2O} = 0.9407), and 7.0 m MEA (x_{H2O} = 0.888) seem to fit a straight line, and thus suggest that their activity is indeed temperature independent. The same cannot be said for the 23.8 m MEA (x_{H2O} = 0.7) solution. Because its prediction curve and data are not flat over this temperature range, it appears that the activity of water in this solution has some temperature dependence. Thus it appears that below some nominal value for x_{H2O}, the solution activity displays a temperature effect that should be accounted for in models.

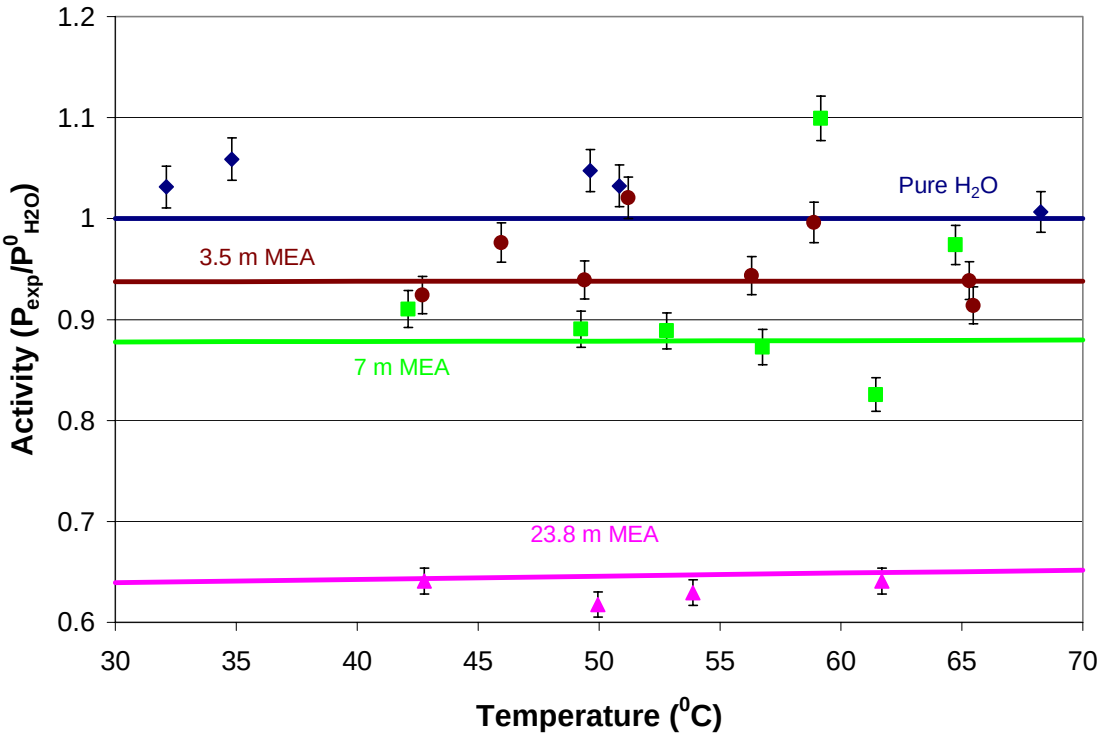

Figure 6.3. Water activity data for MEA-H_2O system for all four concentrations as a function of temperature

One final interesting result of this particular system is its relative volatility. Relative volatility is defined as the ratio between the equilibrium constants (i.e., K-

values) in the system, which would be water and MEA, respectively, in this case. A K-value is simply the ratio of the equilibrium vapor mole fraction to the equilibrium liquid mole fraction (y/x). Figure 6.4 below, however, shows that the 7 m MEA solution actually has a higher relative volatility than the 3.5 m MEA solution, which is quite unexpected.

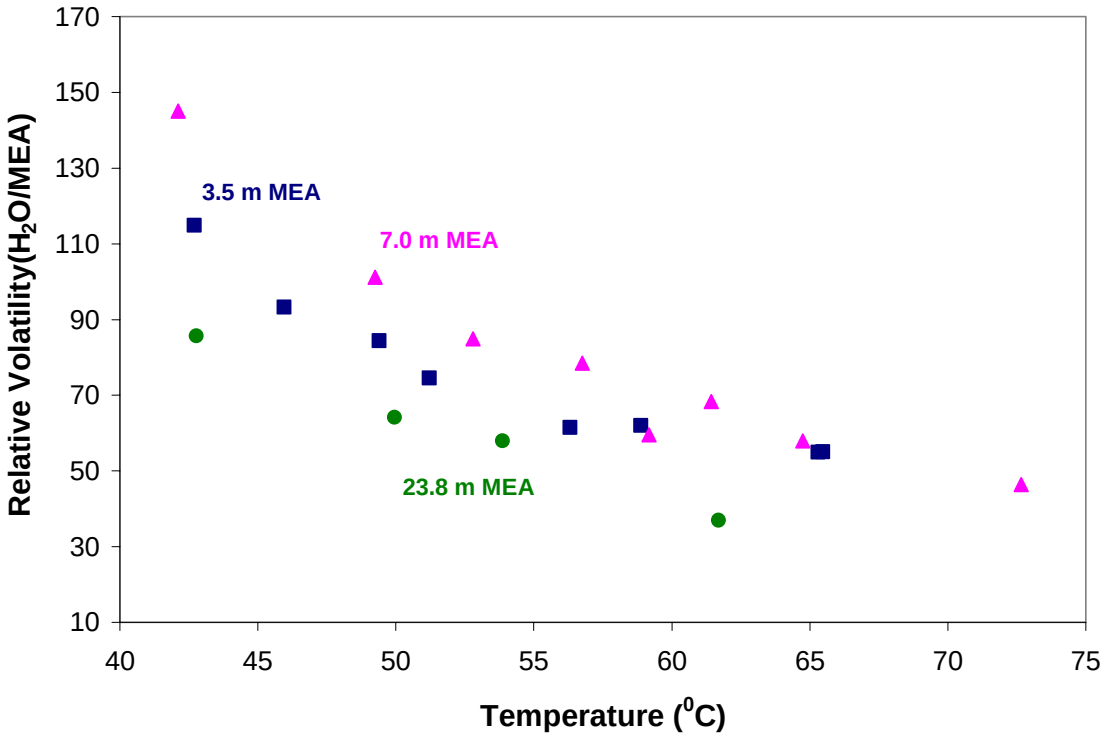

Figure 6.4. Relative volatility of MEA-H_2O

6.3. PZ-H_2O Experimental Results

As was shown in Chapter 2, there is not much partial pressure data for PZ-H_2O systems available at this time as compared to MEA-H_2O systems. Because of this lack of data, the DIPPR parameters used to calculate PZ vapor pressures have been regressed using predicted vapor pressure values by Riedel (1954). Additionally, the minimum

temperature used in Riedel's predictions was 106 ^{0}C, which is far outside the temperature range of interest for this work. Therefore, all PZ saturation pressures calculated using the DIPPR parameters for this work were done so under the assumption that these parameters extrapolate reasonably well to the lower temperature range that this work is exploring.

The experimental data are given below in Table 6.3, and Figure 6.5 shows how the measured partial pressure of PZ (points) compared to the NRTL sub model predictions from the Aspen™ regressions (solid curves). As evidenced by the graph, the measured partial pressures of PZ have about a range of error from 5 – 23% over the four compositions measured when compared to the model predictions.

Table 6.3. Measured vapor pressures for PZ – H_2O system

Date	Composition	T (^{o}C)	PZ (ppm)	H_2O (%vol)	Total P (kPa)
4/3/2006	0.9 m PZ	35.95	4.9	6.04	113.8
4/3/2006		44.29	12.8	9.47	113.9
4/3/2006		52.77	21.5	13.94	113.9
4/3/2006		63.41	54.3	22.16	114.3
4/5/2006	1.8 m PZ	36.18	11.0	5.93	112.7
4/5/2006		44.43	21.1	9.20	112.4
4/5/2006		52.83	43.6	13.62	112.3
4/5/2006		60.40	76.2	19.50	112.2
4/6/2006	2.5 m PZ	32.72	16.2	6.24	113.9
4/6/2006		39.70	30.3	9.25	114.3
4/6/2006		52.92	73.0	16.85	114
4/6/2006		61.01	125.4	23.42	115.6
4/7/2006	3.6 m PZ	34.66	19.6	5.76	114.9
4/7/2006		45.08	47.7	10.09	115.3
4/7/2006		53.22	89.6	14.78	116.9
4/7/2006		61.16	158.2	21.1	114.6

One important result from Figure 6.6 is that this particular set of NRTL sub model parameters did a much better job of predicting PZ volatility for the PZ – H2O system than the K_2CO_3/PZ/CO_2 model used for pilot plant data analysis (see Chapter 5). From the raw data shown in Table 6.3, any PZ solvent composition in this range would not

have adverse economic effects below about 40 ^{0}C as the volatility is less than the 40 ppm threshold calculated in Chapter 1. Therefore, these data suggest that a PZ –H_2O solvent may be economically viable for CO_2 capture at absorber temperatures up to approximately 40 ^{0}C.

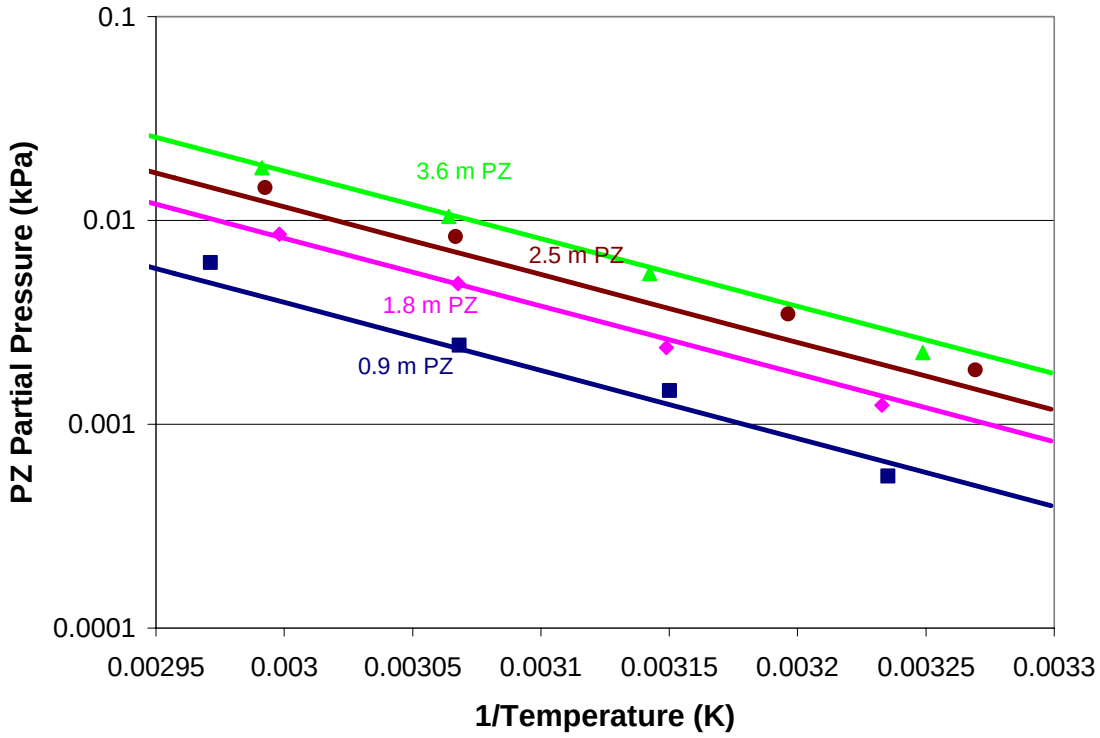

Figure 6.5. PZ equilibrium partial pressure over PZ/water, curves predicted by NRTL sub model 33

After the experimental data had been tabulated and the NRTL sub model binary interaction parameters regressed, it was possible to calculate PZ activity coefficients. Figure 6.6 plots experimentally calculated (points) and predicted values (solid curves) as given by the final NRTL sub model. These activity coefficients do not show the same agreement as the values for MEA discussed previously, and the reason for this is presumed to be the uncertainty dealing with the pure component vapor pressures

calculated for PZ by the DIPPR equation. Perhaps the most important result that can be gained from this plot is that even though some discrepancy exists between experimental and predicted values, PZ remains a fairly non-volatile compound and thus PZ loss through volatility is not significant over these composition and temperature ranges.

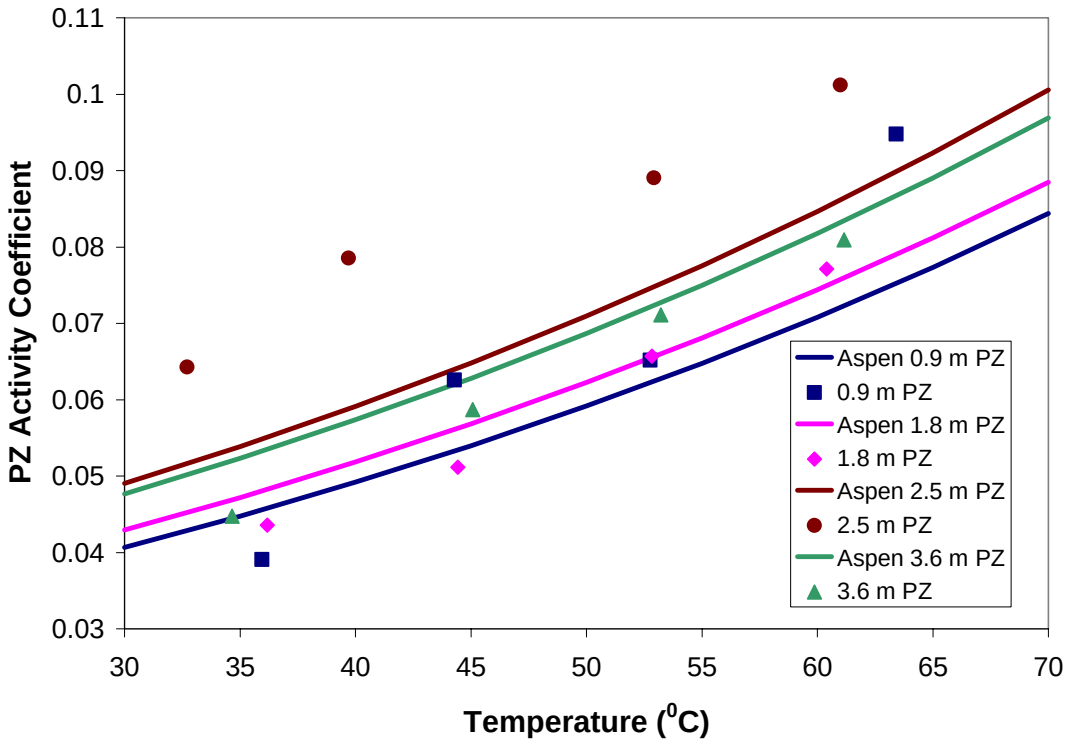

Figure 6.6. Measured and predicted PZ activity coefficients as a function of temperature

The H_2O activity data are plotted in Figure 6.7 below. The error bars on the experimental data represent the 2% error range associated with the FTIR. The experimental data in this case do not share the same agreement with the model predictions as the H_2O activity data associated with the MEA – H_2O system. In fact, the error associated with these measurements is in the 10 – 15% range for every composition except for the 2.5 m PZ, which was the anomaly above as well. The error for this

particular solvent was in the 35 – 45% range for the experimentally measured activities when compared to the software predictions. Another important trend to notice is that none of the experimental activities display the temperature independence as suggested by the software predictions. The experimental measurements seem to vary somewhat with temperature, as they follow some curve that is anything but flat.

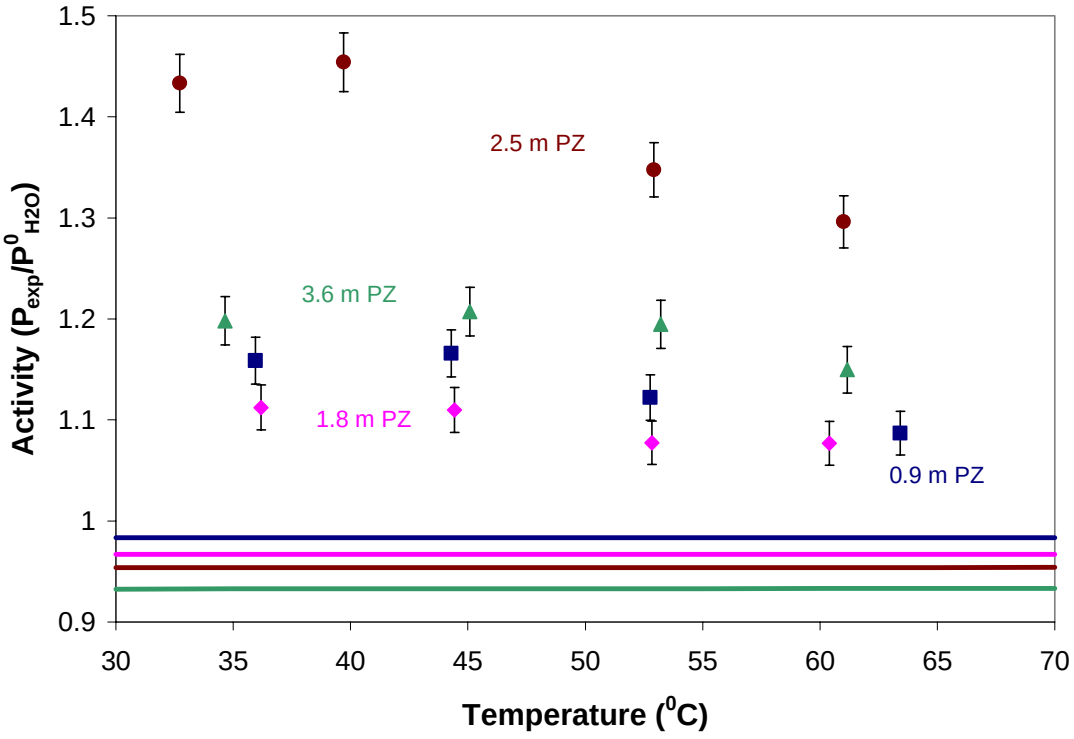

Figure 6.7. Measured and predicted H_2O activities as a function of temperature for the PZ-H_2O system

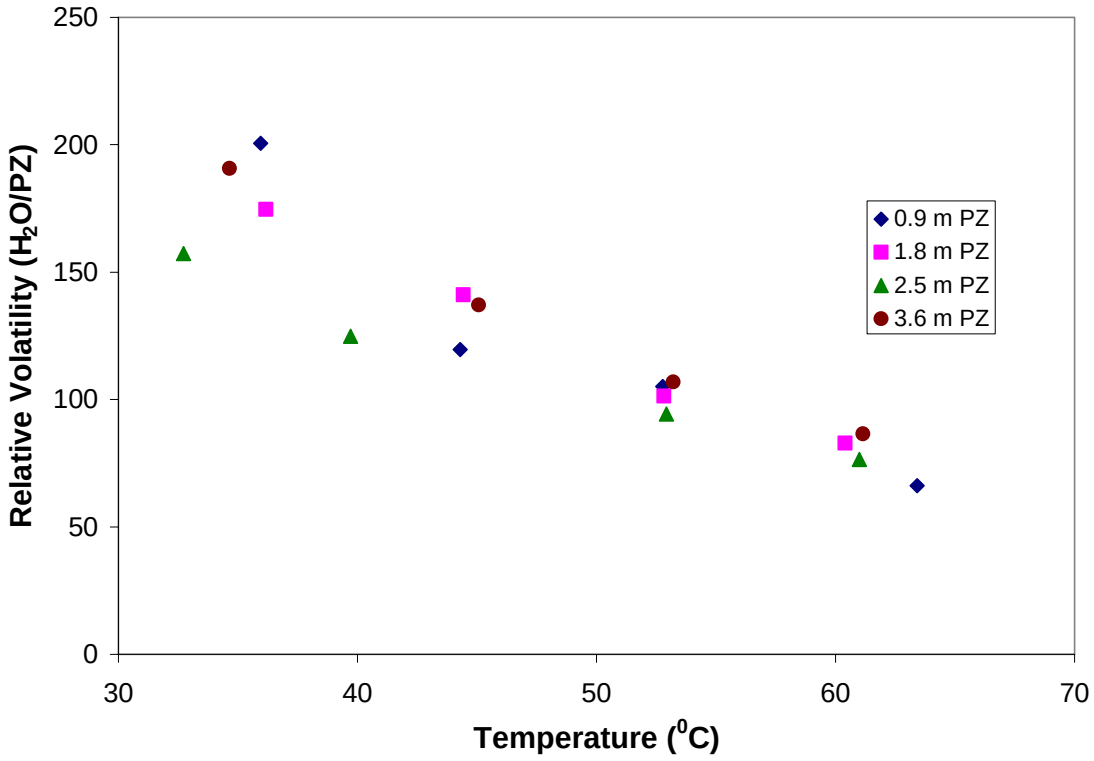

Figure 6.8. Relative volatility for H_2O-PZ

Figure 6.8 shows the experimental relative volatility for the H_2O-PZ system. With the exception of the two outlier points at the lower temperatures for the 2.5 m PZ solution, it appears all the data are tightly clustered and follow the same downward curve trend. This suggests that possibly those two points for the 2.5 m PZ solution could possibly be bad data points. Furthermore, the data appear to have less scatter at the higher temperatures, possibly implying more reproducibility in these measurements than in the lower temperatures.

6.4. MEA-PZ-H_2O Experimental Results

Now that the results of the separate MEA-H_2O and PZ-H_2O systems have been reported, it was important to gather partial pressure data for the ternary MEA-PZ-H_2O

blended amine system to see how the two amines interacted with one another. Table 6.4 summarizes the results of the experiments.

Table 6.4. Measured vapor pressures for the MEA-PZ-H_2O system

Date	Composition	T (^{0}C)	MEA (ppm)	PZ (ppm)	H_2O (vol%)	Total P (kPa)
4/10/2006	3.5 m MEA/1.8 m PZ	37.32	24.7	14.1	5.56	115
4/10/2006		44.93	46.2	20.2	8.61	115.2
4/10/2006		52.65	89.9	43.8	12.89	115.4
4/10/2006		60.36	161.1	70.3	18.48	116.4
4/11/2006	3.5 m MEA/3.6 m PZ	37.24	26.4	21.8	5.32	113.3
4/11/2006		44.78	49.6	48.3	8.08	113.3
4/11/2006		53.44	98.0	74.4	12.35	113.2
4/11/2006		60.32	189.4	153.7	17.82	113.1
4/12/2006	7 m MEA/1.8 m PZ	36.82	49.3	10.5	5.19	114.1
4/12/2006		44.47	98.3	23.6	7.92	114.2
4/12/2006		53.73	179.7	47.9	12.04	114.2
4/12/2006		61.45	334.6	71.5	17.54	114.3
4/13/2006	7 m MEA/3.6 m PZ	35.78	49.8	21.4	4.92	115.8
4/13/2006		44.52	107.6	46.9	7.50	116
4/13/2006		53.04	196.3	86.8	11.46	116.4
4/13/2006		60.69	364.4	168.6	16.65	117.6

In comparing the above data to the experimental results for the MEA-H_2O and PZ-H_2O systems, it is apparent that the MEA concentrations are higher at the same temperature for the same molality while the PZ are approximately the same. Thus, in a blended system it would appear that PZ loss through volatility would not be a concern as much as MEA volatility. PZ volatility would become important at above 40 ^{0}C for the two 3.6 m PZ blend solvents as the concentrations here are above the 40 ppm economic threshold from Chapter 1.

Figure 6.9 below is a plot of MEA partial pressures as a function of temperature for all four solvent compositions studied (refer to Table 6.4). Each solvent pair corresponding to similar MEA concentrations (i.e., 3.5 m MEA and 7 m MEA blends) have approximately the same partial pressures at the same temperature, and the additional PZ tends to drive the MEA partial pressure down slightly as evidenced by the graph.

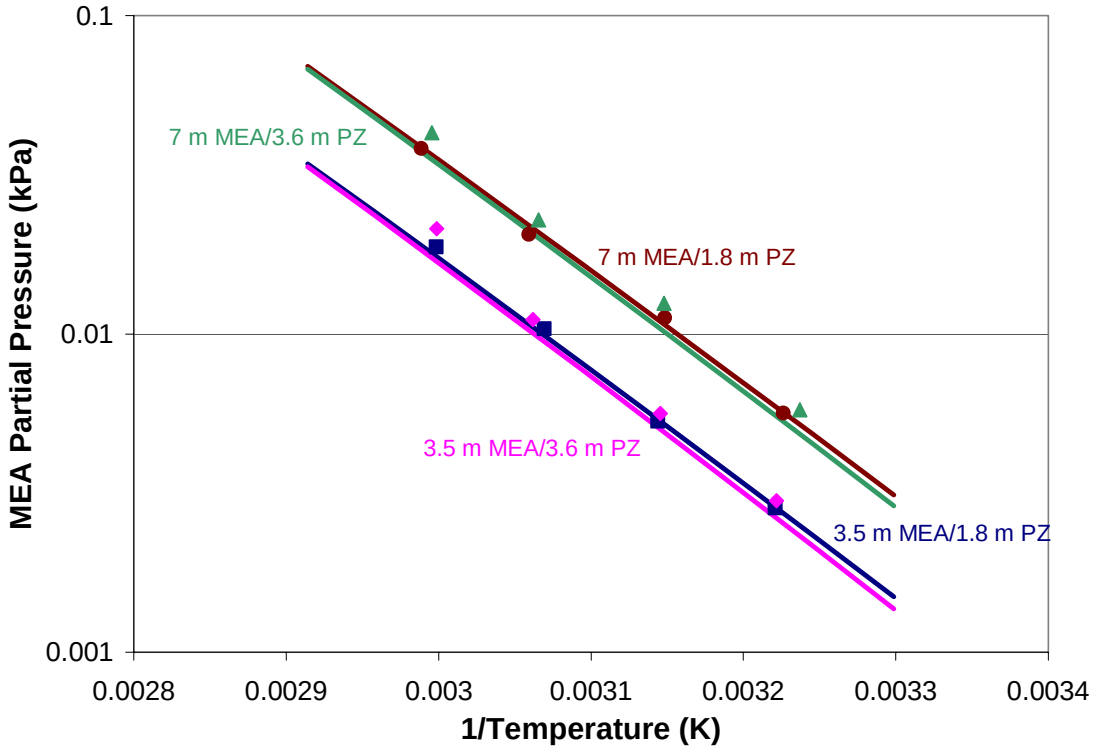

Figure 6.9. Experimental and predicted MEA partial pressures as a function of temperature for MEA-PZ-H_2O systems

It can be seen that the NRTL parameter regression using the entire set of experimental data does a very good job of predicting partial pressures that mirror actual experimental results. In fact, over this temperature range, the error was only 19% at the highest point, which was the 7 m MEA/3.6 m PZ solution. Two of the other solvent compositions (3.5 m MEA/1.8 m PZ and 7 m MEA/1.8 m PZ) had errors in the 3% range, which looks to be attributable to the lower PZ concentrations. The remaining 3.5 m MEA/3.6 m PZ solvent had an average error of about 15% compared to the NRTL predictions.

The NRTL also accurately predicted the PZ partial pressures, which can be seen below in Figure 6.10.

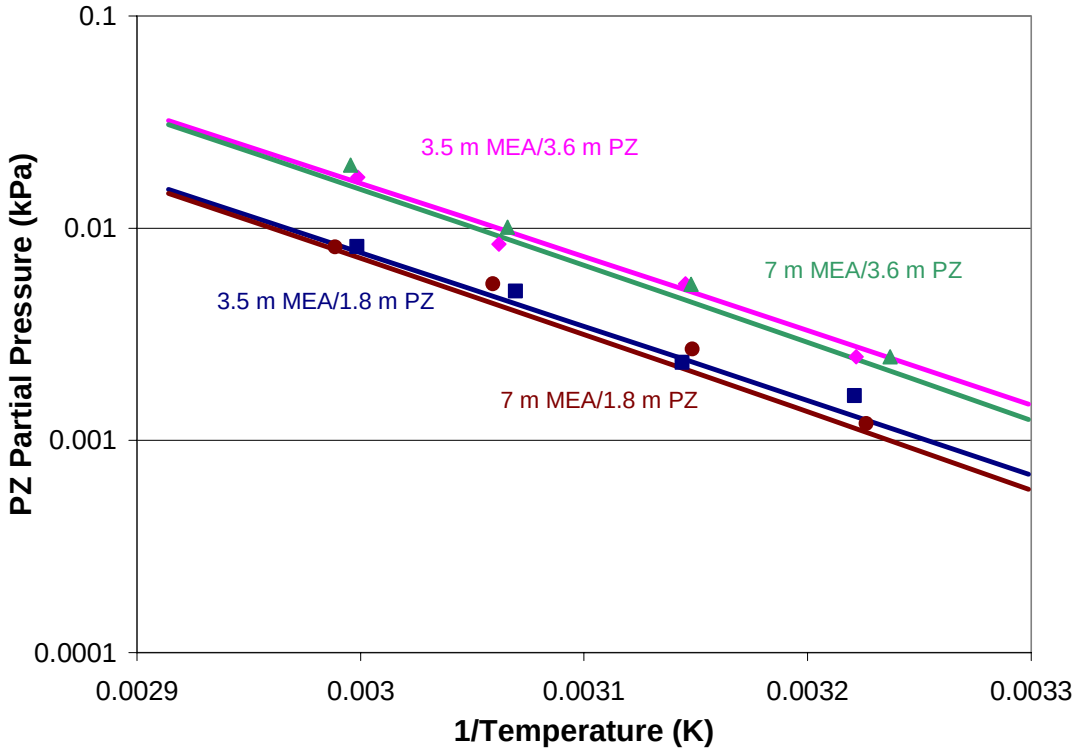

Figure 6.10. Measured and predicted PZ partial pressures as a function of temperature for the MEA-PZ-H_2O system

While not quite as precise as the MEA measurements, the predicted PZ partial pressures were off by an average of 10% for the two solutions at the lower MEA concentration, but the two 7 m MEA blend solvents showed an error of 15 – 20% in the PZ partial pressure predictions. This is a significant improvement to the K_2CO_3/PZ pilot plant data which exhibited a large percentage error.

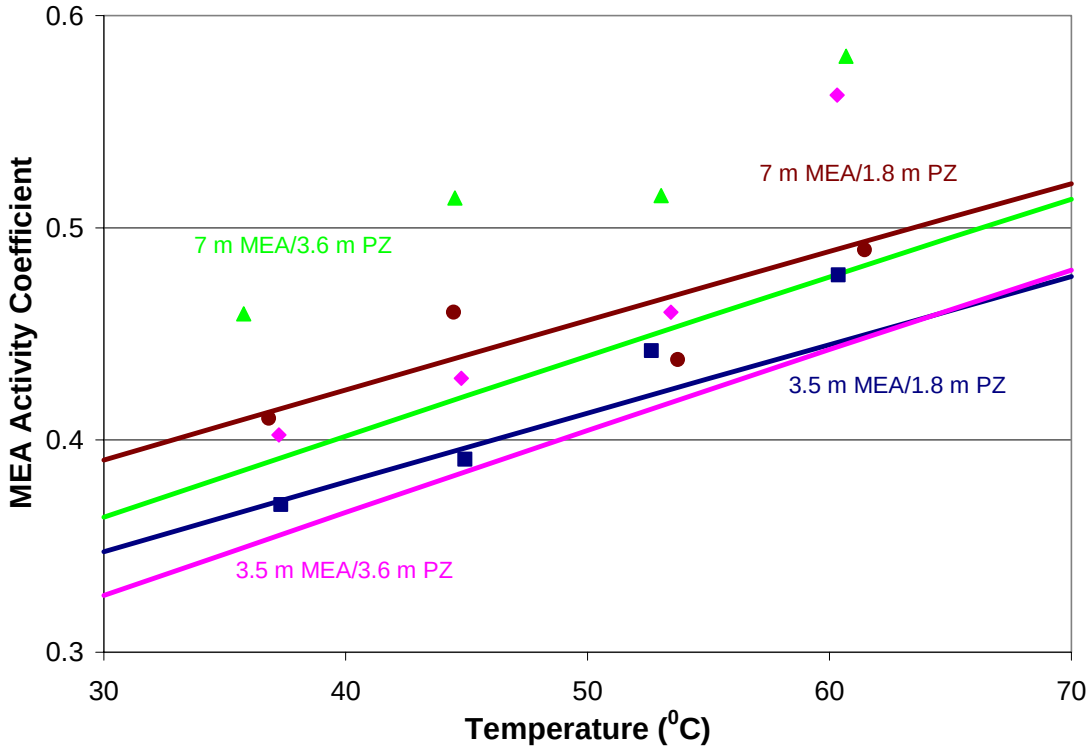

Figure 6.11. MEA activity coefficients for the MEA-PZ- H_2O system, curves predicted by NRTL sub model 33

Figure 6.11 above shows the measured as well as predicted MEA activity coefficients over the temperature range studied for each different solvent composition. The scatter in the data shows that there is still some error associated with the NRTL parameter regression, although a few of the experimental points lie very close to the model prediction curves. The average error of the measurements was around 15%, and it can be seen that the addition of PZ tends to shift the MEA activity down at the same temperature. Therefore, since PZ by itself is not a very volatile compound, it would make sense from an economic standpoint to add PZ to an MEA solvent to decrease the MEA volatility.

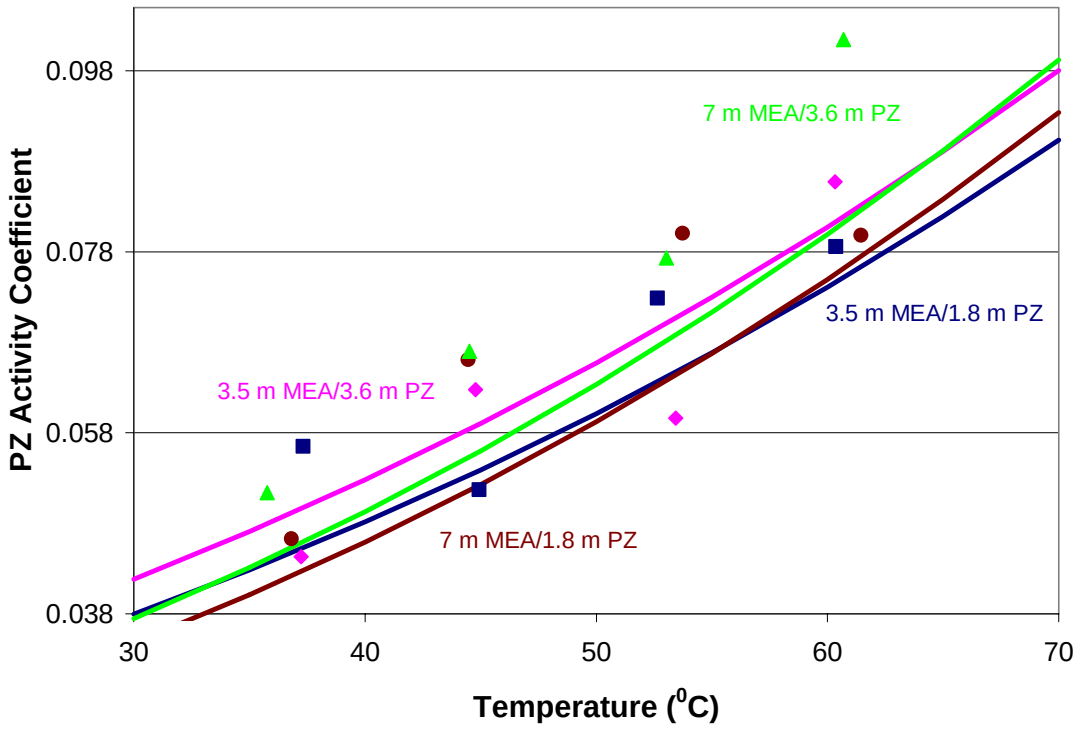

Figure 6.12. PZ activity coefficients for the MEA-PZ-H_2O system, curves predicted from NRTL sub model 33

Figure 6.12 plots the measured and predicted PZ activity coefficients calculated from the MEA-PZ-H_2O blend data. As was the case with the MEA activity coefficients for this system, there is some error involved with the NRTL predictions, and the average is around 20%. Similar to the MEA activity coefficients above, the PZ activity coefficients for a blend solution with the same PZ molality decrease with the addition of MEA.

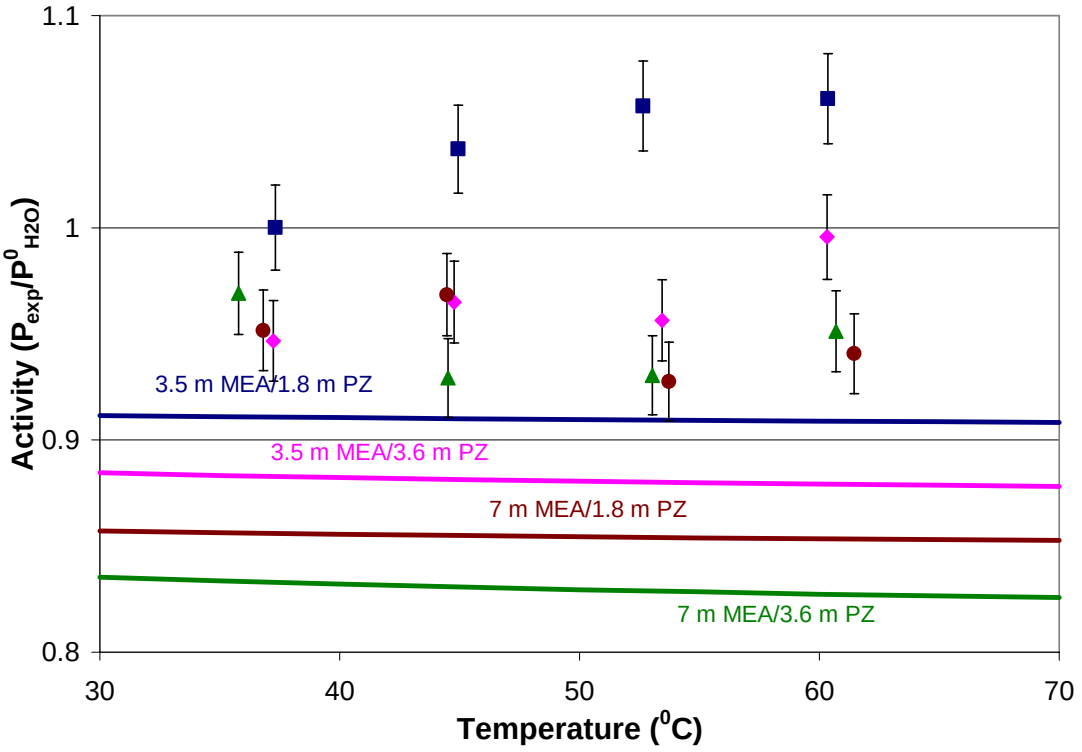

Figure 6.13. H_2O activity for the MEA-PZ-H_2O system, curves predicted by NRTL sub model 33

Finally, the H_2O activity data for the MEA-PZ-H_2O system is given in Figure 6.13. The NRTL sub model predicts a relatively flat behavior for H_2O activity based on temperature, suggesting that activity is a temperature independent function. The experimental data show some slight curvature over this same temperature range, thus raising the possibility that there could be some slight temperature dependence associated with this parameter that the model is not accounting for. The error bars on the experimental data points represent the 2% range of error associated with the FTIR analyzer, and thus it seems there is about a 10 – 15% error between the experimental and predicted values for H_2O activity.

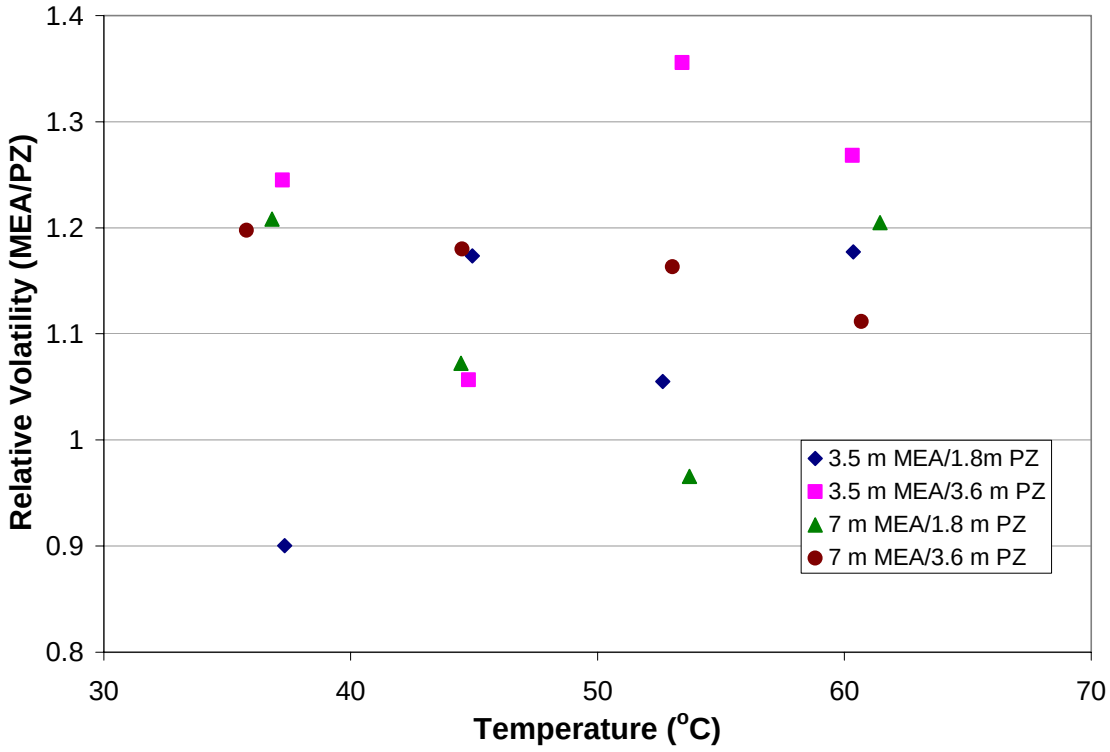

Figure 6.14. Relative volatility of MEA-PZ-H_2O

Figure 6.14 shows the experimental relative volatility for the MEA-PZ-H_2O blend systems. Ignoring the one outlier point each for the 3.5 m MEA/1.8 m PZ, 3.5 m MEA/3.6 m PZ and 7 m MEA/1.8 m PZ systems, it appears the relative volatility for MEA/PZ is anywhere between 1 – 1.2. Thus, to a zero order approximation, it can be concluded that MEA and PZ have the same volatility at the same liquid mole fraction.

6.5. NRTL BINARY INTERACTION PARAMETERS FOR MEA-PZ-H_2O DATA

Upon completion of the partial pressure experiments, all experimental data for the various binary and ternary systems was entered into the Aspen™ software where attempts were made to model the experimental data by regressing NRTL binary interaction parameters for the full model described earlier. That is, A_{ij} and B_{ij} values were

regressed for H_2O-MEA, MEA-H_2O, H_2O-PZ, PZ-H_2O, MEA-PZ, and PZ-MEA interactions. Once the full model parameters were established, they were tabulated along with their respective standard deviations, and a logic test was performed. The logic test simply describes whether or not the standard deviation was smaller than the parameter estimate, and a logic test result of "Yes" indicates that the parameter estimate is not very good due to the fact that its magnitude is smaller than that of its standard deviation. A correlation matrix was also created to quantify the extent of the correlation of a certain parameter and the others. A value greater than or equal to ± 0.9 indicates that there is no correlation where a value of approximately 0.5 indicates there is slight correlation and a value near 0 indicates strong correlation. Finally, a weighted sum of squares average was calculated for the full model and used as a reference point to compare to the weighted sum of squares average (as calculated by Aspen™) of the sub models.

Once the full NRTL model was established, the process of adding and subtracting parameters was used to ultimately find the simplest sub model possible that could model the experimental data with the least error between its weighted sum of squares average and that of the full model. Starting with the full model, there was a separate regression done for each sub model that subtracted only one B_{ij} parameter at a time, and the results were ranked in order of lowest SSQ. Whichever sub model had the lowest SSQ as compared to the full model was chosen as the starting point for the next set of sub model cases, where A_{ij} and B_{ij} parameters were added and subtracted one at a time until eventually the sub model got down to a single A_{ij} parameter used to model the entire data set. Table 6.5 gives the results of the sub models that were ranked first on logic test and then on correlation.

Table 6.5. NRTL sub model rankings based on logic test and correlation matrix values

Model	SSQ	Logic Test	Correlation	Rank		Model	SSQ	Logic Test	Correlation	Rank
3	8745	10	7	1		15	8783	7	13	13
11	8746	8	3	4		24	8915	6	1	19
19	8747	7	13	5		30	9096	4	1	24
25	8778	6	6	12		31	9295	1	0	30
27	8803	5	7	16		36	13226	2	1	38
33	9084	1	3	23		39	20193	1	1	41
37	9505	0	2	31		41	103740	0	1	44
38	10795	0	1	33		2	8752	11	9	8
43	14799	0	1	40		9	8783	9	7	14
45	25324	0	0	43		17	9010	6	12	20
46	188104	0	0	46		23	9015	4	2	21
5	8746	10	9	3		26	9258	4	2	29
13	8748	9	8	7		32	13094	3	2	37
18	8758	7	13	9		6	8760	11	12	11
21	8785	6	3	15		10	8833	8	5	18
29	9046	4	2	22		20	9187	5	4	27
34	9115	1	2	25		14	9188	6	13	28
35	9510	0	2	32		28	13062	4	1	36
40	13442	0	2	39		4	8829	10	11	17
42	20839	0	0	42		8	9150	8	8	26
44	176895	0	1	45		16	12050	12	9	34
47	1720338	0	0	47		22	12289	5	1	35
7	8748	11	14	6		full	8746	12	13	2

The first criterion for selecting the appropriate sub model was the logic test; that is, a value of 0 for logic test indicates that none of the parameter estimates had a magnitude less than the standard deviation. Thus, it was important to select a sub model with a relatively low number for logic test The next criterion used to evaluate the sub model performance was the value assigned to each sub model's correlation matrix. This value is the number of sub model parameters that are greater than or equal to ± 0.9. A high number for the correlation matrix indicates that a high number of parameters are not correlated very well with each other, and thus they could probably be removed from the model to simplify it further. Finally, the Rank column was just a ranking done on the deviation of each sub model's weighted sum of squares average as compared to that of the full model; that is the closer the two SSQs, the closer to 1 the sub model was ranked.

Out of all the sub model cases shown in Table 6.5, the final sub model chosen was sub model 33. Certainly arguments can be made for other sub models depending on the

weight placed on the three different criteria outlined above, but the justification for sub model 33 was that it had a low logic test (1) as well as a low correlation (3), and finally the deviation from the full model's SSQ was less than 4%. Thus, sub model 33 seems to meet the requirements established above that it is a simple model that can still reflect the experimental data with good precision. The form of sub model 33 is given below in Equations 6.7 – 6.9 (T is in K). Tables 6.7 and 6.8 give the confidence intervals associated with each A_{ij} and B_{ij} and correlation matrix, respectively.

$$\tau_{H_2O-MEA} = 1.166 - \frac{688}{T} \tag{6.7}$$

$$\tau_{H_2O-PZ} = 4.007 - \frac{2253}{T} \tag{6.8}$$

$$\tau_{MEA-PZ} = 17.194 - \frac{6845}{T} \tag{6.9}$$

Table 6.7. NRTL submodel 33 parameter estimates and standard deviations

Parameter	Component *i*	Component *j*	Value (SI units)	Standard deviation	Logic Test
A	H_2O	MEA	1.166	1.34	Yes
B	H_2O	MEA	-689	433.47	No
A	H_2O	PZ	4.007	1.80	No
B	H_2O	PZ	-2254	579.60	No
A	MEA	PZ	17.194	13.10	No
B	MEA	PZ	-6845	4179.85	No

Table 6.8. NRTL sub model 33 correlation matrix

Parameter	A (H_2O-MEA	B (H_2O-MEA)	A (H_2O-PZ)	B (H_2O-PZ)	A (MEA-PZ)	B (MEA-PZ)
A (H_2O-MEA	1					
B (H_2O-MEA)	-1.000	1				
A (H_2O-PZ)	0.436	-0.435	1			
B (H_2O-PZ)	-0.437	0.437	-1.000	1		
A (MEA-PZ)	-0.456	0.453	-0.738	0.734	1	
B (MEA-PZ)	0.459	-0.456	0.740	-0.737	-1.000	1

The first thing to note about the form of sub model 33 is that the first two interactions are the H_2O-amine interactions. This makes physical sense in that all the solutions (with the exception of pure MEA) are comprised of H_2O for the most part, so these interactions would probably be more representative of the actual solutions than the omitted amine-H_2O terms. The three parameters that have the high correlation values from Table 6.5 are the B_{ij} parameters for each equation. Thus, these parameters are not really correlated and could be removed. However, removing the three B_{ij} parameters results in an increase in deviation from the full model SSQ from less than 4% (sub model 33) to over 58% (sub model 42). Therefore, it is shown that there is some room for interpretation when deciding the amount of precision that is acceptable to sacrifice for the sake of modeling simplicity.

Now that the final sub model form has been established, the parameters were input into an Aspen™ flash calculation along with the experimental values of temperature, liquid mole fraction, and gas partial pressure. The constraints placed on the liquid mole fractions (0.1%) and gas partial pressures (2%) were purposely set tight and the constraint around temperature (0.1 ^{0}C) was set so that Aspen™ would essentially adjust the value of the regressed temperature to match the liquid mole fractions and partial pressures. Tables 6.6 through 6.8 below show the experimental and regressed data using sub model 33 parameters in Aspen™.

Table 6.6. Experimental and regressed data for all MEA experiments

MEA								
EXPERIMENTAL					REGRESSED			
T (^{0}C)	x_{MEA}	P_{MEA} (bar)	γ	Composition	T (^{0}C)	x_{MEA}	P_{MEA} (bar)	γ
42.77	0.3	2.74E-04	0.453	23.8 m MEA	42.37	0.2998	3.48E-04	0.592
49.95	0.3	5.08E-04	0.501		49.68	0.2998	6.00E-04	0.603
53.87	0.3	6.95E-04	0.523		53.65	0.2999	7.99E-04	0.610
61.69	0.3	1.60E-03	0.719		61.92	0.3001	1.38E-03	0.610
72.7	0.112	1.00E-03	0.610	7 m MEA	72.96	0.1121	8.43E-04	0.505
31	0.112	5.10E-05	0.561		31.60	0.1121	3.68E-05	0.385
35.8	0.112	9.00E-05	0.676		36.66	0.1121	5.55E-05	0.390
40.8	0.112	1.76E-04	0.902		42.08	0.1122	8.39E-05	0.390
48.2	0.112	2.96E-04	0.884		49.32	0.1122	1.50E-04	0.414
64.7	0.112	5.24E-04	0.520		64.79	0.1120	4.96E-04	0.490
42.1	0.112	6.50E-05	0.302		41.48	0.1119	9.32E-05	0.454
49.3	0.112	1.32E-04	0.365		48.95	0.1119	1.64E-04	0.464
52.8	0.112	1.87E-04	0.405		52.59	0.1120	2.13E-04	0.468
56.8	0.112	2.40E-04	0.397		56.53	0.1120	2.85E-04	0.481
61.4	0.112	3.25E-04	0.398		61.10	0.1119	3.95E-04	0.493
45.95	0.0593	6.60E-05	0.437	3.5 m MEA	46.07	0.0593	6.17E-05	0.405
51.21	0.0593	1.13E-04	0.516		51.55	0.0593	9.25E-05	0.413
58.87	0.0593	1.91E-04	0.520		59.13	0.0593	1.62E-04	0.435
65.29	0.0593	2.73E-04	0.493		65.41	0.0593	2.54E-04	0.456
42.7	0.0593	4.30E-05	0.361		42.53	0.0593	4.76E-05	0.406
49.4	0.0593	8.40E-05	0.435		49.47	0.0593	8.06E-05	0.416
56.31	0.0593	1.62E-04	0.523		56.61	0.0593	1.35E-04	0.427
65.47	0.0593	2.68E-04	0.479		65.54	0.0593	2.58E-04	0.458

Table 6.6 (cont.). Experimental and regressed data for all MEA experiments

MEA								
EXPERIMENTAL					REGRESSED			
T (^{0}C)	x_{MEA}	P_{MEA} (bar)	γ	Composition	T (^{0}C)	x_{MEA}	P_{MEA} (bar)	γ
50.61	1	3.18E-03	0.898		50.44	1	3.50E-03	1.000
58.03	1	4.75E-03	0.812		57.72	1	5.74E-03	1.000
38.79	1	1.60E-03	1.069	Pure MEA	38.90	1	1.51E-03	1.000
45.78	1	2.52E-03	1.003		45.78	1	2.51E-03	1.000
53.92	1	4.27E-03	0.960		53.86	1	4.43E-03	1.000
37.32	0.0576	2.84E-05	0.370	3.5 m	37.48	0.0575	2.90E-05	0.372
44.93	0.0576	5.32E-05	0.391	MEA/1.8 m	44.34	0.0575	5.14E-05	0.395
52.65	0.0576	1.04E-04	0.442		52.54	0.0575	9.81E-05	0.421
60.36	0.0576	1.88E-04	0.478	PZ	60.11	0.0575	1.72E-04	0.446
37.24	0.0560	2.99E-05	0.402	3.5 m	37.03	0.0560	2.59E-05	0.354
44.78	0.0560	5.61E-05	0.429	MEA/3.6 m	44.86	0.0560	5.06E-05	0.385
53.44	0.0560	1.11E-04	0.460		53.01	0.0560	9.73E-05	0.416
60.32	0.0560	2.14E-04	0.562	PZ	60.54	0.0560	1.72E-04	0.444
36.82	0.1067	5.63E-05	0.410	7 m MEA/1.8	36.75	0.1066	5.63E-05	0.413
44.47	0.1067	1.12E-04	0.460		44.84	0.1067	1.10E-04	0.440
53.73	0.1067	2.05E-04	0.438		53.90	0.1066	2.22E-04	0.470
61.45	0.1067	3.82E-04	0.490	m PZ	61.28	0.1066	3.81E-04	0.493
35.78	0.1059	5.77E-05	0.459	7 m MEA/3.6	36.01	0.1059	4.94E-05	0.386
44.52	0.1059	1.25E-04	0.514		45.05	0.1060	1.06E-04	0.421
53.04	0.1059	2.28E-04	0.515		53.22	0.1059	2.03E-04	0.452
60.69	0.1059	4.29E-04	0.581	m PZ	61.13	0.1060	3.65E-04	0.481

Table 6.7. Experimental and regressed data for all PZ experiments

PZ								
EXPERIMENTAL					REGRESSED			
T (^{0}C)	x_{PZ}	P_{PZ}(bar)	γ	Composition	T (^{0}C)	x_{PZ}	P_{PZ} (bar)	γ
35.95	0.0159	5.55E-06	0.039	0.9 m PZ	35.69	0.0159	6.36E-06	0.045
44.29	0.0159	1.46E-05	0.063		44.56	0.0159	1.27E-05	0.054
52.77	0.0159	2.45E-05	0.065		52.85	0.0159	2.36E-05	0.062
63.41	0.0159	6.2E-05	0.095		63.77	0.0159	5.06E-05	0.076
36.18	0.0314	1.24E-05	0.044	1.8 m PZ	36.01	0.0314	1.36E-05	0.048
44.43	0.0314	2.38E-05	0.051		44.28	0.0314	2.59E-05	0.056
52.83	0.0314	4.89E-05	0.066		52.85	0.0314	4.88E-05	0.066
60.40	0.0314	8.55E-05	0.077		60.46	0.0314	8.34E-05	0.075
32.72	0.0393	1.85E-05	0.064	2.5 m PZ	33.29	0.0393	1.56E-05	0.052
39.70	0.0393	3.47E-05	0.079		40.37	0.0393	2.73E-05	0.059
52.92	0.0393	8.33E-05	0.089		53.37	0.0393	7.22E-05	0.075
61.01	0.0393	0.000145	0.101		61.42	0.0393	0.000127	0.087
34.66	0.0609	2.25E-05	0.045	3.6 m PZ	34.40	0.0609	2.56E-05	0.052
45.08	0.0609	5.5E-05	0.059		44.98	0.0609	5.84E-05	0.063
53.22	0.0609	0.000105	0.071		53.19	0.0609	0.000107	0.073
61.16	0.0609	0.000181	0.081		61.12	0.0609	0.000186	0.083
37.32	0.029545	1.62E-05	0.056	3.5 m MEA/	37.48	0.0296	1.32E-05	0.045
44.93	0.029545	2.33E-05	0.052		44.34	0.0295	2.31E-05	0.053
52.65	0.029545	5.05E-05	0.073		52.54	0.0295	4.38E-05	0.064
60.36	0.029545	8.19E-05	0.079	1.8 m PZ	60.11	0.0295	7.64E-05	0.074
37.24	0.0576	2.47E-05	0.044	3.5 m MEA/	37.03	0.0575	2.72E-05	0.049
44.78	0.0576	5.47E-05	0.063		44.86	0.0576	5.15E-05	0.059
53.44	0.0576	8.42E-05	0.060		53.01	0.0575	9.64E-05	0.070
60.32	0.0576	1.74E-04	0.086	3.6 PZ	60.54	0.0576	1.67E-04	0.082
36.82	0.0275	1.20E-05	0.046	7 m MEA/	36.75	0.0275	1.08E-05	0.042
44.47	0.0275	2.70E-05	0.066		44.84	0.0275	2.17E-05	0.052
53.73	0.0275	5.47E-05	0.080		53.90	0.0275	4.49E-05	0.065
61.45	0.0275	8.17E-05	0.080	1.8 m PZ	61.28	0.0274	7.83E-05	0.077
35.78	0.0545	2.48E-05	0.051	7 m MEA/	36.01	0.0545	2.16E-05	0.044
44.52	0.0545	5.44E-05	0.067		45.05	0.0545	4.69E-05	0.056
53.04	0.0545	1.01E-04	0.077		53.22	0.0545	9.01E-05	0.068
60.69	0.0545	1.98E-04	0.101	3.6 m PZ	61.13	0.0546	1.64E-04	0.082

Table 6.8. Experimental and regressed data for all H_2O experiments

H_2O								
EXPERIMENTAL					REGRESSED			
T (^{0}C)	x_{H2O}	P_{H2O} (bar)	γ	Composition	T (^{0}C)	x_{H2O}	P_{H2O} (bar)	γ
42.77	0.7	5.48E-02	0.915	23.8 m MEA	42.37	0.7002	5.50E-02	0.938
49.95	0.7	7.61E-02	0.882		49.68	0.7002	7.96E-02	0.935
53.87	0.7	9.40E-02	0.899		53.65	0.7001	9.66E-02	0.934
61.69	0.7	1.38E-01	0.916		61.92	0.6999	1.40E-01	0.918
72.70	0.888	3.69E-01	1.186	7 m MEA	72.96	0.8879	3.08E-01	0.980
31.00	0.888	6.43E-02	1.610		31.60	0.8879	3.95E-02	0.956
35.80	0.888	8.35E-02	1.599		36.66	0.8879	5.17E-02	0.943
40.80	0.888	1.12E-01	1.631		42.08	0.8878	6.77E-02	0.925
48.20	0.888	1.55E-01	1.548		49.32	0.8878	9.92E-02	0.936
64.70	0.888	2.41E-01	1.098		64.79	0.8880	2.17E-01	0.986
42.10	0.888	7.52E-02	1.026		41.48	0.8881	7.25E-02	1.022
49.30	0.888	1.06E-01	1.000		48.95	0.8881	1.05E-01	1.007
52.80	0.888	1.26E-01	1.001		52.59	0.8880	1.25E-01	1.000
56.80	0.888	1.49E-01	0.980		56.53	0.8880	1.51E-01	1.002
61.40	0.888	1.76E-01	0.931		61.10	0.8881	1.87E-01	1.004
45.95	0.9407	9.84E-02	1.038	3.5 m MEA	46.07	0.9407	9.45E-02	0.991
51.21	0.9407	1.34E-01	1.085		51.55	0.9407	1.23E-01	0.981
58.87	0.9407	1.89E-01	1.059		59.13	0.9407	1.77E-01	0.985
65.29	0.9407	2.38E-01	0.998		65.41	0.9407	2.38E-01	0.992
42.70	0.9407	7.87E-02	0.982		42.53	0.9407	7.99E-02	1.006
49.40	0.9407	1.13E-01	0.998		49.47	0.9407	1.12E-01	0.993
56.31	0.9407	1.58E-01	1.003		56.61	0.9407	1.57E-01	0.983
65.47	0.9407	2.34E-01	0.972		65.54	0.9407	2.40E-01	0.994
35.95	0.9841	5.48E-02	0.938	0.9 m PZ	35.69	0.9841	5.75E-02	0.999
44.29	0.9841	7.61E-02	0.836		44.56	0.9841	9.23E-02	0.999
52.77	0.9841	9.40E-02	0.675		52.85	0.9841	1.40E-01	0.999
63.41	0.9841	1.38E-01	0.602		63.77	0.9841	2.33E-01	1.000

Table 6.8 (cont.). Experimental and regressed data for all H_2O experiments

H_2O								
EXPERIMENTAL					REGRESSED			
T (^{0}C)	x_{H2O}	P_{H2O} (bar)	γ	Composition	T (^{0}C)	x_{H2O}	P_{H2O} (bar)	γ
36.18	0.9686	6.68E-02	1.148	1.8 m PZ	36.01	0.9686	5.75E-02	0.998
44.43	0.9686	1.03E-01	1.146		44.28	0.9686	8.94E-02	0.998
52.83	0.9686	1.53E-01	1.112		52.85	0.9686	1.37E-01	0.998
60.40	0.9686	2.19E-01	1.112		60.46	0.9686	1.97E-01	0.998
32.72	0.9607	7.11E-02	1.492	2.5 m PZ	33.29	0.9607	4.88E-02	0.993
39.70	0.9607	1.06E-01	1.514		40.37	0.9607	7.19E-02	0.993
52.92	0.9607	1.92E-01	1.403		53.37	0.9607	1.39E-01	0.993
61.01	0.9607	2.71E-01	1.349		61.42	0.9607	2.03E-01	0.993
34.66	0.9391	6.62E-02	1.276	3.6 m PZ	34.40	0.9391	5.08E-02	0.993
45.08	0.9391	1.16E-01	1.285		44.98	0.9391	8.94E-02	0.993
53.22	0.9391	1.73E-01	1.272		53.19	0.9391	1.35E-01	0.994
61.16	0.9391	2.42E-01	1.224		61.12	0.9391	1.96E-01	0.994
37.32	0.9129	6.39E-02	1.095	3.5 m MEA/	37.48	0.9129	5.87E-02	0.998
44.93	0.9129	9.92E-02	1.136		44.34	0.9130	8.44E-02	0.997
52.65	0.9129	1.49E-01	1.158		52.54	0.9130	1.27E-01	0.996
60.36	0.9129	2.15E-01	1.162	1.8 m PZ	60.11	0.9130	1.82E-01	0.996
37.24	0.8864	6.03E-02	1.068	3.5 m MEA/	37.03	0.8865	5.56E-02	0.996
44.78	0.8864	9.15E-02	1.089		44.86	0.8864	8.40E-02	0.994
53.44	0.8864	1.40E-01	1.079		53.01	0.8866	1.26E-01	0.993
60.32	0.8864	2.02E-01	1.124	3.6 m PZ	60.54	0.8864	1.80E-01	0.992
36.82	0.8658	5.92E-02	1.099	7 m MEA/	36.75	0.8659	5.30E-02	0.988
44.47	0.8658	9.04E-02	1.119		44.84	0.8658	8.14E-02	0.987
53.73	0.8658	1.37E-01	1.071		53.90	0.8659	1.28E-01	0.986
61.45	0.8658	2.00E-01	1.086	1.8 m PZ	61.28	0.8659	1.80E-01	0.986
35.78	0.8396	5.70E-02	1.154	7 m MEA/	36.01	0.8396	4.96E-02	0.992
44.52	0.8396	8.70E-02	1.107		45.05	0.8395	7.99E-02	0.990
53.04	0.8396	1.33E-01	1.108		53.22	0.8396	1.20E-01	0.987
60.69	0.8396	1.96E-01	1.133	3.6 m PZ	61.13	0.8395	1.74E-01	0.985

6.5 CONCLUSIONS AND RECOMMENDATIONS

The experimental method used to gather partial pressure data via FTIR analysis proved to be viable and the results reproducible. All of the component results in the Calcmet® software had residuals of less than 0.01, meaning they were accurate and precise. This was proven by repeating the MEA-H_2O measurements several times on separate days with the results showing good reproducibility (hence more than 4 experimental data points). Due to time constraints, however, the only experiments that

had been repeated at the time of this work had been the MEA-H_2O experiments, and so it is recommended to repeat all of the PZ-H_2O and MEA-PZ-H_2O systems to ensure the precision of the results used in the model regression.

MEA partial pressures were measured to within 10% of the values predicted by the NRTL sub model. One interesting result of the MEA-H_2O measurements is that the 7 m MEA solution actually has a higher relative volatility than the 3.5 m solution. The final form of the sub model to calculate the NRTL binary interaction parameters for this system only accounts for temperature dependence between H_2O-MEA, and not vice versa. Because the MEA predictions were fairly accurate, this means that volatility loss is an issue with MEA, and thus should be taken into account when selecting a solvent for CO_2 capture.

The NRTL sub model also predicted PZ partial pressure data more accurately than the previous K_2CO_3/PZ/CO_2 electrolyte NRTL model. The experimental data showed no temperature dependence relative to the PZ activity, which was predicted by the Aspen™ software. The new NRTL parameters regressed as a result of these experiments give new partial pressure predictions to within 10-20% error. The calculations for activity coefficients involving PZ should be taken cautiously as the DIPPR model for calculating PZ vapor pressures was extrapolated to the temperature range pertaining to the experimental conditions. These experiments should be repeated to ensure reproducibility of the data and to further test the model.

The entire MEA-PZ-H_2O data set was initially modeled using a full NRTL model to account for all amine-H_2O and amine-amine interactions. Through systematic addition and subtraction of parameters, a sub model was chosen to represent the data using only H2O-amine interactions and MEA-PZ interactions. This sub model had a deviation of less than 4% from the weighted sum of squares average of the full model.

Appendix A: Detailed FTIR Analysis Procedure

This appendix serves to detail the process by which the FTIR is calibrated and shutdown, gas phase analysis is carried out, and the production of reference spectra for components in the gas, liquid, and solid phases.

A.1 MULTI-COMPONENT GAS PHASE ANALYSIS

A.1.1. FTIR Setup and Zero Calibration Procedure

The FTIR analyzer is capable of analyzing any gas sample provided the particular reference spectra, interferences, and analysis regions have been specified for each particular component to be analyzed (more detail will follow on this). Because of the wide range of applications of this instrument as well as the variety of Swagelok® fittings and valves available, it is possible to plumb the pump(s), heated line(s), and analyzer in many different ways, so this work will mainly focus on the typical setup for the stirred reactor system in the laboratory. This setup will involve both 15 ft heated lines as well as both SB4000 sample pumps in addition to the DX4000 analyzer. Plug one heated line's power cord and thermocouple into their respective outlets on the SB4000, and plug the sample pump's plugs into the special outlets on the laboratory wall. The temperature readings should come on for both, and should read room temperature. (If there is an "Err 4" reading, it means the thermocouple is not plugged in.) Connect the ends of one heated line to the "Sample Inlet" port on the SB4000 on one end and at the other connect to an N_2 source (for background spectrum generation). The other 15 ft heated hose should be connected to the "Exhaust Vent" port on the SB4000 and the other end placed inside the fume hood. (Under this setup, only one SB4000 pump will be used as a pump, and the other will function as only a temperature controller for the heated line.) It is important that all connections to the sample pump and analyzer be well-insulated so that sample

cannot condense anywhere during the recirculation loop. The next step is to connect the SB4000 to the DX4000 analyzer using the two small (approximately 3 in long) ¼ in diameter PFA tubing connections. Specifically, connect the "Analyzer Inlet" on the SB4000 to "Analyzer IN" on the DX4000 and "Analyzer Outlet" to "OUT" in the same manner. It is important that the analyzer be connected to a constant N_2 purge to rid the optics casing of the small amount of CO_2 and water that is present due to the fact that the optics casing is not hermetically sealed. The use of the N_2 purge will significantly improve analysis in the regions where CO_2 and H_2O absorb as opposed to operating without a N_2 purge. To do this in the laboratory, connect the "Purge" port on the analyzer to the N_2 valve located directly outside the fume hood using the supplied plastic tubing and Swagelok® connections. Finally, connect the RS-232 cable from the analyzer to the back of the computer tower. (If for some reason the cable is connected to the wrong port on the computer tower, there will be a message saying "Error Starting Measurement" when a measurement is started.)

Assuming this has been done, the first step to be taken before the sample can be analyzed is to run a background spectrum using pure N_2. Before the background spectrum can be created, however, it is necessary to first warm the heated lines to a temperature of 180 ^{0}C by setting the temperature on the sample pump under the switch labeled "Umbilical Temperature." Once the lines get to within approximately 20 ^{0}C of the setpoint, the sample pump module should be heated up to 180 ^{0}C by turning on the switch labled "Pump Heater" and adjusting the temperature to its set value below. The DX4000 analyzer should make a buzzing type sound if it is on, which is possible to check audibly. If not, then there is an on/off switch located to the left of the "Sample In" port, directly beside the N_2 purge port. During the time required to come up to temperature, it is necessary to begin flowing pure N_2 through the heated lines to try to rid them of any

residual impurities left over from previous experiments. Once the heated lines and pumps have reached their desired setpoint temperatures, open the Calcmet™ software, and click "Options," "View Hardware Status". A small box will appear that counts down from 1 s and then a table is displayed. It is important that the analyzer temperature be 180 ^{0}C, which can be verified by on this table. (Incidentally, if the analyzer is not up to temperature, there will be an error message saying "Error Starting Measurement" and a red light at the bottom of the screen.) Once the analyzer temperature is 180 ^{0}C, click "Options," "Measuring Times," and then select "20 s" from the drop down menu and click OK. Click on the circular arrow icon at the top of the screen to begin making continuous measurements. All components should read 0.00 vol% or ppm, but if not, continue flowing N_2 through the heated lines until all components read zero. Once this is accomplished, click "Cancel" on the box with the time, and click "Yes" when the software asks "Are you sure you want to cancel the measurement?" Select, "Options," then from the "Measuring Times" drop down box change from 20 s to 5 min, then click "Measure" and "Zero Calibration." A small box will appear on the screen that will count down from 600 s. This is the background scan, which should look similar to Figure 3.6 below.

Meaningful data can only be garnered by the analyzer if the single beam intensity is below 65,000 as 65,000 is the physical saturation limit of the detector. It is important before analyzing any samples, therefore, to verify that the maximum absorbance is greater than 20,000 and less than 65,000, which are shown on the screen directly below the N_2 background spectrum in the Calcmet™ software.

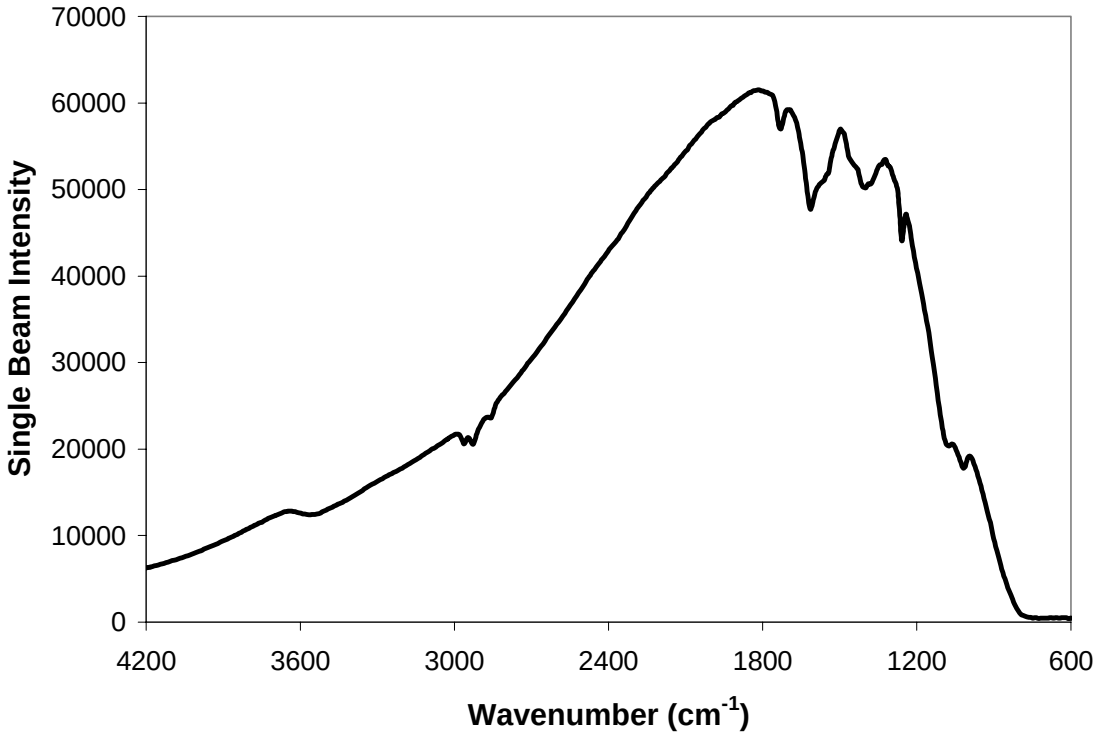

Figure A.1: Typical N_2 Background Scan for FTIR Analysis.

A.1.2. FTIR Gas Sampling Analysis

Once the N_2 background step has been completed, it is now possible to analyze a sample. At this point, it may be necessary to switch over any valves or reconnect any Swagelok® fittings necessary to allow the gas sample to flow through the heated lines. Before proceeding any further, it is recommended at this stage to go into the Calcmet™ software and create a file to save the samples. To do this, click "Options," "Autosaving" and make sure the box for "All" is checked beside "Autosave Sample Spectra." Once this is checked, it is possible to save the spectra that will be generated under some name; typically, the root for the experiments in this work was "C:\\CALCMETSAMPLES\Date_AmineConcentration_Temperature." Then, click

"Options," "Result Output" and verify that the box next to "Autosave Results" is checked, and then name the folder the same name as under Autosaving. (If more than one temperature or concentration is to be measured during one sitting, it is recommended to repeat this step after each successful run so that it is easier to find the corresponding spectra to match the conditions for later analysis.) For the stirred reactor apparatus in the laboratory, fill the reactor with approximately 500 mL of liquid solution and then disconnect the end of the heated line from the N_2 source and connect it to the proper ¼ - in Swagelok® fitting located on the top of the reactor. After putting the liquid into the reactor, turn on the IsoTemp heat bath via the on/off switch on the back of the apparatus and set the bath temperature by pressing "Set/Enter" and use the up and down arrows to pick a temperature, and press "Set/Enter" again to make this the setpoint temperature. (Note: There is an approximate 3 – 5 ^{0}C temperature difference between bath and reactor temperature for most runs.) Connect the branch of the 3/8 – in PFA Swagelok® Tee to the line that goes to the two gas washing bottles. (This serves as a pressure relief system.) The entire series of connections from the reactor to the heated line should then be wrapped in the BriskHeat electronic heating wrap and the Variac turned to 70. Attach the other heated line (the one that was open to vent) to the bottom of the glass reactor, and open the valve. The N_2 source line should be connected to the valve at the top of the reactor (with the valve opened). Flowing N_2 into the top of the reactor for the initial 10 minutes of the experiment serves to eliminate a big initial plug of entrainment that can throw off the analysis, and the valve should be closed after 10 minutes. Since this process involves analyzing a vapor composition from the stirred reactor, then it is necessary to turn on the switch labeled "Pump Motor" on the SB4000 sample pump. However, if the gas to be analyzed is coming from a pressurized cylinder (as is the case when creating some reference files or measurement verification purposes), this step is not

necessary. Observe the "Sample Pressure" gauge, and open the drain valve slightly at the bottom of the reactor until the "Sample Pressure" reads less than 3 psig. The last step is to go in the Calcmet™ software and change the Measuring Times from 5 minutes to 3 minutes and click the circular arrow button on the far right of the top toolbar to begin taking continuous 3 minute samples.

A.1.3. Shutting Down the Analyzer

Once experiments have concluded, it is necessary to properly shut down the software and clean the reactor apparatus. The first step is to cancel the measuring in the Calcmet™ software, and then turn off the "Pump Motor" switch on the SB4000. Turn off the IsoTemp heat bath. Turn off the BriskHeat wrap, and unwrap it so it is possible to disconnect the heated line from the top of the reactor. Connect this heated line with the N_2 source and begin flowing pure N_2 through the lines. Close both the Swagelok® ¼ - in on/off valve and the drain valve at the bottom of the reactor and disconnect the heated line from the valve. Remove the entire series of Swagelok® fittings (including the white AceSafe tap) from the reactor and rinse with deionized water from the sink. After rinsing the fittings, connect them to the heated line that was initially connected to the gas inlet at the bottom of the reactor so that N_2 can flow through them and remove any potential impurities that may be present. Attach a piece of tubing to the ¼ -in Swagelok® valve at the bottom of the reactor and open the valve (as well as the drain valve) to drain the liquid into a container and properly dispose of the waste. Once the liquid has been drained, close both valves and fill the reactor with deionized water from the sink, open the valves, drain, and repeat this process several times. Once the reactor has been sufficiently rinsed, turn off the N_2 flowing through the heated lines, and turn on the air so that gas can flow overnight. At this point, it is optional whether to leave the heated lines at 180 ^{0}C (if an experiment is to be started the next day), or to turn them down to a lower

temperature (50 ^{0}C), or to turn them off completely (to relocate the FTIR or if an experiment is not planned for the near future.)

A.2. REFERENCE SPECTRA GENERATION

The Calcmet™ software has a vast library of reference spectra for many different compounds at various concentrations, but the need sometimes arises to create a new reference file when analyzing for a new compound whose reference does not exist, or to create new ones for a compound whose old reference spectra may be erroneous. The FTIR analyzer system is useful for this purpose, although the setup has to be modified a bit from the partial pressure experimental apparatus.

Before one can actually go through the process of creating reference spectra, it is useful to calculate the necessary N_2 gas flowrate (and hence flow controller setting) to achieve the desired reference concentration. The Brooks mass flow controllers each have different flowrates that correspond to a different reference gas used in their calibration, so it is important to use the correct flow controller as well as calibration curve for these calculations (see Appendix for current calibration curves.) Once the properties of the specific compound such as molecular weight and density are known, it is possible to calculate the N_2 flowrate to give desired concentrations for the reference spectra.

Creating reference files for gases such as CO_2 or NH_3 is a relatively straightforward process. Simply connect the cylinder of gas to be measured to the appropriate flow controller, and use the Brose control box to set the flow controllers to the appropriate settings (Channel 1 – Air, Channel N_2 – Air, Channel 3 – CO_2) as calculated previously. (Note: It is possible to use the flow controllers for some gas mixtures at low concentrations, i.e., using Channel 2 for 1000 ppm in N_2 or Channel 1 for 2% CO_2 in air). Take 20 s samples using the Calcmet® software until the maximum absorbance becomes stable. At that point, switch over to 3 min scans and take 10 sample

spectra. Take the spectra from the ten 3 min scans that is the most representative of the scans, and change the extension on the sample file from .SPE to .REF and re-save the file. Then, in the Calcmet® software, select "Edit", "Analysis Settings" and verify that the compound you are adding a reference for is included in the analysis method. If not, check a box that is unchecked, and type in the name of the compound. Once the name of the compound is highlighted, click "Add" under the "Reference Files" section on the right side of the box, and select the reference file(s) from the appropriate directory that it is saved and click "Add". With one of those files selected, click "Parameters" and type in the exact concentration as calculated by the spreadsheet (to 3 decimal places) and specify units of vol% or ppm. Verify that the path length is 500 cm, and click OK.

Creating reference files for compounds that are liquids at room temperature requires a slightly different approach than that described above. For this process, it is necessary to use the GASMET™ Calibrator, which is a self-contained apparatus inside a black briefcase that integrates with the DX4000 analyzer. The first step is to connect a N_2 line to the port labeled "N_2 1.4 Bar". Next, connect the included heated line from the right side of the injection chamber to the "Analyzer IN" port on the DX4000. At this point, the "OUT" port on the DX4000 should just have a line that stretches to the fume hood to vent. Now the unit can be plugged in and turned on, and the oven and heated line temperature controllers can be set at 180 ^{0}C. Set the N2 flow controller to a flowrate of 2 L/min. Like the gas reference generation procedure, it is helpful to use a spreadsheet to calculate a flowrate (in either mL/hr or mL/hr depending on desired concentration) of liquid based on specific properties such as molecular weight and density. Assuming that value has been calculated, fill the appropriate syringe with liquid and place in the syringe pump, and move the needle valve to rest against the back of the syringe. On the buttons near the handle of the case, press "Select", which will bring up the main menu. Use the

left and right arrows to scroll over to “Table” and press “Select”, where it will ask you to choose the appropriate syringe manufacturer (Hamilton in this case). Choose the manufacturere, press “Select”, and toggle over using the left and right arrows to select the total volume of the syringe (in mL or mL), and input that value and press “Select”. The display should read “Volume: 0.00 ml”, and press “Select”. Use the left and right arrows to enter the calculated dispensing rate of the syringe (in mL/hr or mL/hr) and press “Select.” A black arrow should appear on the right of the display, and press “Run”. The same arrow should now be blinking, signaling the apparatus is in use. As was the case in the gas reference generation procedure, take 20 s scans with the Calcmet™ software until the maximum absorbance value is not changing drastically, and then take ten 3 min scans as before. To change to a different concentration, press “Stop” on the GASMET™ Calibrator, and repeat the above steps with the only difference being a different dispensing rate for the syringe. Once all spectra have been made, the process for changing a .SPE file to a .REF file are the same as outlined above for a gas reference spectrum.

Creating a reference file for a compound that is solid at room temperature can be done in two ways. First, it is possible to place the pure solid inside a heated bomb in the IsoTemp bath, and measure the partial pressure of the vapor using the FTIR and associated Swagelok® fittings on the bomb at a given temperature. Secondly, it is possible (although not trivial) to dissolve the solid in a solvent (at a predetermined concentration) with a well-known reference spectra (i.e., water) and then “subtract out” the solvent’s spectra to leave the spectra of the unknown. This particular method is possible using the GASMET™ Calibrator, although the first method is generally the first choice.

Appendix B: Experimental Results for MEA-H_2O

Table B.1. MEA measured and regressed data for MEA-H_2O

EXPERIMENTAL					REGRESSED		
Date	T (^{0}C)	x_{MEA}	P_{MEA} (bar)	Composition	T (^{0}C)	x_{MEA}	P_{MEA} (bar)
3/23/2006	42.77	0.300	2.74E-04		42.37	0.300	3.48E-04
3/23/2006	49.95	0.300	5.08E-04		49.68	0.300	6.00E-04
3/23/2006	53.87	0.300	6.95E-04		53.65	0.300	7.99E-04
3/23/2006	61.69	0.300	1.60E-03	23.8 m MEA	61.92	0.300	1.38E-03
3/10/2006	72.7	0.112	1.00E-03		72.96	0.112	8.43E-04
3/14/2006	64.7	0.112	5.24E-04		64.79	0.112	4.96E-04
3/22/2006	42.1	0.112	6.50E-05		41.48	0.112	9.32E-05
3/22/2006	49.3	0.112	1.32E-04		48.95	0.112	1.64E-04
3/22/2006	52.8	0.112	1.87E-04		52.59	0.112	2.13E-04
3/22/2006	56.8	0.112	2.40E-04		56.53	0.112	2.85E-04
3/22/2006	61.4	0.112	3.25E-04	7 m MEA	61.10	0.112	3.95E-04
3/15/2006	45.95	0.059	6.60E-05		46.07	0.059	6.17E-05
3/15/2006	51.21	0.059	1.13E-04		51.55	0.059	9.25E-05
3/15/2006	58.87	0.059	1.91E-04		59.13	0.059	1.62E-04
3/15/2006	65.29	0.059	2.73E-04		65.41	0.059	2.54E-04
3/21/2006	42.7	0.059	4.30E-05		42.53	0.059	4.76E-05
3/21/2006	49.4	0.059	8.40E-05		49.47	0.059	8.06E-05
3/21/2006	56.31	0.059	1.62E-04		56.61	0.059	1.35E-04
3/21/2006	65.47	0.059	2.68E-04	3.5 m MEA	65.54	0.059	2.58E-04
3/2/2006	50.61	1.000	3.18E-03		50.44	1.000	3.50E-03
3/3/2006	58.03	1.000	4.75E-03		57.72	1.000	5.74E-03
3/24/2006	38.79	1.000	1.60E-03		38.90	1.000	1.51E-03
3/24/2006	45.78	1.000	2.52E-03		45.78	1.000	2.51E-03
3/24/2006	53.92	1.000	4.27E-03	Pure MEA	53.86	1.000	4.43E-03

Table B.2. H_2O measured and regressed data for MEA-H_2O

EXPERIMENTAL					REGRESSED		
Date	T (^{0}C)	x_{H2O}	P_{H2O} (bar)	Composition	T (^{0}C)	x_{H2O}	P_{H2O} (bar)
3/23/2006	42.77	0.700	5.48E-02		42.37	0.700	5.22E-02
3/23/2006	49.95	0.700	7.61E-02		49.68	0.700	7.62E-02
3/23/2006	53.87	0.700	9.40E-02		53.65	0.700	9.29E-02
3/23/2006	61.69	0.700	1.38E-01	23.8 m MEA	61.92	0.700	1.36E-01
3/10/2006	72.7	0.888	3.69E-01		72.96	0.888	3.06E-01
3/14/2006	64.7	0.888	2.41E-01		64.79	0.888	2.17E-01
3/22/2006	42.1	0.888	7.52E-02		41.48	0.888	7.20E-02
3/22/2006	49.3	0.888	1.06E-01		48.95	0.888	1.04E-01
3/22/2006	52.8	0.888	1.26E-01		52.59	0.888	1.24E-01
3/22/2006	56.8	0.888	1.49E-01		56.53	0.888	1.50E-01
3/22/2006	61.4	0.888	1.76E-01	7 m MEA	61.10	0.888	1.86E-01
3/15/2006	45.95	0.941	9.84E-02		46.07	0.941	9.46E-02
3/15/2006	51.21	0.941	1.34E-01		51.55	0.941	1.23E-01
3/15/2006	58.87	0.941	1.89E-01		59.13	0.941	1.77E-01
3/15/2006	65.29	0.941	2.38E-01		65.41	0.941	2.38E-01
3/21/2006	42.7	0.941	7.87E-02		42.53	0.941	8.00E-02
3/21/2006	49.4	0.941	1.13E-01		49.47	0.941	1.12E-01
3/21/2006	56.31	0.941	1.58E-01		56.61	0.941	1.57E-01
3/21/2006	65.47	0.941	2.34E-01	3.5 m MEA	65.54	0.941	2.40E-01

Appendix C: Experimental Results for PZ-H_2O

Table C.1. PZ measured and regressed data for PZ-H_2O

EXPERIMENTAL				REGRESSED		
T (^{0}C)	x_{PZ}	P_{PZ}(bar)		T (^{0}C)	x_{PZ}	P_{PZ}(bar)
35.95	0.0159	5.55E-06		35.69	0.0159	6.36E-06
44.29	0.0159	1.46E-05		44.56	0.0159	1.27E-05
52.77	0.0159	2.45E-05		52.85	0.0159	2.36E-05
63.41	0.0159	6.20E-05	0.9 m PZ	63.77	0.0159	5.06E-05
36.18	0.0314	1.24E-05		36.01	0.0314	1.36E-05
44.43	0.0314	2.38E-05		44.28	0.0314	2.59E-05
52.83	0.0314	4.89E-05		52.85	0.0314	4.88E-05
60.40	0.0314	8.55E-05	1.8 m PZ	60.46	0.0314	8.34E-05
32.72	0.0393	1.85E-05		33.29	0.0393	1.56E-05
39.70	0.0393	3.47E-05		40.37	0.0393	2.73E-05
52.92	0.0393	8.33E-05		53.37	0.0393	7.22E-05
61.01	0.0393	1.45E-04	2.5 m PZ	61.42	0.0393	1.27E-04
34.66	0.0609	2.25E-05		34.40	0.0609	2.56E-05
45.08	0.0609	5.50E-05		44.98	0.0609	5.84E-05
53.22	0.0609	1.05E-04		53.19	0.0609	1.07E-04
61.16	0.0609	1.81E-04	3.6 m PZ	61.12	0.0609	1.86E-04

Table C.2. H_2O measured and regressed data for PZ-H_2O

EXPERIMENTAL				REGRESSED		
T (^{0}C)	x_{H2O}	P_{H2O}(bar)		T (^{0}C)	x_{H2O}	P_{H2O}(bar)
35.95	0.9841	0.0687352		35.69	0.9841	0.058352
44.29	0.9841	0.1078633		44.56	0.9841	0.090996
52.77	0.9841	0.1587766		52.85	0.9841	0.139185
63.41	0.9841	0.2532888	0.9 m PZ	63.77	0.9841	0.229229
36.18	0.9686	0.0668311		36.01	0.9686	0.058088
44.43	0.9686	0.103408		44.28	0.9686	0.090088
52.83	0.9686	0.1529526		52.85	0.9686	0.137263
60.40	0.9686	0.21879	1.8 m PZ	60.46	0.9686	0.196456
32.72	0.9607	0.0710736		33.29	0.9607	0.047285
39.70	0.9607	0.1057275		40.37	0.9607	0.069343
52.92	0.9607	0.19209		53.37	0.9607	0.135973
61.01	0.9607	0.2707352	2.5 m PZ	61.42	0.9607	0.199235
34.66	0.9391	0.0661824		34.40	0.9391	0.051517
45.08	0.9391	0.1163377		44.98	0.9391	0.089903
53.22	0.9391	0.1727782		53.19	0.9391	0.134944
61.16	0.9391	0.241806	3.6 m PZ	61.12	0.9391	1.96E-01

Appendix D: Experimental Results for MEA-PZ-H_2O

Table D.1. MEA measured and regressed data for MEA-PZ-H_2O

EXPERIMENTAL				REGRESSED		
T (^{0}C)	x_{MEA}	P_{MEA} (bar)	Composition	T (^{0}C)	x_{MEA}	P_{MEA} (bar)
37.32	0.0576	2.84E-05		37.48	0.0575	2.90E-05
44.93	0.0576	5.32E-05	3.5 m	44.34	0.0575	5.14E-05
52.65	0.0576	1.04E-04	MEA/1.8 m	52.54	0.0575	9.81E-05
60.36	0.0576	1.88E-04	PZ	60.11	0.0575	1.72E-04
37.24	0.0560	2.99E-05		37.03	0.0560	2.59E-05
44.78	0.0560	5.61E-05	3.5 m	44.86	0.0560	5.06E-05
53.44	0.0560	1.11E-04	MEA/3.6 m	53.01	0.0560	9.73E-05
60.32	0.0560	2.14E-04	PZ	60.54	0.0560	1.72E-04
36.82	0.1067	5.63E-05		36.75	0.1066	5.63E-05
44.47	0.1067	1.12E-04		44.84	0.1067	1.10E-04
53.73	0.1067	2.05E-04	7 m MEA/1.8	53.90	0.1066	2.22E-04
61.45	0.1067	3.82E-04	m PZ	61.28	0.1066	3.81E-04
35.78	0.1059	5.77E-05		36.01	0.1059	4.94E-05
44.52	0.1059	1.25E-04		45.05	0.1060	1.06E-04
53.04	0.1059	2.28E-04	7 m MEA/3.6	53.22	0.1059	2.03E-04
60.69	0.1059	4.29E-04	m PZ	61.13	0.1060	3.65E-04

Table D.2. PZ measured and regressed data for MEA-PZ-H_2O

EXPERIMENTAL				REGRESSED		
T (^{0}C)	x_{PZ}	P_{PZ}(bar)	Composition	T (^{0}C)	x_{PZ}	P_{PZ} (bar)
37.32	0.0295	1.62E-05		37.48	0.0296	1.32E-05
44.93	0.0295	2.33E-05	3.5 m	44.34	0.0295	2.31E-05
52.65	0.0295	5.05E-05	MEA/1.8 m	52.54	0.0295	4.38E-05
60.36	0.0295	8.19E-05	PZ	60.11	0.0295	7.64E-05
37.24	0.0576	2.47E-05		37.03	0.0575	2.72E-05
44.78	0.0576	5.47E-05	3.5 m	44.86	0.0576	5.15E-05
53.44	0.0576	8.42E-05	MEA/3.6 m	53.01	0.0575	9.64E-05
60.32	0.0576	1.74E-04	PZ	60.54	0.0576	1.67E-04
36.82	0.0275	1.20E-05		36.75	0.0275	1.08E-05
44.47	0.0275	2.70E-05		44.84	0.0275	2.17E-05
53.73	0.0275	5.47E-05	7 m MEA/1.8	53.90	0.0275	4.49E-05
61.45	0.0275	8.17E-05	m PZ	61.28	0.0274	7.83E-05
35.78	0.0545	2.48E-05		36.01	0.0545	2.16E-05
44.52	0.0545	5.44E-05		45.05	0.0545	4.69E-05
53.04	0.0545	1.01E-04	7 m MEA/3.6	53.22	0.0545	9.01E-05
60.69	0.0545	1.98E-04	m PZ	61.13	0.0546	1.64E-04

Table D.3. H_2O measured and regressed data for MEA-PZ-H_2O

EXPERIMENTAL				REGRESSED		
T (^{0}C)	x_{H2O}	P_{H2O} (bar)	Composition	T (^{0}C)	x_{H2O}	P_{H2O} (bar)
37.32	0.9129	6.39E-02		37.48	0.9129	5.87E-02
44.93	0.9129	9.92E-02	3.5 m	44.34	0.9130	8.44E-02
52.65	0.9129	1.49E-01	MEA/1.8 m	52.54	0.9130	1.27E-01
60.36	0.9129	2.15E-01	PZ	60.11	0.9130	1.82E-01
37.24	0.8864	6.03E-02		37.03	0.8865	5.56E-02
44.78	0.8864	9.15E-02	3.5 m	44.86	0.8864	8.40E-02
53.44	0.8864	1.40E-01	MEA/3.6 m	53.01	0.8866	1.26E-01
60.32	0.8864	2.02E-01	PZ	60.54	0.8864	1.80E-01
36.82	0.8658	5.92E-02		36.75	0.8659	5.30E-02
44.47	0.8658	9.04E-02		44.84	0.8658	8.14E-02
53.73	0.8658	1.37E-01	7 m MEA/1.8	53.90	0.8659	1.28E-01
61.45	0.8658	2.00E-01	m PZ	61.28	0.8659	1.80E-01
35.78	0.8396	5.70E-02		36.01	0.8396	4.96E-02
44.52	0.8396	8.70E-02		45.05	0.8395	7.99E-02
53.04	0.8396	1.33E-01	7 m MEA/3.6	53.22	0.8396	1.20E-01
60.69	0.8396	1.96E-01	m PZ	61.13	0.8395	1.74E-01

Appendix E: MEA Baseline Pilot Plant Campaign

This appendix serves to give an actual sample spectrum and Calcmet™ analysis for a sample point during the MEA Baseline Campaign carried out from April 6 – 13, 2005. Secondly, all experimental data for CO_2, H_2O, NH_3, and MEA will be tabulated in this section.

Figure E.1 and Table E.1 below correspond to actual Calcmet™ samples from the MEA Baseline Campaign. Specifically, the spectrum and gas phase analysis correspond to sample number 00768, which was recorded on April 8, 2005 at 06:34:35 AM. All samples for the campaign were analyzed using the PilotPlantMEA.LIB application.

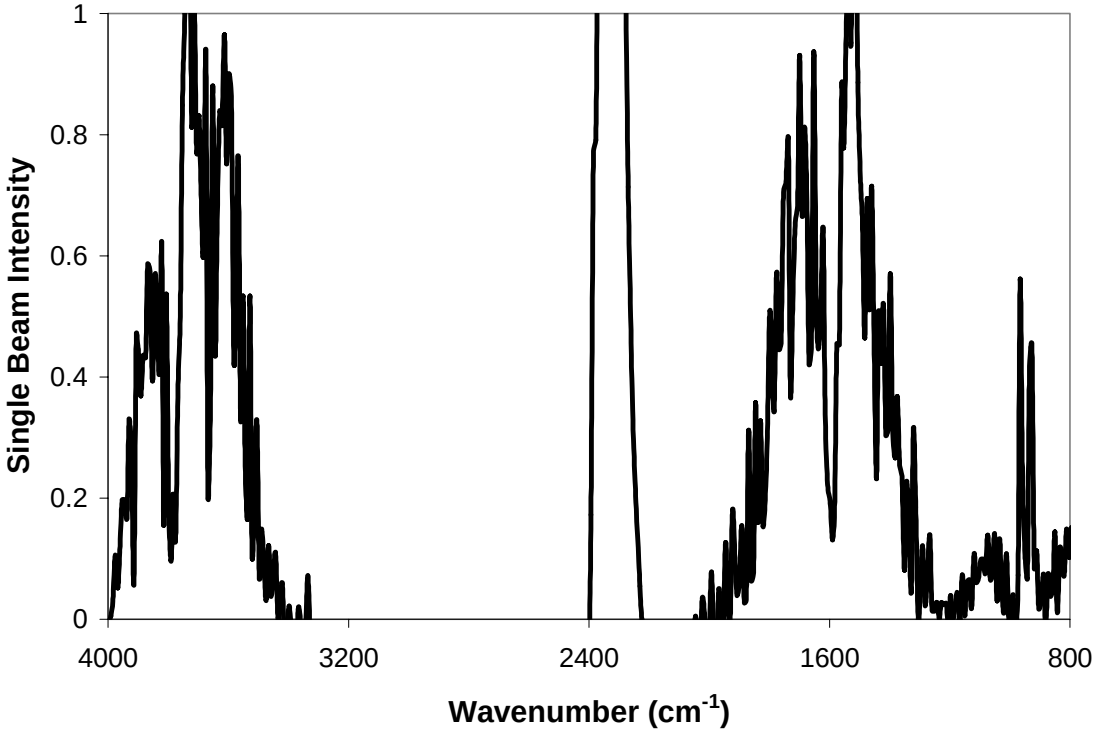

Figure E.1. Calcmet™ sample spectrum prc#1_00768.SPE

Table E.1. Calcmet™ analysis of prc#1_00768.SPE (all spectra analyzed using PilotPlantMEA.LIB application file)

Channel	Component	Concentration	Units	Range	Residual
1	Water vapor H2O	4.2	vol%	10	0.0096
2	Carbon dioxide CO2	1.7	vol%	5	0.0060
3	Carbon monoxide CO	0.00	ppm	10	0.0069
5	Nitrous oxide N2O	7.0	ppm	100	0.0063
6	Nitrogen monoxide NO	16.4	ppm	20	0.0095
7	Nitrogen dioxide NO2	0.00	ppm	20	0.0034
9	Ammonia NH3	965	ppm	1000	0.0083
21	Formaldehyde	-3.9	ppm	10	0.0042
25	MEA	36.3	ppm	100	0.0041
29	Methane CH4	2.8	ppm	10	0.0037

Table E.2. Experimental times, temperatures, and calculated absorber lean loadings for MEA Baseline Campaign (April 6 – 13, 2005)

Date	Time	Adjusted Time (min)	Adjusted Time (hr)	Temperature TT4078 (F)	Lean Loading
4/6/2005	4:20 PM	0	0.00	100.84	0.302
4/6/2005	5:30 PM	70	1.17	100.75	0.298
4/7/2005	1:00 AM	520	8.67	96.94	0.308
4/7/2005	2:05 AM	585	9.75	96.32	0.311
4/7/2005	5:30 AM	790	13.17	105.25	0.309
4/7/2005	6:30 AM	850	14.17	108.40	0.307
4/7/2005	10:45 AM	1105	18.42	89.72	0.304
4/7/2005	11:45 AM	1165	19.42	91.78	0.302
4/7/2005	5:00 PM	1480	24.67	98.89	0.307
4/7/2005	6:00 PM	1540	25.67	99.06	0.305
4/8/2005	2:05 AM	2025	33.75	90.29	0.303
4/8/2005	3:10 AM	2090	34.83	91.11	0.308
4/8/2005	11:00 AM	2560	42.67	97.10	0.305
4/8/2005	12:00 PM	2620	43.67	96.00	0.304
4/11/2005	11:30 AM	6950	115.83	95.83	0.247
4/11/2005	12:30 PM	6910	115.17	96.56	0.248
4/11/2005	2:30 PM	7030	117.17	115.38	0.254
4/11/2005	3:30 PM	7090	118.17	118.09	0.252
4/12/2005	1:30 AM	7690	128.17	134.96	0.250
4/12/2005	2:30 AM	7750	129.17	136.65	0.250
4/13/2005	10:00 AM	9640	160.67	96.60	0.309
4/13/2005	11:00 AM	9700	161.67	97.25	0.310
4/13/2005	2:45 PM	9925	165.42	136.73	0.305
4/13/2005	3:45 PM	9985	166.42	134.81	0.309

Table E.3. Absorber outlet CO_2 concentrations for MEA Baseline Campaign (April 6 – 13, 2005)

Date	Time	Vaisala AI404 Analyzer (vol% CO_2)	FTIR 1 (vol% CO_2)	FTIR 2 (vol% CO_2)	FTIR 3 (vol% CO_2)	FTIR 4 (vol% CO_2)	FTIR 5 (vol% CO_2)	FTIR AVG (vol % CO_2)
4/6/2005	4:20 PM	0.97	1.3	1.2	1.2	0.88	1.3	1.18
4/6/2005	5:30 PM	0.87	0.93	0.76	0.8	1	1.1	0.92
4/7/2005	1:00 AM	1.79	1.5	1.9	1.4	2	2.2	1.80
4/7/2005	2:05 AM	1.79	1.6	1.8	1.9	1.9	1.5	1.74
4/7/2005	5:30 AM	3.66	3.2	2.9	3.1	3.2	3.3	3.14
4/7/2005	6:30 AM	4.07	3.3	3.5	3.4	3.3	3.7	3.44
4/7/2005	10:45 AM	0.65	0.84	0.83	0.82	0.84	0.93	0.85
4/7/2005	11:45 AM	0.83	1	1	1	0.98	0.89	0.97
4/7/2005	5:00 PM	2.76	2.5	2.4	2.4	2.5	2.4	2.44
4/7/2005	6:00 PM	2.73	2.7	2.7	2.6	2.6	2.7	2.66
4/8/2005	2:05 AM	0.48	0.69	0.69	0.72	0.75	0.78	0.73
4/8/2005	3:10 AM	0.73	0.84	0.79	0.81	1.3	1.1	0.97
4/8/2005	11:00 AM	0.54	1.2	1.1	1.1	0.88	0.9	1.04
4/8/2005	12:00 PM	0.56	1.5	1.3	1	1	0.84	1.13
4/11/2005	11:30 AM	0.79	0.97	0.95	1.1	0.96	0.92	0.98
4/11/2005	12:30 PM	0.88	1.1	1.2	1.1	1.1	1.1	1.12
4/11/2005	2:30 PM	1.76	1.6	1.6	1.7	1.6	1.7	1.64
4/11/2005	3:30 PM	1.65	1.6	1.5	1.6	1.6	1.6	1.58
4/12/2005	1:30 AM	3.72	3.2	3.1	3.3	3.2	3.2	3.20
4/12/2005	2:30 AM	3.59	3.5	2.9	3	2.5	2.6	2.90
4/13/2005	10:00 AM	0.67	0.55	0.18	0.56	0.3	0.68	0.45
4/13/2005	11:00 AM	0.52	0.92	0.61	0.94	0.83	0.33	0.73
4/13/2005	2:45 PM	4.22	2.8	2.9	2.7	2.6	2.7	2.74
4/13/2005	3:45 PM	4.07	2.4	2.8	2.8	2.5	2.5	2.60

Table E.4. Absorber outlet H_2O concentrations for MEA Baseline Campaign (April 6 – 13, 2005)

Date	Time	FTIR 1 (vol% H_2O)	FTIR 2 (vol% H_2O)	FTIR 3 (vol% H_2O)	FTIR 4 (vol% H_2O)	FTIR 5 (vol% H_2O)	FTIR AVG (vol% H_2O)
4/6/2005	4:20 PM	4.4	4.3	4.2	4.5	4.6	4.4
4/6/2005	5:30 PM	4.4	4.4	4.4	4.3	4.4	4.38
4/7/2005	1:00 AM	3.3	3	3.1	2.7	3	3.02
4/7/2005	2:05 AM	3.5	3.5	3.3	3	3.5	3.36
4/7/2005	5:30 AM	5.7	5.7	5.4	5.6	5.4	5.56
4/7/2005	6:30 AM	6	6.1	6.3	6.1	6.2	6.14
4/7/2005	10:45 AM	3.8	4.3	4.2	4.3	4	4.12
4/7/2005	11:45 AM	4.4	4.3	4.5	4.4	4.4	4.4
4/7/2005	5:00 PM	4.3	4.2	4.3	4.4	4.5	4.34
4/7/2005	6:00 PM	4.3	4.4	4.5	4.5	4.4	4.42
4/8/2005	2:05 AM	3.8	3.9	3.9	3.7	3.8	3.82
4/8/2005	3:10 AM	3.7	3.7	3.6	4	4	3.8
4/8/2005	11:00 AM	4.7	4.7	5	4.4	4.5	4.66
4/8/2005	12:00 PM	4.5	4.7	4.4	4.3	4.4	4.46
4/11/2005	11:30 AM	3.6	3.4	3.5	3.2	3.7	3.48
4/11/2005	12:30 PM	3.6	4	3.7	4.2	4	3.9
4/11/2005	2:30 PM	7.3	7.5	7.7	7.3	7.8	7.52
4/11/2005	3:30 PM	8.1	8.1	7.8	8.1	8.1	8.04
4/12/2005	1:30 AM	11.1	12.5	11.5	11.5	11.4	11.6
4/12/2005	2:30 AM	8.7	8.6	9.4	9.4	9.9	9.2
4/13/2005	10:00 AM	0	0	0	0	0	0
4/13/2005	11:00 AM	3.5	3.9	4.2	4.3	4.4	4.06
4/13/2005	2:45 PM	13.4	13	13.1	13	12.6	13.02
4/13/2005	3:45 PM	12.4	12.6	12.6	12.2	12.5	12.46

Table E.5. Absorber outlet NH_3 concentrations for MEA Baseline Campaign (April 6 – 13, 2005)

Date	Time	FTIR 1 (ppm NH_3)	FTIR 2 (ppm NH_3)	FTIR 3 (ppm NH_3)	FTIR 4 (ppm NH_3)	FTIR 5 (ppm NH_3)	FTIR AVG (ppm NH_3)
4/6/2005	4:20 PM	280	278	272	272	283	277
4/6/2005	5:30 PM	382	396	405	396	400	395.8
4/7/2005	1:00 AM	634	527	517	616	520	562.8
4/7/2005	2:05 AM	718	607	678	673	713	677.8
4/7/2005	5:30 AM	1294	1305	1273	1294	1276	1288.4
4/7/2005	6:30 AM	1328	1368	1345	1361	1356	1351.6
4/7/2005	10:45 AM	861	937	937	941	932	921.6
4/7/2005	11:45 AM	931	931	963	961	955	948.2
4/7/2005	5:00 PM	849	847	864	841	860	852.2
4/7/2005	6:00 PM	873	922	852	857	839	868.6
4/8/2005	2:05 AM	1037	1037	1032	1013	1018	1027.4
4/8/2005	3:10 AM	988	987	969	995	1004	988.6
4/8/2005	11:00 AM	974	971	985	975	973	975.6
4/8/2005	12:00 PM	962	977	961	967	981	969.6
4/11/2005	11:30 AM	72	69	70	71	71	70.6
4/11/2005	12:30 PM	102	105	107	118	110	108.4
4/11/2005	2:30 PM	451	461	458	463	473	461.2
4/11/2005	3:30 PM	469	469	466	465	471	468
4/12/2005	1:30 AM	760	815	780	760	769	776.8
4/12/2005	2:30 AM	533	521	507	523	526	522
4/13/2005	10:00 AM	0	0	0	0	0	0.01
4/13/2005	11:00 AM	7.6	4.2	0	16.4	15.6	8.76
4/13/2005	2:45 PM	51	51	55	52	55	52.8
4/13/2005	3:45 PM	57	58	60	60	64	59.8

Table E.6. Absorber outlet MEA concentrations for MEA Baseline Campaign (April 6 – 13, 2005)

Date	Time	FTIR 1 (ppm MEA)	FTIR 2 (ppm MEA)	FTIR 3 (ppm MEA)	FTIR 4 (ppm MEA)	FTIR 5 (ppm MEA)	FTIR AVG (ppm MEA)
4/6/2005	4:20 PM	79	78	72	63	75	73.4
4/6/2005	5:30 PM	99	89	91	92	82	90.6
4/7/2005	1:00 AM	55	46.6	23.6	22	22.9	34.02
4/7/2005	2:05 AM	34.5	22.9	13.8	16.3	24.9	22.48
4/7/2005	5:30 AM	45.8	67	59	41.2	40	50.6
4/7/2005	6:30 AM	71	46.9	43.9	55	32.3	49.82
4/7/2005	10:45 AM	44.1	19	37.9	49.1	26	35.22
4/7/2005	11:45 AM	26	39.2	42.3	30.2	56	38.74
4/7/2005	5:00 PM	17.7	12.5	12.9	13.2	11.6	13.58
4/7/2005	6:00 PM	24	12.2	22.8	21.4	32	22.48
4/8/2005	2:05 AM	43.5	42	34.5	45.9	34.9	40.16
4/8/2005	3:10 AM	30.1	34.8	33	30.4	41.6	33.98
4/8/2005	11:00 AM	41.7	38.2	80	58	68	57.18
4/8/2005	12:00 PM	54	146	59	80	42.5	76.3
4/11/2005	11:30 AM	144	128	118	102	89	116.2
4/11/2005	12:30 PM	44.7	38.6	42.1	39.9	36.3	40.32
4/11/2005	2:30 PM	135	132	116	160	87	126
4/11/2005	3:30 PM	174	129	112	108	155	135.6
4/12/2005	1:30 AM	208	284	190	205	217	220.8
4/12/2005	2:30 AM	125	183	156	161	147	154.4
4/13/2005	10:00 AM	0	0	0	0	0	0
4/13/2005	11:00 AM	269	421	524	654	690	511.6
4/13/2005	2:45 PM	232	237	233	231	187	224
4/13/2005	3:45 PM	216	229	212	225	221	220.6

Appendix F: K_2CO_3/PZ Pilot Plant Campaign

This appendix serves to tabulate all experimental data from the K_2CO_3/PZ Pilot Plant Campaign at the JJ Pickle Research Campus from January 10 – 26, 2006. All spectra were analyzed using the AQAPRCAmine.LIB application file.

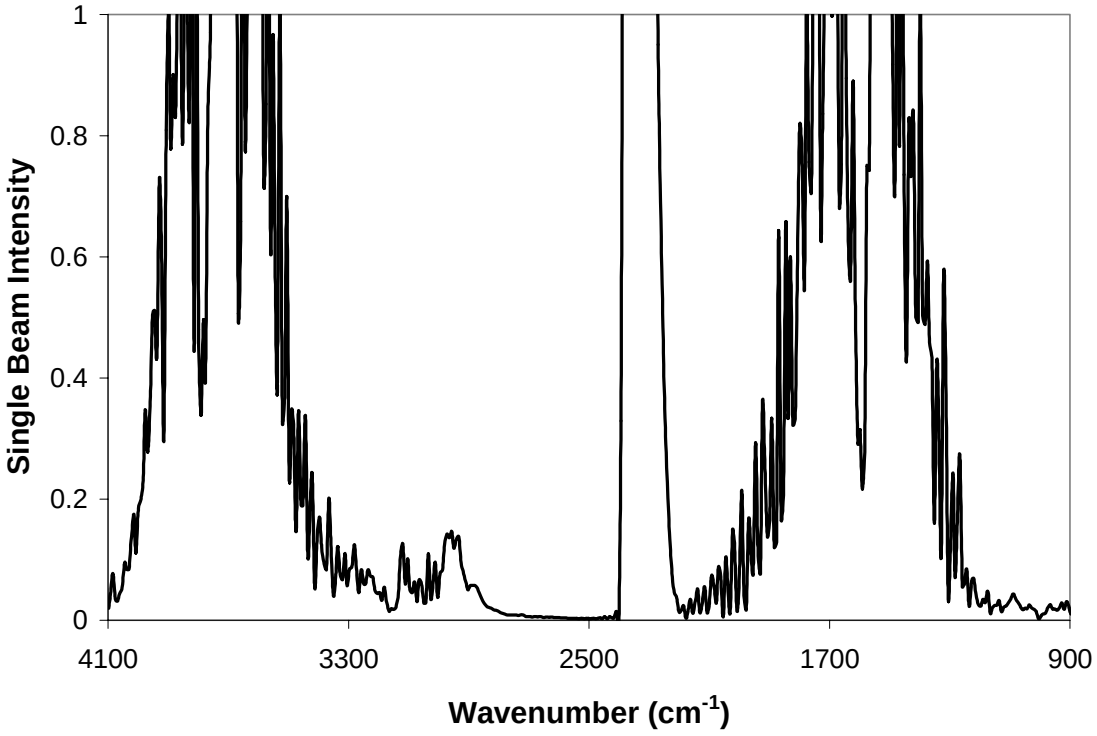

Figure F.1. Sample spectrum PZ_Campaign3_1660.SPE (absorber outlet sample point)

Table F.1. Calcmet™ analysis of PZ_Campaign3_1660.SPE (all spectra analyzed using AQAPRCAmine.LIB)

Channel	Component	Concentration	Units	Range	Residual
1	Water vapor H2O	8.7	vol%	10	0.0046
2	Carbon dioxide CO2	2.7	vol%	30	0.0058
5	Nitrous oxide N2O	0.53	ppm	100	0.0009
7	Nitrogen dioxide NO2	0.13	ppm	20	0.0073
9	Ammonia NH3	13.4	ppm	200	0.0017
16	Hexane C6H14	34.9	ppm	250	0.0017
21	Formaldehyde	6.4	ppm	25	0.0008
22	Acetaldehyde	0.75	ppm	25	0.0004
27	Methylamine	14.8	ppm	50	0.0015
30	Piperazine	7.2	ppm	50	0.0013
33	Unknown	49.9	ppm	100	0.0084

Table F.2. Experimental times, temperatures, measured lean loadings, and solvent compositions for absorber outlet sample point during K_2CO_3/PZ Campaign

Date	Time	Adjusted Time (hour)	Absorber Lean Ldg (mol CO_2/mol TAlk)	Gas Temp C (Gas Out TT400)	Solvent Concentration (m K^+/m PZ)
1/10/2006	3:31 PM	15.52	0.431	42.43	5/2.5
1/10/2006	9:04 PM	21.07	0.418	45.91	5/2.5
1/10/2006	10:08 PM	22.13	0.408	45.86	5/2.5
1/11/2006	3:59 PM	39.98	0.432	41.91	5/2.5
1/12/2006	6:28 AM	54.47	0.407	46.99	5/2.5
1/12/2006	7:35 AM	55.58	0.405	40.44	5/2.5
1/12/2006	2:04 PM	62.07	0.386	45.00	5/2.5
1/12/2006	10:31 PM	70.52	0.446	39.75	5/2.5
1/12/2006	11:31 PM	71.52	0.448	37.12	5/2.5
1/13/2006	3:03 AM	75.05	0.434	35.81	5/2.5
1/13/2006	5:12 AM	77.20	0.427	38.09	5/2.5
1/13/2006	5:59 AM	77.98	0.436	38.57	5/2.5
1/19/2006	10:27 AM	226.45	0.391	37.68	5/2.5
1/19/2006	1:56 PM	229.93	0.433	35.69	5/2.5
1/19/2006	3:10 PM	231.17	0.434	35.66	5/2.5
1/19/2006	7:34 PM	235.57	0.406	38.17	5/2.5
1/19/2006	9:03 PM	237.05	0.440	37.39	5/2.5
1/20/2006	4:13 AM	244.22	0.393	37.09	5/2.5
1/20/2006	1:30 PM	253.50	0.417	37.27	5/2.5
1/24/2006	11:30 AM	347.50	0.175	34.05	6.4/1.6
1/24/2006	12:35 PM	348.58	0.432	34.25	6.4/1.6
1/24/2006	7:33 PM	355.55	0.447	34.51	6.4/1.6
1/24/2006	9:34 PM	357.57	0.477	35.37	6.4/1.6
1/25/2006	4:58 AM	364.97	0.462	33.16	6.4/1.6
1/25/2006	3:00 PM	375.00	0.460	36.91	6.4/1.6
1/25/2006	4:00 PM	376.00	0.472	37.69	6.4/1.6
1/25/2006	9:00 PM	381.00	0.468	37.06	6.4/1.6
1/25/2006	10:04 PM	382.07	0.449	35.80	6.4/1.6
1/26/2006	12:58 AM	396.97	0.461	35.07	6.4/1.6
1/26/2006	2:00 AM	386.00	0.467	34.15	6.4/1.6
1/26/2006	5:32 AM	389.53	0.454	35.34	6.4/1.6
1/26/2006	6:32 AM	390.53	0.449	35.61	6.4/1.6
1/26/2006	10:00 AM	394.00	0.378	35.76	6.4/1.6
1/26/2006	3:00 PM	399.00	0.456	38.42	6.4/1.6
1/26/2006	4:00 PM	400.00	0.466	38.48	6.4/1.6
1/26/2006	7:00 PM	403.00	0.464	40.96	6.4/1.6
1/26/2006	8:00 PM	404.00	0.476	40.85	6.4/1.6

Table F.3. Absorber outlet CO_2 concentrations for K_2CO_3/PZ Campaign

Date	Time	Avg FTIR CO_2 (vol%)	Corrected CO_2 (vol%)	Vaisala CO_2 out (mol%)	Solvent Concentration (m K^+/m PZ)
1/10/2006	3:31 PM	0.84	0.81	0.43	5/2.5
1/10/2006	9:04 PM	2.91	2.66	2.67	5/2.5
1/10/2006	10:08 PM	4.47	4.07	3.67	5/2.5
1/11/2006	3:59 PM	5.34	4.83	3.60	5/2.5
1/12/2006	6:28 AM	2.60	2.36	1.56	5/2.5
1/12/2006	7:35 AM	2.41	2.24	1.45	5/2.5
1/12/2006	2:04 PM	2.21	2.02	0.83	5/2.5
1/12/2006	10:31 PM	5.61	5.22	2.93	5/2.5
1/12/2006	11:31 PM	5.79	5.40	3.22	5/2.5
1/13/2006	3:03 AM	6.31	5.92	3.93	5/2.5
1/13/2006	5:12 AM	5.46	5.13	3.19	5/2.5
1/13/2006	5:59 AM	6.17	5.78	3.77	5/2.5
1/19/2006	10:27 AM	2.37	2.22	1.84	5/2.5
1/19/2006	1:56 PM	1.53	1.44	1.26	5/2.5
1/19/2006	3:10 PM	1.94	1.83	1.31	5/2.5
1/19/2006	7:34 PM	5.05	4.73	4.16	5/2.5
1/19/2006	9:03 PM	3.08	2.89	2.68	5/2.5
1/20/2006	4:13 AM	3.49	3.29	3.37	5/2.5
1/20/2006	1:30 PM	1.32	1.24	1.28	5/2.5
1/24/2006	11:30 AM	8.17	7.84	5.85	6.4/1.6
1/24/2006	12:35 PM	8.40	8.02	5.65	6.4/1.6
1/24/2006	7:33 PM	6.92	6.58	4.53	6.4/1.6
1/24/2006	9:34 PM	6.38	6.03	4.75	6.4/1.6
1/25/2006	4:58 AM	4.77	4.53	3.52	6.4/1.6
1/25/2006	3:00 PM	3.17	3.01	2.41	6.4/1.6
1/25/2006	4:00 PM	3.87	3.66	2.78	6.4/1.6
1/25/2006	9:00 PM	4.75	4.48	3.27	6.4/1.6
1/25/2006	10:04 PM	4.66	4.41	3.12	6.4/1.6
1/26/2006	12:58 AM	5.68	5.38	6.70	6.4/1.6
1/26/2006	2:00 AM	4.83	4.57	6.70	6.4/1.6
1/26/2006	5:32 AM	3.54	3.34	2.87	6.4/1.6
1/26/2006	6:32 AM	4.89	4.61	3.25	6.4/1.6
1/26/2006	10:00 AM	2.71	2.55	2.07	6.4/1.6
1/26/2006	3:00 PM	8.01	7.50	6.01	6.4/1.6
1/26/2006	4:00 PM	7.78	7.26	5.87	6.4/1.6
1/26/2006	7:00 PM	9.25	8.59	6.88	6.4/1.6
1/26/2006	8:00 PM	8.68	8.09	6.48	6.4/1.6

Table F.4. Absorber outlet H_2O concentrations for K_2CO_3/PZ Campaign

Date	Time	Avg FTIR H_2O (vol%)	Solvent Concentration (m K^+/m PZ)
1/10/2006	3:31 PM	4.46	5/2.5
1/10/2006	9:04 PM	9.404	5/2.5
1/10/2006	10:08 PM	9.818	5/2.5
1/11/2006	3:59 PM	7.5	5/2.5
1/12/2006	6:28 AM	10.448	5/2.5
1/12/2006	7:35 AM	7.636	5/2.5
1/12/2006	2:04 PM	9.244	5/2.5
1/12/2006	10:31 PM	7.374	5/2.5
1/12/2006	11:31 PM	7.13	5/2.5
1/13/2006	3:03 AM	6.494	5/2.5
1/13/2006	5:12 AM	6.38	5/2.5
1/13/2006	5:59 AM	6.618	5/2.5
1/19/2006	10:27 AM	6.432	5/2.5
1/19/2006	1:56 PM	6.232	5/2.5
1/19/2006	3:10 PM	5.924	5/2.5
1/19/2006	7:34 PM	6.716	5/2.5
1/19/2006	9:03 PM	6.44	5/2.5
1/20/2006	4:13 AM	6.126	5/2.5
1/20/2006	1:30 PM	6.016	5/2.5
1/24/2006	11:30 AM	4.264	6.4/1.6
1/24/2006	12:35 PM	4.716	6.4/1.6
1/24/2006	7:33 PM	5.238	6.4/1.6
1/24/2006	9:34 PM	5.904	6.4/1.6
1/25/2006	4:58 AM	5.334	6.4/1.6
1/25/2006	3:00 PM	5.35	6.4/1.6
1/25/2006	4:00 PM	5.698	6.4/1.6
1/25/2006	9:00 PM	5.962	6.4/1.6
1/25/2006	10:04 PM	5.712	6.4/1.6
1/26/2006	12:58 AM	5.624	6.4/1.6
1/26/2006	2:00 AM	5.728	6.4/1.6
1/26/2006	5:32 AM	5.866	6.4/1.6
1/26/2006	6:32 AM	5.96	6.4/1.6
1/26/2006	10:00 AM	6.088	6.4/1.6
1/26/2006	3:00 PM	6.794	6.4/1.6
1/26/2006	4:00 PM	7.144	6.4/1.6
1/26/2006	7:00 PM	7.616	6.4/1.6
1/26/2006	8:00 PM	7.234	6.4/1.6

Table F.5. Absorber outlet PZ concentrations for K_2CO_3/PZ Campaign

Date	Time	Measured PZ (ppm)	Solvent Concentration (m K+/m PZ)
1/10/2006	3:31 PM	-1.69	5/2.5
1/10/2006	9:04 PM	33.44	5/2.5
1/10/2006	10:08 PM	39.75	5/2.5
1/11/2006	3:59 PM	14.52	5/2.5
1/12/2006	6:28 AM	7.15	5/2.5
1/12/2006	7:35 AM	5.73	5/2.5
1/12/2006	2:04 PM	10.40	5/2.5
1/12/2006	10:31 PM	3.87	5/2.5
1/12/2006	11:31 PM	5.50	5/2.5
1/13/2006	3:03 AM	2.62	5/2.5
1/13/2006	5:12 AM	2.33	5/2.5
1/13/2006	5:59 AM	1.82	5/2.5
1/19/2006	10:27 AM	0.33	5/2.5
1/19/2006	1:56 PM	0.74	5/2.5
1/19/2006	3:10 PM	0.78	5/2.5
1/19/2006	7:34 PM	0.17	5/2.5
1/19/2006	9:03 PM	0.17	5/2.5
1/20/2006	4:13 AM	0.27	5/2.5
1/20/2006	1:30 PM	2.36	5/2.5
1/24/2006	11:30 AM	21.01	6.4/1.6
1/24/2006	12:35 PM	-6.30	6.4/1.6
1/24/2006	7:33 PM	-7.38	6.4/1.6
1/24/2006	9:34 PM	-10.63	6.4/1.6
1/25/2006	4:58 AM	-3.26	6.4/1.6
1/25/2006	3:00 PM	-4.28	6.4/1.6
1/25/2006	4:00 PM	-1.79	6.4/1.6
1/25/2006	9:00 PM	-2.96	6.4/1.6
1/25/2006	10:04 PM	-2.28	6.4/1.6
1/26/2006	12:58 AM	-1.33	6.4/1.6
1/26/2006	2:00 AM	-0.43	6.4/1.6
1/26/2006	5:32 AM	-0.81	6.4/1.6
1/26/2006	6:32 AM	-0.50	6.4/1.6
1/26/2006	10:00 AM	0.09	6.4/1.6
1/26/2006	3:00 PM	-1.05	6.4/1.6
1/26/2006	4:00 PM	0.37	6.4/1.6
1/26/2006	7:00 PM	-1.03	6.4/1.6
1/26/2006	8:00 PM	-0.31	6.4/1.6

Table F.6. Absorber outlet Unknown Amine concentrations for K_2CO_3/PZ Campaign

Date	Time	Measured UNK (ppm)	Solvent Concentration (m K^+/m PZ)
1/10/2006	3:31 PM	49.094	5/2.5
1/10/2006	9:04 PM	50.132	5/2.5
1/10/2006	10:08 PM	51.526	5/2.5
1/11/2006	3:59 PM	51.174	5/2.5
1/12/2006	6:28 AM	59.606	5/2.5
1/12/2006	7:35 AM	50.106	5/2.5
1/12/2006	2:04 PM	44.888	5/2.5
1/12/2006	10:31 PM	43.336	5/2.5
1/12/2006	11:31 PM	45.068	5/2.5
1/13/2006	3:03 AM	39.708	5/2.5
1/13/2006	5:12 AM	38.652	5/2.5
1/13/2006	5:59 AM	39.924	5/2.5
1/19/2006	10:27 AM	23.982	5/2.5
1/19/2006	1:56 PM	21.172	5/2.5
1/19/2006	3:10 PM	19.43	5/2.5
1/19/2006	7:34 PM	23.114	5/2.5
1/19/2006	9:03 PM	19.232	5/2.5
1/20/2006	4:13 AM	18.096	5/2.5
1/20/2006	1:30 PM	22.224	5/2.5
1/24/2006	11:30 AM	68.344	6.4/1.6
1/24/2006	12:35 PM	162.61	6.4/1.6
1/24/2006	7:33 PM	117.514	6.4/1.6
1/24/2006	9:34 PM	109.682	6.4/1.6
1/25/2006	4:58 AM	114.368	6.4/1.6
1/25/2006	3:00 PM	89.3	6.4/1.6
1/25/2006	4:00 PM	81.01	6.4/1.6
1/25/2006	9:00 PM	92.08	6.4/1.6
1/25/2006	10:04 PM	71.422	6.4/1.6
1/26/2006	12:58 AM	62.588	6.4/1.6
1/26/2006	2:00 AM	53.794	6.4/1.6
1/26/2006	5:32 AM	48.444	6.4/1.6
1/26/2006	6:32 AM	57.844	6.4/1.6
1/26/2006	10:00 AM	46.786	6.4/1.6
1/26/2006	3:00 PM	50.202	6.4/1.6
1/26/2006	4:00 PM	35.338	6.4/1.6
1/26/2006	7:00 PM	41.462	6.4/1.6
1/26/2006	8:00 PM	29.1	6.4/1.6

Table F.7. Absorber outlet Formaldehyde concentrations for K_2CO_3/PZ Campaign

Date	Time	Measured FORM (ppm)	Solvent Concentration (m K^+/m PZ)
1/10/2006	3:31 PM	7.76	5/2.5
1/10/2006	9:04 PM	6.19	5/2.5
1/10/2006	10:08 PM	7.52	5/2.5
1/11/2006	3:59 PM	6.13	5/2.5
1/12/2006	6:28 AM	7.06	5/2.5
1/12/2006	7:35 AM	6.68	5/2.5
1/12/2006	2:04 PM	5.33	5/2.5
1/12/2006	10:31 PM	5.31	5/2.5
1/12/2006	11:31 PM	5.4	5/2.5
1/13/2006	3:03 AM	5.11	5/2.5
1/13/2006	5:12 AM	4.49	5/2.5
1/13/2006	5:59 AM	5	5/2.5
1/19/2006	10:27 AM	1.13	5/2.5
1/19/2006	1:56 PM	1.69	5/2.5
1/19/2006	3:10 PM	0.38	5/2.5
1/19/2006	7:34 PM	4.2	5/2.5
1/19/2006	9:03 PM	0.84	5/2.5
1/20/2006	4:13 AM	2.29	5/2.5
1/20/2006	1:30 PM	2.06	5/2.5
1/24/2006	11:30 AM	13.86	6.4/1.6
1/24/2006	12:35 PM	14.66	6.4/1.6
1/24/2006	7:33 PM	10.28	6.4/1.6
1/24/2006	9:34 PM	12.38	6.4/1.6
1/25/2006	4:58 AM	8.98	6.4/1.6
1/25/2006	3:00 PM	4.73	6.4/1.6
1/25/2006	4:00 PM	5.94	6.4/1.6
1/25/2006	9:00 PM	11.44	6.4/1.6
1/25/2006	10:04 PM	9.75	6.4/1.6
1/26/2006	12:58 AM	6.44	6.4/1.6
1/26/2006	2:00 AM	10.08	6.4/1.6
1/26/2006	5:32 AM	9.86	6.4/1.6
1/26/2006	6:32 AM	7.34	6.4/1.6
1/26/2006	10:00 AM	6.62	6.4/1.6
1/26/2006	3:00 PM	9.06	6.4/1.6
1/26/2006	4:00 PM	7.07	6.4/1.6
1/26/2006	7:00 PM	9.54	6.4/1.6
1/26/2006	8:00 PM	7.48	6.4/1.6

Table F.8. Absorber outlet Methylamine concentrations for K_2CO_3/PZ Campaign

Date	Time	Measured MA (ppm)	Solvent Concentration (m K^+/m PZ)
1/10/2006	15:31	20.24	5/2.5
1/10/2006	21:04	23.59	5/2.5
1/10/2006	22:08	20	5/2.5
1/11/2006	15:59	15.74	5/2.5
1/12/2006	6:28	16.71	5/2.5
1/12/2006	7:35	15.38	5/2.5
1/12/2006	14:04	14.83	5/2.5
1/12/2006	22:31	16.45	5/2.5
1/12/2006	23:31	17.05	5/2.5
1/13/2006	3:03	13.66	5/2.5
1/13/2006	5:12	14.59	5/2.5
1/13/2006	5:59	13.15	5/2.5
1/19/2006	10:27	13.15	5/2.5
1/19/2006	13:56	13.89	5/2.5
1/19/2006	15:10	11.84	5/2.5
1/19/2006	19:34	14.15	5/2.5
1/19/2006	21:03	11.28	5/2.5
1/20/2006	4:13	11.64	5/2.5
1/20/2006	13:30	13.67	5/2.5
1/24/2006	11:30	28.12	6.4/1.6
1/24/2006	12:35	17.57	6.4/1.6
1/24/2006	19:33	21.35	6.4/1.6
1/24/2006	21:34	24.92	6.4/1.6
1/25/2006	4:58	24.98	6.4/1.6
1/25/2006	15:00	17.27	6.4/1.6
1/25/2006	16:00	18.07	6.4/1.6
1/25/2006	21:00	29.37	6.4/1.6
1/25/2006	22:04	14.38	6.4/1.6
1/26/2006	0:58	20.73	6.4/1.6
1/26/2006	2:00	19.61	6.4/1.6
1/26/2006	5:32	23.04	6.4/1.6
1/26/2006	6:32	20.05	6.4/1.6
1/26/2006	10:00	16.46	6.4/1.6
1/26/2006	15:00	17.64	6.4/1.6
1/26/2006	16:00	12.96	6.4/1.6
1/26/2006	19:00	14.29	6.4/1.6
1/26/2006	20:00	10.01	6.4/1.6

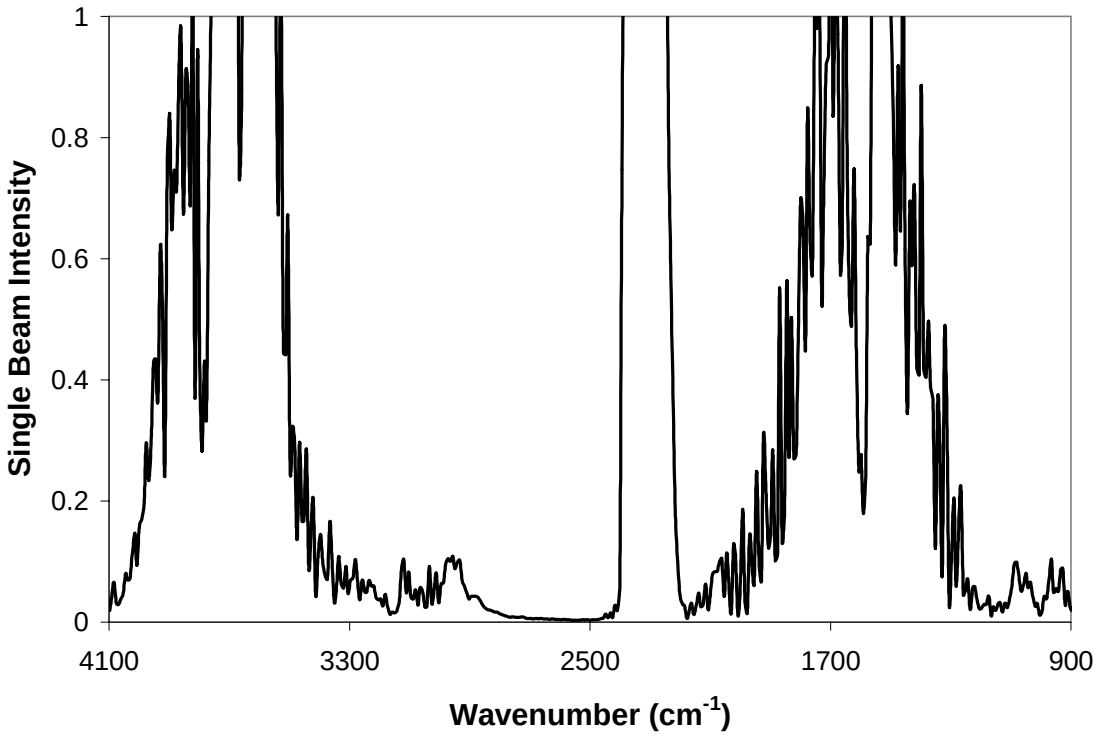

Figure F.2. Sample spectrum PZ_Campaign3_1699.SPE (absorber inlet sample point)

Table F.9. Calcmet™ analysis of sample spectrum PZ_Campaign3_1699.SPE

Channel	Component	Concentration	Units	Range	Residual
1	Water vapor H2O	6.8	vol%	10	0.0032
2	Carbon dioxide CO2	12.5	vol%	30	0.0029
5	Nitrous oxide N2O	0.9	ppm	100	0.0008
7	Nitrogen dioxide NO2	4.4	ppm	20	0.0114
9	Ammonia NH3	6.9	ppm	200	0.0023
16	Hexane C6H14	23.4	ppm	250	0.0015
21	Formaldehyde	5.6	ppm	25	0.0017
22	Acetaldehyde	0.12	ppm	25	0.0008
27	Methylamine	27.6	ppm	50	0.0014
30	Piperazine	6.5	ppm	50	0.0017
33	Unknown	48.9	ppm	100	0.0064

Table F.10. Experimental times, temperatures, measured lean loadings, and solvent compositions at absorber inlet sample point for K_2CO_3/PZ Campaign (red boxes correspond to samples taken when conditions were not steady state)

Date	Time	Adjusted Time (hour)	Absorber Lean Ldg (mol CO_2/mol TAlk)	Gas Temp C (Gas In TT406)	Solvent Concentration (m K+/m PZ)
1/11/2006	12:00 PM	36.00	0.443	38.18	5/2.5
1/11/2006	1:01 PM	37.02	0.437	40.97	5/2.5
1/11/2006	5:28 PM	41.47	0.439	39.62	5/2.5
1/11/2006	9:19 PM	45.32	0.435	39.79	5/2.5
1/11/2006	10:20 PM	46.33	0.438	40.30	5/2.5
1/12/2006	3:00 PM	63.00	0.388	43.73	5/2.5
1/12/2006	5:06 PM	65.10	0.390	39.67	5/2.5
1/12/2006	6:03 PM	66.05	0.382	40.09	5/2.5
1/12/2006	6:31 PM	66.52	0.386	40.18	5/2.5
1/13/2006	2:07 AM	74.12	0.386	39.33	5/2.5
1/13/2006	3:17 AM	75.28	0.434	40.19	5/2.5
1/19/2006	11:11 AM	227.18	0.391	40.39	5/2.5
1/19/2006	12:24 PM	228.40	0.444	39.65	5/2.5
1/20/2006	5:13 AM	245.22	0.407	39.37	5/2.5
1/24/2006	1:41 PM	349.68	0.432	41.74	6.4/1.6
1/25/2006	5:31 AM	365.52	0.462	40.80	6.4/1.6
1/26/2006	1:07 AM	385.12	0.461	39.40	6.4/1.6
1/26/2006	2:17 AM	386.28	0.467	40.63	6.4/1.6
1/26/2006	5:46 AM	389.77	0.454	40.42	6.4/1.6
1/26/2006	6:47 AM	390.78	0.449	40.32	6.4/1.6
1/26/2006	11:09 AM	395.15	0.452	40.24	6.4/1.6

Table F.11. Absorber inlet CO_2 concentrations for K_2CO_3/PZ Campaign

Date	Time	Avg FTIR CO_2 (vol%)	Corrected CO_2 (vol%)	Solvent Concentration (m K+/m PZ)
1/11/2006	12:00 PM	14.48	13.57	5/2.5
1/11/2006	1:01 PM	15.03	14.09	5/2.5
1/11/2006	5:28 PM	16.05	15.04	5/2.5
1/11/2006	9:19 PM	15.75	14.79	5/2.5
1/11/2006	10:20 PM	10.90	10.07	5/2.5
1/12/2006	3:00 PM	12.38	11.60	5/2.5
1/12/2006	5:06 PM	10.16	9.52	5/2.5
1/12/2006	6:03 PM	15.36	14.35	5/2.5
1/12/2006	6:31 PM	15.49	14.48	5/2.5
1/13/2006	2:07 AM	14.45	13.64	5/2.5
1/13/2006	3:17 AM	14.33	13.53	5/2.5
1/19/2006	11:11 AM	12.96	12.14	5/2.5
1/19/2006	12:24 PM	14.55	13.62	5/2.5
1/20/2006	5:13 AM	15.53	14.54	5/2.5
1/24/2006	1:41 PM	14.71	13.97	6.4/1.6
1/25/2006	5:31 AM	16.00	15.02	6.4/1.6
1/26/2006	1:07 AM	14.90	13.68	6.4/1.6
1/26/2006	2:17 AM	13.40	12.34	6.4/1.6
1/26/2006	5:46 AM	14.44	13.45	6.4/1.6
1/26/2006	6:47 AM	15.02	14.03	6.4/1.6
1/26/2006	11:09 AM	15.78	14.68	6.4/1.6

Table F.12. Absorber inlet H_2O concentrations for K_2CO_3/PZ Campaign

Date	Time	Avg FTIR H_2O (vol%)	Solvent Concentration (m K+/m PZ)
1/11/2006	12:00 PM	6.76	5/2.5
1/11/2006	1:01 PM	6.63	5/2.5
1/11/2006	5:28 PM	6.71	5/2.5
1/11/2006	9:19 PM	6.49	5/2.5
1/11/2006	10:20 PM	8.27	5/2.5
1/12/2006	3:00 PM	6.71	5/2.5
1/12/2006	5:06 PM	6.76	5/2.5
1/12/2006	6:03 PM	7.00	5/2.5
1/12/2006	6:31 PM	6.99	5/2.5
1/13/2006	2:07 AM	5.94	5/2.5
1/13/2006	3:17 AM	5.90	5/2.5
1/19/2006	11:11 AM	6.78	5/2.5
1/19/2006	12:24 PM	6.88	5/2.5
1/20/2006	5:13 AM	6.79	5/2.5
1/24/2006	1:41 PM	5.25	6.4/1.6
1/25/2006	5:31 AM	6.53	6.4/1.6
1/26/2006	1:07 AM	8.92	6.4/1.6
1/26/2006	2:17 AM	8.61	6.4/1.6
1/26/2006	5:46 AM	7.35	6.4/1.6
1/26/2006	6:47 AM	7.08	6.4/1.6
1/26/2006	11:09 AM	7.50	6.4/1.6

Table F.13. Absorber inlet PZ concentrations for K_2CO_3/PZ Campaign

Date	Time	Measured PZ (ppm)	Solvent Concentration (m K^+/m PZ)
1/11/2006	12:00 PM	0.29	5/2.5
1/11/2006	1:01 PM	1.32	5/2.5
1/11/2006	5:28 PM	7.99	5/2.5
1/11/2006	9:19 PM	6.19	5/2.5
1/11/2006	10:20 PM	6.83	5/2.5
1/12/2006	3:00 PM	8.21	5/2.5
1/12/2006	5:06 PM	11.59	5/2.5
1/12/2006	6:03 PM	11.22	5/2.5
1/12/2006	6:31 PM	9.44	5/2.5
1/13/2006	2:07 AM	5.25	5/2.5
1/13/2006	3:17 AM	4.37	5/2.5
1/19/2006	11:11 AM	3.79	5/2.5
1/19/2006	12:24 PM	2.98	5/2.5
1/20/2006	5:13 AM	12.95	5/2.5
1/24/2006	1:41 PM	-12.68	6.4/1.6
1/25/2006	5:31 AM	11.55	6.4/1.6
1/26/2006	1:07 AM	8.40	6.4/1.6
1/26/2006	2:17 AM	9.07	6.4/1.6
1/26/2006	5:46 AM	5.35	6.4/1.6
1/26/2006	6:47 AM	5.72	6.4/1.6
1/26/2006	11:09 AM	18.37	6.4/1.6

Table F.14. Absorber inlet Unknown Amine concentrations for K_2CO_3/PZ Campaign

Date	Time	FTIR UNK (ppm)	Solvent Concentration (m K^+/m PZ)
1/11/2006	12:00 PM	56.87	5/2.5
1/11/2006	1:01 PM	56.36	5/2.5
1/11/2006	5:28 PM	39.86	5/2.5
1/11/2006	9:19 PM	35.80	5/2.5
1/11/2006	10:20 PM	51.94	5/2.5
1/12/2006	3:00 PM	49.40	5/2.5
1/12/2006	5:06 PM	53.71	5/2.5
1/12/2006	6:03 PM	48.99	5/2.5
1/12/2006	6:31 PM	47.51	5/2.5
1/13/2006	2:07 AM	38.79	5/2.5
1/13/2006	3:17 AM	37.40	5/2.5
1/19/2006	11:11 AM	26.51	5/2.5
1/19/2006	12:24 PM	25.39	5/2.5
1/20/2006	5:13 AM	27.25	5/2.5
1/24/2006	1:41 PM	45.99	6.4/1.6
1/25/2006	5:31 AM	126.22	6.4/1.6
1/26/2006	1:07 AM	64.87	6.4/1.6
1/26/2006	2:17 AM	59.49	6.4/1.6
1/26/2006	5:46 AM	57.69	6.4/1.6
1/26/2006	6:47 AM	63.33	6.4/1.6
1/26/2006	11:09 AM	51.15	6.4/1.6

Table F.15. Absorber inlet Formaldehyde concentrations for K_2CO_3/PZ Campaign

Date	Time	FTIR FORM (ppm)	Solvent Concentration (m K^+/m PZ)
1/11/2006	12:00	6.99	5/2.5
1/11/2006	13:01	6.56	5/2.5
1/11/2006	17:28	4.95	5/2.5
1/11/2006	21:19	4.47	5/2.5
1/11/2006	22:20	3.92	5/2.5
1/12/2006	15:00	5.65	5/2.5
1/12/2006	17:06	5.52	5/2.5
1/12/2006	18:03	5.22	5/2.5
1/12/2006	18:31	4.44	5/2.5
1/13/2006	2:07	3.75	5/2.5
1/13/2006	3:17	3.62	5/2.5
1/19/2006	11:11	2.27	5/2.5
1/19/2006	12:24	3.56	5/2.5
1/20/2006	5:13	3.43	5/2.5
1/24/2006	13:41	22.97	6.4/1.6
1/25/2006	5:31	6.36	6.4/1.6
1/26/2006	1:07	9.85	6.4/1.6
1/26/2006	2:17	8.94	6.4/1.6
1/26/2006	5:46	7.86	6.4/1.6
1/26/2006	6:47	8.95	6.4/1.6
1/26/2006	11:09	6.54	6.4/1.6

Table F.16. Absorber inlet Methylamine concentrations for K_2CO_3/PZ Campaign

Date	Time	FTIR MA (ppm)	Solvent Concentration (m K^+/m PZ)
1/11/2006	12:00	20.02	5/2.5
1/11/2006	13:01	18.30	5/2.5
1/11/2006	17:28	20.52	5/2.5
1/11/2006	21:19	16.48	5/2.5
1/11/2006	22:20	13.28	5/2.5
1/12/2006	15:00	27.61	5/2.5
1/12/2006	17:06	33.13	5/2.5
1/12/2006	18:03	31.62	5/2.5
1/12/2006	18:31	31.86	5/2.5
1/13/2006	2:07	23.67	5/2.5
1/13/2006	3:17	21.69	5/2.5
1/19/2006	11:11	21.39	5/2.5
1/19/2006	12:24	24.44	5/2.5
1/20/2006	5:13	26.69	5/2.5
1/24/2006	13:41	49.87	6.4/1.6
1/25/2006	5:31	43.76	6.4/1.6
1/26/2006	1:07	31.87	6.4/1.6
1/26/2006	2:17	31.45	6.4/1.6
1/26/2006	5:46	29.64	6.4/1.6
1/26/2006	6:47	28.68	6.4/1.6
1/26/2006	11:09	30.20	6.4/1.6

References

Design Institute for Physical Properties (DIPPR). 2006. New York, American Institute of Chemical Engineers.

Aroua, M.K. and Salleh R.M. 2004. Solubility of CO_2 in Aqueous Piperazine and its Modeling Using the Kent-Eisenberg Approach. Chem. Eng. Tech. 27 (1): 65 – 70.

Bishnoi, S. 2000. Carbon Dioxide Absorption and Solution Equilibrium in Piperazine Activated Methyldiethanolamine. Ph.D. Dissertation. The University of Texas at Austin.

Cai, Z., Xie, R., and Wu, Z. 1996. Binary Isobaric Vapor-Liquid Equilibria of Ethanolamines + Water. J. Chem. Eng. Data. 41: 1101 – 1103.

Chang, H., Posey, M., and Rochelle, G.T. 1993. Thermodynamics of Alkanolamine – Water Solutions from Freezing Point Measurements. Ind. Eng. Chem. Res. 32: 2324 – 2335.

Chiu, L. and Li, M. 1999. Heat Capacity of Alkanolamine Aqueous Solutions. J. Chem. Eng. Data. 44: 1396 – 1401.

Cullinane, J.T. 2005. Thermodynamics and Kinetics of Aqueous Piperazine with Potassium Carbonate for Carbon Dioxide Absorption. Ph.D. Dissertation. The University of Texas at Austin.

Derks, P.W.J., Dijkstra, H.B.S., Hogendoorn, J.A., and Versteeg, G.F. 2005. Solubility of Carbon Dioxide in Aqueous Piperazine Solutions. AIChE. 51 (8): 2311 – 2327.

Goff, G. S. 2005. Oxidative Degradation of Aqueous Monoethanolamine in CO_2 Capture Processes: Iron and Copper Catalysis, Inhibition, and O_2 Mass Transfer. Ph.D. Dissertation. The University of Texas at Austin.

Hilliard, M.D. 2005. Thermodynamics of Aqueous Piperazine/Potassium Carbonate/Carbon Dioxide by the ENRTL Model. M.S. Thesis. The University of Texas at Austin.

Rénard, J., Rousseau, R.W., and Teja, A.S. 1990. Vapor-Liquid Equilibria for Mixtures of 2 – Aminoethanol + Water. AIChE Symposium Series. 86 (279): 1 – 5.

Nath, A. and Bender, E. 1983. Isothermal Vapor-Liquid Equilibria of Binary and Ternary Mixtures Containing Alcohol, Alkanolamine, and Water with a New Static Device. J. Chem. Eng. Data. 26: 370 – 375.

Pagé, M., Huot, J., and Jolicouer, C. 1993. A comprehensive thermodynamic investigation of water-ethanolamine mixtures at 10, 25, and 40 ^{0}C. Can. J. Chem. 71 (7): 1064 – 1072.

Park, S., and Lee, H. 1997. Vapor-Liquid Equilibria for the Binary Monoethanolamine + Water and Methanolamine + Ethanol Systems. Korean J. of Chem. Eng. 14 (2): 146 – 148.

Posey, M.L. 1996. Thermodynamic Model for Acid Gas Loaded Aqueous Alkanolamine Solutions. Ph.D. Dissertation. The University of Texas at Austin.

Seinfeld, J.H. and Pandis, S.N. 1998. Atmospheric Chemistry and Physics: From Air Pollution to Climate Change. John Wiley and Sons, Inc., New York.

Tochigi, K., Akimoto, K., Ochi, K., Liu, F., and Kawase, Y. 1999. Isothermal Vapor-Liquid Equilibria for Water + 2-Aminoethanol + Dimethyl Sulfoxide and Its Constituent Three Binary Systems. J. Chem. Eng. Data. 44: 588 – 590.

Touhara, H., Okazaki, S., Okino, F., Tanaka, H., Ikari, K., and Nakanishi, K. 1982. Thermodynamic Properties of Aqueous Mixtures of Hydrophilic Compounds 2-Aminoethanol and its Methyl Derivatives. J. Chem. Thermodynamics. 14: 145 – 156.

Wilson, H.L., and Wilding, W.V. 1994. Vapor-Liquid and Liquid-Liquid Equilibrium Measurements of Twenty-Two Binary Mixtures. Experimental Results for DIPPR 1990 – 1991 Projects on Phase Equilibria and Pure Component Properties. J.R. Cunningham and D.K. Jones. 63 – 115.

Weiland, R.H., Dingman, J.C., and Cronin, D.B. 1997. Heat Capacity of Aqueous Monoethanolamine, Diethanolamine, N-Methyldiethanolamine, and N-Methyldiethanolamine-Based Blends with Carbon Dioxide. J. Chem. Eng. Data. 42: 1004 – 1006.

Vita

John Arthur McLees, Jr. was born on January 23, 1982 in Greenville, South Carolina to John Arthur McLees and Susan Anne McLees. Upon graduation from Hillcrest High School in Simpsonville, South Carolina in 2000, he enrolled at the University of South Carolina. As an undergraduate, he did summer internships at the South Carolina State Board of Professional Engineers and Land Surveyors as well as Battery Design Company. He graduated with honors with a Bachelor of Science in Chemical Engineering in May 2004, and commenced graduate studies at the University of Texas at Austin in August 2004. He has accepted full-time employment with Samsung Austin Semiconductor in Austin, Texas.

Permanent address: 117 William Street
Fountain Inn, SC 29644

This thesis was typed by the author.